AD_____

Award Number: W81XWH-07-1-0170

TITLE: Calcium Homeostatasis and Mitochondrial Dysfunction in Dopaminergic Neurons of the Substantia Nigra

PRINCIPAL INVESTIGATOR: D. James Surmeier, Ph.D.

CONTRACTING ORGANIZATION: Northwestern University
Evanston, IL 60208

REPORT DATE: March 2010

TYPE OF REPORT: Final

PREPARED FOR: U.S. Army Medical Research and Materiel Command
Fort Detrick, Maryland 21702-5012

# REPORT DOCUMENTATION PAGE

*Form Approved*
*OMB No. 0704-0188*



| **1. REPORT DATE** *(DD-MM-YYYY)* | **2. REPORT TYPE** | **3. DATES COVERED** *(From - To)* |
|---|---|---|
| 01-mar-2010 | Final | 01-03-2007 to 28-02-2010 |

**4. TITLE AND SUBTITLE**
Calcium Homeostasis and Mitochondrial Dysfunction in Dopaminergic Neurons of the Substantia Nigra

**5a. CONTRACT NUMBER**
W81XWH-07-0170

**5b. GRANT NUMBER**

**5c. PROGRAM ELEMENT NUMBER**

**6. AUTHOR(S)**
D. James Surmeier, Ph.D.
Email: j-surmeier@northwestern.edu

**5d. PROJECT NUMBER**

**5e. TASK NUMBER**

**5f. WORK UNIT NUMBER**

**7. PERFORMING ORGANIZATION NAME(S) AND ADDRESS(ES)**
Northwestern University
633 Clark Street
Evanston, IL 60208-1110

**8. PERFORMING ORGANIZATION REPORT NUMBER**

**9. SPONSORING / MONITORING AGENCY NAME(S) AND ADDRESS(ES)**
U.S. Army Medical Research
and Materiel Command
Fort Detrick, Maryland 21702-5012

**10. SPONSOR/MONITOR'S ACRONYM(S)**

**11. SPONSOR/MONITOR'S REPORT NUMBER(S)**

**12. DISTRIBUTION / AVAILABILITY STATEMENT**

Approved for public release; distribution unlimited

**13. SUPPLEMENTARY NOTES**

**14. ABSTRACT**

**Key Research Accomplishments:**

- the discovery that calcium entry through L-type channels during normal pacemaking elevates the sensitivity of SNc dopaminergic neurons to toxins;
- the discovery that L-type calcium channels participate in but are not necessary for pacemaking;
- the discovery that serum concentration of the dihydropyridine isradipine required to achieve protection of SNc dopaminergic neurons against toxins in animal models is similar to that achieved in humans by FDA approved doses;
- the discovery that calcium entry through L-type channels during pacemaking elevates mitochondrial oxidant stress and leads to the engagement of a DJ-1-dependent oxidant defense system involving uncoupling proteins.

**15. SUBJECT TERMS**
L-type calcium channel, mitochondria, Parkinson's disease, dopamine, substantia nigra, neurotoxin

| **16. SECURITY CLASSIFICATION OF:** | | | **17. LIMITATION OF ABSTRACT** | **18. NUMBER OF PAGES** | **19a. NAME OF RESPONSIBLE PERSON** |
|---|---|---|---|---|---|
| **a. REPORT** | **b. ABSTRACT** | **c. THIS PAGE** | | | USAMRMC |
| U | U | U | UU | 57 | **19b. TELEPHONE NUMBER** *(include area code)* |

## Table of Contents

**Introduction:**

Parkinson's disease (PD) is a widespread, disabling neurodegenerative disorder of unknown etiology. PD symptoms are triggered by the death of dopaminergic (DA) neurons of the substantia nigra (SNc). Why SNc DA neurons are preferentially lost in PD is unknown. Our working hypothesis when we started the project was that the selective vulnerability of SNc DA neurons was attributable to their reliance upon dendritic L-type (Cav1.3) calcium channels to drive autonomous pacemaking and resulting mitochondrial oxidant stress created by the burden of pumping calcium out of the cell. The studies proposed in this project were aimed at testing this hypothesis. As outlined below, these studies confirmed this hypothesis and identified a well-tolerated FDA approved drug that reduced calcium entry and vulnerability to toxins without compromising neuronal function. This drug (isradipine) is now moving into clinical neuroprotection trials for early stage PD.

**Our project had four specific aims:**

- *To compare the impact of calcium loading during autonomous pacemaking on mitochondrial function in vulnerable SNc DA neurons with relatively resistant VTA DA neurons;*

  **Progress:** After discovering that the usually employed means of assessing mitochondrial oxidant state were problematic in brain slices, we generated a transgenic mouse that expressed a mitochondrial matrix targeted, redox sensitive variant of GFP (mito-roGFP) under control of the tyrosine hydroxylase (TH) promotor (TH-mito-roGFP). Using tissue from these mice to conduct 2 photon laser scanning microscopy (2PLSM) and patch clamp experiments, we found that mitochondrial matrix oxidant stress was higher in SNc DA neurons than in neighboring VTA DA neurons and that this difference was attributable to calcium entry through L-type calcium channels. Moreover, we discovered that this oxidant stress engaged a largely unknown defense mechanism involving so-called 'uncoupling proteins' (UCPs); when activated by superoxide, this defense system induced transient depolarizations of the inner mitochondrial membrane that diminished oxidant stress. The transient opening of UCPs was manifested as a 'flickering' in mitochondrial membrane potential. This work was submitted to *Nature* and was favorably reviewed; it is now in revision and should be resubmitted by the first week of April.

- *To compare the impact of calcium loading during autonomous pacemaking on mitochondrial function in vulnerable SNc DA neurons from wild-type mice with mice harboring PD-related genetic deletions or mutations;*

  **Progress:** We have examined four genetic models of PD: LRRK2 knockouts, LRRK2 G2019S mutants, PINK1 knockouts and DJ-1 knockouts. There were no obvious deficits in pacemaking or calcium oscillations in any of the models. However, in the PINK1 and DJ-1 knockouts, there were abnormalities in the mitochondrial potential fluctuations that accompanied calcium entry during pacemaking (as described above). Our work on the DJ-1 knockout is closer to completion and will be summarized. In SNc DA neurons from these animals, mitochondrial oxidant stress was elevated compared to wild-type controls. This was determined by crossing DJ-1 knockout mice with our TH-mito-roGFP mice

and conducting 2PLSM experiments with brain slices. Surprisingly, in VTA neurons from knockout mice, oxidant stress was normal, suggesting that the impact of the DJ-1 deletion was only felt in neurons that were already experiencing oxidant stress. This helps to explain how a loss of function mutation in a widely expressed gene could have a preferential effect on SNc DA neurons. A clue about why oxidant stress was higher came from an examination of mitochondrial membrane potential fluctuations induced by UCPs; these were dramatically attenuated in amplitude and frequency. Profiling for UCPs known to be expressed in the SNc (UCP2, UCP4, UCP5) revealed a significant down-regulation in UCP4 and UCP5 expression in DJ-1 knockouts. Because DJ-1 is a redox sensitive transcriptional regulator, the most parsimonious interpretation of these results is that oxidant stress created by calcium entry stimulates DJ-1 transcriptional activity and up-regulates expression of UCP4 and UCP5, which enhance the ability of SNc DA neurons to reduce superoxide levels. These studies are included in the Nature submission.

- To determine the impact of synaptically evoked elevations in cytosolic calcium concentration on mitochondrial function in vulnerable SNc DA neurons;
  **Progress:** Because our pursuit of the first two aims was so successful, this aim has only begun to be addressed. To this end we have developed the capacity to uncage glutamate at somatic and dendritic locations using two photon laser light. This gives us much better spatial and temporal control over receptor stimulation. These studies have shown that activation of metabotropic glutamate receptors mobilize intracellular calcium and elevate mitochondrial oxidant stress. In addition, we have found that activation of NMDA receptors also elevates cytosolic calcium and increases mitochondrial oxidant stress transiently. These studies are the subject of a new grant proposal that has fundamental implications for the progression of PD.
- To determine whether the reliance upon Cav1.3 calcium channels renders SNc DA neurons more prone to neurodegenerative changes following exposure to mitochondrial toxins.
  **Progress:** This aim was approached in two models of PD: the MPTP and 6-OHDA model. To better mimic the slow onset of human disease, a chronic MPTP model was used in which mice were given two MPTP injections a week for five weeks. This regimen normally results in the loss of about half of all SNc DA neurons. Co-administration of isradipine systemically cut this loss in half and prevented mice from developing any behavioral symptoms (Chan et al., 2007). The 6-OHDA model we used involved intrastriatal injection of the toxin to mimic the initial loss of terminals thought to occur in PD. With large intrastriatal injections of 6-OHDA that produced greater than a 90% loss of SNc DA neurons, systemically administered isradipine had little effect on survival. However, if the amount of 6-OHDA injected was reduced to produce a 50-60% loss of SNc DA neurons in a few days, isradipine treatment had a significant effect, cutting the number of neurons lost in half (much like the situation with chronic MPTP treatment). Thus, with both toxin models antagonizing L-type channels led to protection. The next question we asked was whether it mattered how much isradipine was given. To answer this question, we varied the rate of isradipine

delivered by osmotic minipumps placed under the skin. Animals were given intrastriatal injections of 6-OHDA that normally produced the 50-60% percent cell loss. Ten days after this injection, animals were tested behaviorally and then sacrificed for histological analysis. We also took serum samples from mice to determine the amount of circulating isradipine as a measure of what was actually getting into the brain. These studies revealed something very important. If serum concentrations of isradipine were above 1 ng/ml, there was clear protection but not if values fell below this level. This is important because oral dosing of time-released isradipine in the middle of the FDA range (10 mg/day) achieves serum concentrations of 1-2 ng/ml in humans. This dose is very well tolerated in early stage PD patients and has no effect on blood pressure. This work is being prepared for publication now.

The other issue raised by these studies is what treatment with isradipine at these concentrations does to SNc DA neuron activity. The prevailing view had been that L-type channels were necessary for pacemaking and that pacemaking was essential to maintain striatal levels of dopamine needed for motor function. If serum concentrations of isradipine in the low nanomolar range was protective, it must be having a significant impact on calcium channel function. But in vitro experiments typically used concentrations of dihydropyridine that were orders of magnitude greater. Using calcium imaging and electrophysiological approaches we demonstrated two key points that were relevant to taking isradipine into the clinic or battlefield. First, L-type channels participate in pacemaking but are not necessary; in their absence, other channels take over for them. The confusion in the literature about their role was a consequence of using concentrations of the drug that were not selective and resulted in blockade of other channels that participated in pacemaking. This finding was recently published in the *Journal of Neuroscience*. Second, at low nanomolar concentrations of isradipine that were protective, roughly half of the Cav1.3 L-type channels appear to be effectively antagonized. This result is being included in a manuscript that has been submitted as part of a special basal ganglia edition of Brain Research Reviews.

**Key Research Accomplishments:**

- the discovery that calcium entry through L-type channels during normal pacemaking elevates the sensitivity of SNc dopaminergic neurons to toxins;
- the discovery that L-type calcium channels participate in but are not necessary for pacemaking;
- the discovery that serum concentration of the dihydropyridine isradipine required to achieve protection of SNc dopaminergic neurons against toxins in animal models is similar to that achieved in humans by FDA approved doses;
- the discovery that calcium entry through L-type channels during pacemaking elevates mitochondrial oxidant stress and leads to the engagement of a DJ-1-dependent oxidant defense system involving uncoupling proteins;

**Reportable Outcomes:**

Peer-reviewed manuscripts:

Chan, C.S., Guzman, J.N., Ilijic, E., Mercer, J.N., Rick, C., Tkatch, T.,

Meredith, G.E., and Surmeier, D.J. (2007). 'Rejuvenation' protects neurons in mouse models of Parkinson's disease. Nature 447, 1081-1086.
Surmeier, D.J. (2007). Calcium, ageing, and neuronal vulnerability in Parkinson's disease. Lancet Neurol *6*, 933-938.
Chan, C.S., Gertler, T.S., and Surmeier, D.J. (2009). Calcium homeostasis, selective vulnerability and Parkinson's disease. Trends Neurosci 32, 249-256.
Guzman, J.N., Sanchez-Padilla, J., Chan, C.S., and Surmeier, D.J. (2009). Robust pacemaking in substantia nigra dopaminergic neurons. J Neurosci 29, 11011-11019.
Guzman, J.N., Sanchez-Padilla, J., Wokosin, D., Kondapalli, J., Ilijic, E., Schumacker, P.T., and Surmeier, D.J. (2010). Mitochondrial oxidant stress arising from calcium entry during pacemaking in substantia nigra dopaminergic neurons is attenuated by DJ-1. Nature *in revision*.
Surmeier, D.J., Guzman, J.N., Sanchez-Padilla, J., and Goldberg, J.A. (2010). What causes the death of dopaminergic neurons in Parkinson's disease? Brain Res *(in press)*.
Surmeier, D.J., Guzman, J.N., Sanchez-Padilla, J., and Goldberg, J.A. (2010). The origins of oxidant stress in Parkinson's disease and therapeutic strategies. Free Radical Biology & Medicine *(in review)*.

*Seminars related to funded project:*

06/22/07: Marcus Wallenberg Foundation Symposium, Stockholm, Sweden; "Calcium, Neural Rejuvenation and Parkinson's Disease"
10/02/07: University of Chicago Committee on Computational Neuroscience Seminar Series, Chicago, IL; "Calcium, Neural Rejuvenation and Parkinson's Disease"
11/20/07: Neuroscience Seminar Series, University of Tennessee Health Science Center, Memphis, TN; "Calcium, Selective Vulnerability and Parkinson's Disease"
03/13/08: Case Western Reserve University, Cleveland, OH; "Calcium and Selective Vulnerability of Dopaminergic Neurons in Parkinson's Disease"
04/10/08: Emory University, Atlanta, GA; "Calcium and Selective Vulnerability of Dopaminergic Neurons in Parkinson's Disease"
04/14/08: Picower Foundation Parkinson's Disease Consortium, New York, NY
04/15/08: American Academy of Neuroscience Plenary Session, Chicago, IL; "Channels in Parkinson's Disease"
04/24/08: State University of New York at Stony Brook, Neurobiology of Disease Seminar, Stony Brook, NY "Calcium and Selective Vulnerability of Dopaminergic Neurons in Parkinson's Disease"
05/28/08: University of Salamanca, International Symposium on Novel Advances in Parkinson's Disease, Salamanca, Spain; "The Role of Calcium in Selective Vulnerability of Dopaminergic Neurons in Parkinson's Disease" 2
06/03/08: Netherlands Neuroscience Foundation, 6th Annual Endo-Neuro-Psycho meeting, Lund, Switzerland; "Calcium and Selective Vulnerability of Dopaminergic Neurons in Parkinson's Disease"

06/24/08: Movement Disorder Society's 12th International Congress of Parkinson's disease and Movement Disorders, Chicago, IL; "The Molecular Underpinning of the Selective Neuronal Vulnerability in Parkinson's Disease"
09/05/08: Society for General Physiologists 2008 Woods Hole Meeting, Providence, RI; "Calcium Signaling and Disease"
09/11/08: University of Alabama at Birmingham Retreat, Neurobiology Department, Birmingham, AL; presented Keynote talk during retreat. "Calcium and Selective Vulnerability of Dopaminergic Neurons in Parkinson's Disease"
09/15/08: Michael J. Fox Foundation 2008 Parkinson's Disease Therapeutics Conference, Chicago, IL; "Neuroprotective Effects of Isradipine in a Mouse Model of Parkinson's Disease"
09/18/08: Children's Memorial Research Center Seminar, Chicago, IL; "Calcium, Neurodegeneration and Parkinson's Disease"
12/13/08: NeuroFortis at Lund University, Lund, Switzerland; "Calcium and Selective Vulnerability of Dopaminergic Neurons in Parkinson's Disease"
03/24/09: German Physiological Society Symposium, Frankfurt/Giessen, Germany; "Sources and Sensors – Calcium Signaling at the Plasma Membrane and Parkinson's Disease"
04/21/09: University of Texas at San Antonio, San Antonio, TX; "Pacemaking without L-Type Calcium Channels in Dopaminergic Neurons"
05/20/09: Neurodegeneration Conference, Consiglio Nationale della Richerche and the Cell Death and Differentiation Association, Rome, Italy; "Calcium and Selective Vulnerability of Monoaminergic Neurons in Parkinson's Disease." Chair, "Mechanisms of Neurodegeneration."
09/17/09: Seattle Children's Research Institute, Center for Integrative Brain Research; Seminar series talk, "Calcium, Selective Vulnerability and Parkinson's disease: a new therapeutic approach"
11/03/09: London PD Calcium and Parkinson's Disease Conference, The Royal Society of Medicine, London, England; Co-chair, Session 1 - Calcium Channel Blockers and Vitamin D; Presenter, Session 2 - Calcium and Channel Blockers: "Calcium, mitochondria and selective neuronal vulnerability"; Presenter, Session 3 – Translation from Epidemiology and Electrophysiology into Clinical Practice: "The clinical trial with Isradipine in early-stage Parkinson's disease patients"
11/15/09: Harvard University, Harvard NeuroDiscovery Center Symposium; Symposium talk, "Calcium channels, mitochondrial oxidative stress and Parkinson's disease"
11/19/09: 16th Annual Symposium on CA2+- Binding Proteins and CA2+ Function in Health and Disease, Pucón, Chile; Presenter, Session 8 – Calcium and Disease, "Calcium channels, mitochondrial oxidative stress and Parkinson's disease"
12/10/09: University of Miami, Neuroscience Center Seminar Series; Presenter, "Calcium, selective neurodegeneration and protection in Parkinson's disease"

*Grants/Contracts:*
Michael J. Fox Foundation Clinical Trial 11/30/08-11/29/11
Tatyana Simuni (PI)
"A Pilot Phase II Double-Blind, Placebo-Controlled, Dosage Finding and Tolerability Study of Isradipine as a Disease Modifying Agent in Patients with Early Parkinson's Disease"

**Conclusion:**

These studies have provided fundamental insights into the mechanisms underlying the preferential vulnerability of SNc DA neurons in PD. They demonstrate that the engagement of L-type calcium channels during pacemaking elevates cytosolic calcium concentration and creates a metabolic burden on mitochondria. This metabolic burden elevates mitochondrial oxidant stress. Oxidant stress is firmly tied to increased rates of mitochondrial DNA mutation, diminished capacity to maintain normal energy balance and greater propensity for death or degeneration. Moreover, our results show that the calcium entry through these L-type channels can be significantly diminished with an FDA approved drug, known to be very safe in humans; the concentrations of this drug that were protective in two models of PD can be achieved in humans with few or any side-effects. Clinical trials funded by the MJFF are now underway to better define tolerated doses of isradipine in early stage PD patients, laying the foundation for a larger, clinical neuroprotection trial.

There are several questions that remain to be answered. Perhaps the most important of these to understanding the mechanisms underlying the loss of SNc DA neurons in PD is whether the metabolic stress created by glutamatergic synaptic input synergizes with that created by pacemaking to further accelerate neurodegeneration in the later stages of the disease. Recent studies showing that partial lesioning of SNc DA neurons leads to an elevation in extracellular glutamate concentrations in the SNc suggests that sustained activation of glutamate receptors, particularly NMDA and metabotropic receptors, could be a significant factor in accelerating cell loss. A proposal to pursue this question is being prepared.

**References:**


Chan, C.S., Guzman, J.N., Ilijic, E., Mercer, J.N., Rick, C., Tkatch, T., Meredith, G.E., and Surmeier, D.J. (2007). 'Rejuvenation' protects neurons in mouse models of Parkinson's disease. Nature 447, 1081-1086.

Surmeier, D.J. (2007). Calcium, ageing, and neuronal vulnerability in Parkinson's disease. Lancet Neurol *6*, 933-938.

Chan, C.S., Gertler, T.S., and Surmeier, D.J. (2009). Calcium homeostasis, selective vulnerability and Parkinson's disease. Trends Neurosci 32, 249-256.

Guzman, J.N., Sanchez-Padilla, J., Chan, C.S., and Surmeier, D.J. (2009). Robust pacemaking in substantia nigra dopaminergic neurons. J Neurosci 29, 11011-11019.

Guzman, J.N., Sanchez-Padilla, J., Wokosin, D., Kondapalli, J., Ilijic, E., Schumacker, P.T., and Surmeier, D.J. (2010). Mitochondrial oxidant stress

arising from calcium entry during pacemaking in substantia nigra dopaminergic neurons is attenuated by DJ-1. Nature *in revision*.

Surmeier, D.J., Guzman, J.N., Sanchez-Padilla, J., and Goldberg, J.A. (2010). What causes the death of dopaminergic neurons in Parkinson's disease? Brain Res *(in press)*.

Surmeier, D.J., Guzman, J.N., Sanchez-Padilla, J., and Goldberg, J.A. (2010). The origins of oxidant stress in Parkinson's disease and therapeutic strategies. Free Radical Biology & Medicine *(in review)*.

**Appendices (papers published or submitted):**

Chan et al. (2009) pdf attached
Guzman et al., (2009) pdf attached
Guzman et al., (2010 in revision) pdf attached
Surmeier et al. (2010) pdf attached

Review

# Calcium homeostasis, selective vulnerability and Parkinson's disease

C. Savio Chan*, Tracy S. Gertler* and D. James Surmeier

Department of Physiology, Feinberg School of Medicine, Northwestern University, Chicago, IL 60611, USA

**Parkinson's disease (PD) is a common neurodegenerative disorder of which the core motor symptoms are attributable to the degeneration of dopamine (DA) neurons in the substantia nigra pars compacta (SNc). Recent work has revealed that the engagement of L-type $Ca^{2+}$ channels during autonomous pacemaking renders SNc DA neurons susceptible to mitochondrial toxins used to create animal models of PD, indicating that homeostatic $Ca^{2+}$ stress could be a determinant of their selective vulnerability. This view is buttressed by the central role of mitochondria and the endoplasmic reticulum (linchpins of current theories about the origins of PD) in $Ca^{2+}$ homeostasis. Here, we summarize this evidence and suggest the dual roles had by these organelles could compromise their function, leading to accelerated aging of SNc DA neurons, particularly in the face of genetic or environmental stress. We conclude with a discussion of potential therapeutic strategies for slowing the progression of PD.**

## Introduction

Parkinson's disease (PD) is a disabling neurodegenerative disorder that is strongly associated with aging, increasing exponentially in incidence above the age of 65 [1,2]. The incidence of PD is expected to rise dramatically worldwide in the next 25 years with the extension of life expectancy by improved health care [3]. Although there are signs of distributed neuropathology, as judged by Lewy body (LB) formation, the motor symptoms of PD, including bradykinesia, rigidity and resting tremor, are clearly linked to the degeneration and death of substantia nigra pars compacta (SNc) dopamine (DA) neurons [4,5]. The efficacy of the clinical gold-standard treatment of L-DOPA (3,4-dihydroxy-L-phenylalanine; a DA precursor) is testament to the centrality of these neurons in PD. Here, we examine the evidence that the selective vulnerability of these neurons is attributable to their expression of a physiological phenotype that creates a sustained challenge to $Ca^{2+}$ homeostasis.

## What causes SNc DA neurons to die in PD?

The mechanisms responsible for the preferential loss of DA neurons in PD have been debated for decades. A widely held theory implicates DA itself, suggesting that oxidation of cytosolic DA (and its metabolites) leads to the production of cytotoxic free radicals [6]. However, there are reasons to doubt this type of cellular stress is responsible for either normal aging or the loss of DA neurons in PD. For example, there is considerable regional variability in the vulnerability of DA neurons in PD, with some being devoid of pathological markers [7–11]. Moreover, L-DOPA administration (which relieves symptoms by elevating DA levels in PD patients) does not accelerate disease progression [12], indicating that DA is not a substantial source of reactive oxidative stress.

In recent years, attention has turned to the role of mitochondrial dysfunction in PD [13–15]. In addition to the ability of several toxins that target mitochondria to create a parkinsonian phenotype [16,17], compelling evidence for mitochondrial involvement in PD comes from the study of human PD patients. In postmortem tissue samples of the SNc from sporadic PD patients, there is a substantial decrease in the activity of mitochondrial NADH ubiquinone reductase, referred to as complex I of the electron transport chain (ETC) [18]; this deficit is specific to PD patients [19] and seems to reflect oxidative damage to complex I [20]. Oxidative damage to other cellular components such as lipids, proteins and DNA also has been found in the SNc of PD brains [21]. The source of this oxidative stress is largely mitochondrial: reactive oxygen species (ROS) and other radicals are generated by inefficiencies in the ETC; the ETC is responsible for creating the electrochemical gradient across the inner mitochondrial membrane that drives ATP synthase and the conversion of adenosine diphosphate to ATP [22]. ROS also are thought to be responsible for the high level of somatic DNA mutations in SNc DA neurons [23]. The physical proximity of mitochondrial DNA (mtDNA) to the site of ROS generation probably makes them an even more vulnerable target. The mitochondrial genome encodes 13 proteins involved in the mitochondria respiratory chain, 7 of which are involved in the formation of complex I [13]. The number of mtDNA mutations present in clonally expanded clusters of SNc mitochondria is positively correlated with age and negatively correlated with cytochrome oxidase activity (a marker for functional respiratory activity) [24]. Their clonal nature argues that these mutations are due to the expansion of a somatic mutation, not a genetic mutation present at birth. Because many of these mtDNA mutations impair ETC function [25], they are likely to contribute to the loss of SNc DA neurons. Lastly, although deficits in the complex I activity of platelets, skeletal muscle, fibroblasts and lymphocytes have been reported in some PD patients [26], this is not a consistent feature of the disease, arguing that mitochondrial dysfunction is regionally selective [27].

*Corresponding author:* Surmeier, D.J. (j-surmeier@northwestern.edu)
* These authors contributed equally..

0166-2236/$ – see front matter  doi:10.1016/j.tins.2009.01.006 Available online 21 March 2009

**Box 1. Genetic PD mutations and mitochondria**

Several of the genetic mutations associated with familial PD are directly linked to mitochondrial dysfunction. DJ-1 (*PARK7*), a genetic mutation associated with early-onset PD, has been putatively categorized as an atypical mitochondrial 'peroxiredoxin-like peroxidase', decreasing the accumulation of hydrogen peroxide and, thus, damage from downstream ROS production [106]. Parkin (*PARK2*) is a ubiquitin ligase tied to mitochondrial function in knockout studies in both mice and Drosophila. Fruit flies with functional deletions of Parkin posses fragmented and apoptotic mitochondria with compromised structural integrity [107]; knockout mice have a less dramatic but noteworthy syndromic phenotype (including decreased mitochondrial [respiratory] function, decreased metabolic drive and increased lipid and protein phosphorylation), indicative of functional mitochondrial impairment [108]. Phosphatase and tensin homolog (PTEN)-induced putative kinase 1 (PINK1; *PARK6*), which also is associated with familial PD, leads to an identical phenotype in Drosophila loss-of-function mutants as does Parkin: fragmented cristae and apoptotic mitochondria; this phenotype can be rescued by Parkin overexpression, indicating involvement in some common biochemical pathway [109,110]. Although found both in cytosolic and mitochondrial preparations, PINK1 has an N-terminus mitochondrial targeting sequence [111]. Mutations of leucine-rich repeat kinase (LRRK2; *PARK8*) are associated with a much larger fraction of PD cases in some ethnic groups [112]; LRRK2 is largely cytosolic but a fraction of the protein is associated with mitochondria [113].

Further support for a mitochondrial link in PD comes from the rapidly expanding literature on genetic mutations associated with familial forms of PD [28]. Although much remains to be done in defining the roles of the proteins coded for by these genes, an extraordinary number of them are localized in or interact with mitochondria (Box 1).

Another organelle that has been widely linked to pathogenesis in PD is the endoplasmic reticulum (ER). The ER is an integral component of the cellular machinery responsible for the production, delivery and degradation of proteins, a process referred to as proteostasis [29]. One of the hallmarks of PD is the formation of LBs, an abnormal protein aggregate found in SNc DA neurons and elsewhere in the brain [30]. These depositions reflect a deficiency in proteostasis that is accompanied by signs of ER stress and an attempt to sequester cytotoxic proteins [31]. In part, LBs in PD reflect the decline in proteostatic competence that accompanies normal aging [29]. What seems to distinguish PD is the presence of an additional proteostatic burden that causes an aged DA neuronal ensemble to fail *en masse* (see later) [15,32,33].

Taken together, the evidence for the involvement of mitochondria and ER in the PD pathogenesis is unequivocal. The crucial question is whether or not the disease begins with the dysfunction of these organelles. The striking regional distribution of deficits argues against the primacy of mitochondrial or ER dysfunction in PD. There is no evidence that mitochondria in cortical pyramidal neurons (which show little to no sign of pathology in PD) differ in any important respect from mitochondria in SNc DA neurons. There is no evidence for substantive variation in the ER (or other proteostatic elements) between vulnerable and resistant neurons either. Furthermore, there is no evidence of selective regional expression of genes associated with familial forms of PD that would be predictive of disease progression [28]. The most straightforward conclusion to be drawn from the evidence at hand is that the cellular environment in which these organelles find themselves accelerates their decline with age, making them more vulnerable to genetic or environmental stress. What then is distinctive about the organelle environment created by SNc DA neurons?

## SNc DA neurons have a distinctive physiological phenotype

SNc DA neurons have an unusual physiological phenotype. Unlike the vast majority of neurons in the brain, adult SNc DA neurons are autonomously active, generating action potentials in a clock-like (2–4 Hz) manner in the absence of synaptic input [34]. This pacemaking activity is believed to be important in maintaining ambient DA levels in regions that are innervated by these neurons, particularly the striatum [35]. Whereas most neurons rely on monovalent cation channels to drive pacemaking, SNc DA neurons also engage ion channels that enable $Ca^{2+}$ to enter the cytoplasm [36–38], leading to elevated intracellular $Ca^{2+}$ concentrations [39,40]. The L-type $Ca^{2+}$ channels used by SNc DA neurons in pacemaking have a distinctive $Ca_v1.3$ pore-forming subunit encoded by *Cacna1d* [40,41]; channels with this subunit differ from other L-type $Ca^{2+}$ channels in that they open at relatively hyperpolarized potentials, enabling them to help push the cell to spike threshold [38,40]. $Ca_v1.3$ $Ca^{2+}$ channels are relatively rare, constituting only ~10% of the all the L-type $Ca^{2+}$ channels found in the brain [42]. Not only are they rare but in many of the other neurons where they are found they have a different role than the one in SNc DA neurons; for example, in striatal medium spiny neurons, $Ca_v1.3$ $Ca^{2+}$ channels are positioned near to synapses where they are only activated episodically in response to synaptic depolarization or dendritic action potentials [43].

The sustained engagement of $Ca_v1.3$ $Ca^{2+}$ channels during pacemaking comes at an obvious metabolic cost to SNc DA neurons. Because of its involvement in cellular processes ranging from the regulation of enzyme activity to programmed cell death, $Ca^{2+}$ is under very tight homeostatic control, with a cytosolic set point near to 100 nM; that is 10 000 times lower than the concentration of $Ca^{2+}$ in the extracellular space [44–46]. $Ca^{2+}$ entering neurons is rapidly sequestered or pumped back across the steep plasma membrane concentration gradient; this process requires energy stored in ATP or in ion gradients that are maintained with ATP-dependent pumps (Figure 1). In most neurons, $Ca^{2+}$ channel opening is a rare event, occurring primarily during very brief action potentials. This makes the task and the metabolic cost to the cell readily manageable. But in SNc DA neurons, where $Ca_v1.3$ $Ca^{2+}$ channels are open much of the time, the magnitude and the spatial extent of $Ca^{2+}$ influx is much larger [39]. The two organelles most responsible for handling $Ca^{2+}$ crossing the plasma membrane are the two organelles most closely linked to PD: the ER and the mitochondrion.

## The ER and mitochondria partner in $Ca^{2+}$ homeostasis

The ER sits squarely at the center of the machinery responsible for $Ca^{2+}$ homeostasis [47]. The ER forms a

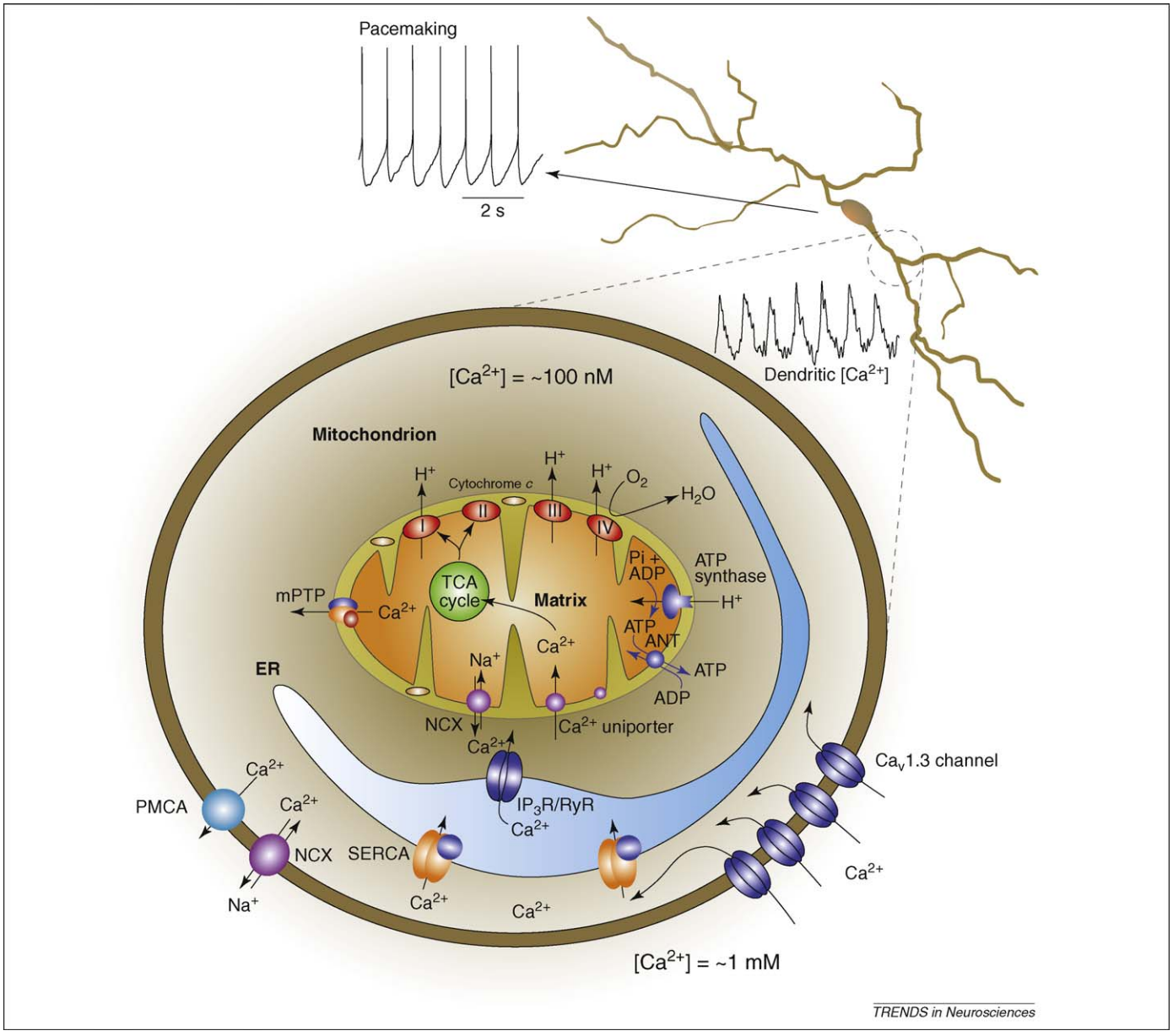


**Figure 1**. $Ca^{2+}$ transport in SNc DA neurons. The steep concentration gradient for $Ca^{2+}$ enables it to cross the plasma membrane readily into cells through open pores such as L-type $Ca^{2+}$ channels. Once inside neurons, it is either transported back across the plasma membrane or sequestered in intracellular organelles. $Ca^{2+}$ is transported across the plasma membrane through either the $Ca^{2+}$-ATPase (PMCA) or through a $Na^+/Ca^{2+}$ exchanger (NCX) that relies upon the $Na^+$ gradient. $Ca^{2+}$ is rapidly sequestered either by ionic interactions with buffering proteins or by transport into cytosolic organelles (i.e. the mitochondria and the ER). The ER uses high-affinity smooth ER $Ca^{2+}$ (SERCA) pumps that depend upon ATP to take $Ca^{2+}$ from the cytoplasm into the ER lumen. $Ca^{2+}$ flows back into the cytoplasm after the opening of inositol trisphosphate receptors ($IP_3R$) and ryanodine receptors (RyR) studding the ER membrane. Mitochondria are often found in close apposition to the ER and plasma membrane, creating a region of high (but localized) $Ca^{2+}$ concentration that drives $Ca^{2+}$ into the matrix of mitochondria through a $Ca^{2+}$ uniporter. $Ca^{2+}$ can leave the mitochondrion through a number of mechanisms. The dominant mitochondrial $Ca^{2+}$-efflux path in neurons is through mitochondrial NCXs. $Ca^{2+}$ release through higher conductance ion channels, such as the mitochondrial permeability transition pore (mPTP), has also been proposed. The mPTP is posited to have two conductance states: a low-conductance state that is reversible and participates in physiological $Ca^{2+}$ handling, and a high-conductance state that is irreversible and leads to mitochondrial swelling and loss of molecules such as cytochrome *c* that trigger apoptosis (Figure 2). Also shown schematically are elements of the tricarboxylic acid (TCA) cycle that produces reducing equivalents for the electron transport chain; complexes I–IV are shown in red. The electrochemical gradient created drives ATP synthase and the conversion of ATP from adenosine diphosphate (ADP) delivered to the matrix by the adenine nucleotide translocator (ANT).

continuous, intracellular network, enabling it to regulate both local and global $Ca^{2+}$ signals. As in other neurons, the ER network in SNc DA neurons extends throughout the somatodendritic tree [48,49]. High-affinity ATP-dependent transporters move $Ca^{2+}$ from the cytoplasm into the ER lumen. The absence of high-affinity, anchored intraluminal $Ca^{2+}$ buffers and the physical continuity of the lumen within the cell [50,51] enables the ER to rapidly (~30 μm/s) redistribute $Ca^{2+}$ between intracellular compartments, thus avoiding pro-apoptotic accumulations in the cytosol [49]. $Ca^{2+}$ sequestered in the ER is released at sites where it can be pumped back across the plasma membrane or where it can be used to modulate cellular function [52–56]. However, the storage capacity of the ER is limited. BCL-2 family proteins, which are implicated in apoptosis, control the ER $Ca^{2+}$ concentration and are capable of adjusting it in response to stress [57]. Movement away from this set point can compromise proteostasis. In

part, this is a consequence of the fact that $Ca^{2+}$ is an allosteric regulator of protein processing and folding [58,59]. Depleting ER $Ca^{2+}$ stores induces ER stress and the unfolded protein response [58,59]. Conversely, proteostatic deficits in Alzheimer's disease have been associated with high ER $Ca^{2+}$ concentrations and large changes in cytosolic $Ca^{2+}$ concentration upon ER release [60], mirroring what has been found in wild-type SNc DA neurons [61].

$Ca^{2+}$ released from the ER through inositol trisphosphate ($IP_3$) or ryanodine receptors can enter mitochondria at points of apposition between the organelles which form functional $Ca^{2+}$ microdomains [62,63]. The steep potential gradient (~−200 mV) across the inner mitochondrial membrane drives $Ca^{2+}$ into the matrix through a pore called the $Ca^{2+}$ uniporter [64]. This ER–mitochondrial system not only serves a role in $Ca^{2+}$ buffering but also increases ATP production by stimulating enzymes of the tricarboxylic acid (TCA) cycle [65], helping to meet the metabolic demands associated with electrical activity and influx of $Ca^{2+}$. However, it is possible that, despite this normally stimulatory role, the large $Ca^{2+}$-buffering burden created by pacemaking in SNc DA neurons ultimately compromises mitochondrial ATP synthesis. In isolated brain mitochondria, elevating the $Ca^{2+}$ concentration in the media induces a transient collapse of the matrix potential, reflecting the reversible opening of an inner membrane pore in response to the rise in matrix $Ca^{2+}$ concentration [66]; elevating the concentration of $Ca^{2+}$ further induces an irreversible mitochondrial depolarization attributable to the opening of the mitochondrial permeability transition pore (mPTP) [22]. During these transient periods of depolarization there is no electrochemical gradient to power ATP synthase, and ATP production halts [22]. Unpublished studies by our group have revealed that mitochondrial potential in SNc DA neurons oscillates during normal pacemaking, much like that of isolated mitochondria challenged by $Ca^{2+}$, indicating that mitochondrial ATP production is compromised by elevations in cytosolic $Ca^{2+}$ concentration during pacemaking.

Judging by aging-related changes in phenotypic markers [67], the stress created by playing two roles seems to be inconsequential for either the ER or mitochondria in most neurons. However, it is not clear that this is true for SNc DA neurons. As outlined earlier, elevated intraluminal ER $Ca^{2+}$ concentration could compromise the ability of the ER to properly fold and process proteins (Figure 2). Passing this $Ca^{2+}$ on to mitochondria could compromise their ability to generate ATP, despite the concomitant increased demand for ATP posed by the need to move $Ca^{2+}$ out of the cell. Attempts to meet this demand by accelerating ETC activity between periods of depolarization brought on by $Ca^{2+}$ buffering might overwhelm oxidative defenses, leading to the escape of damaging ROS.

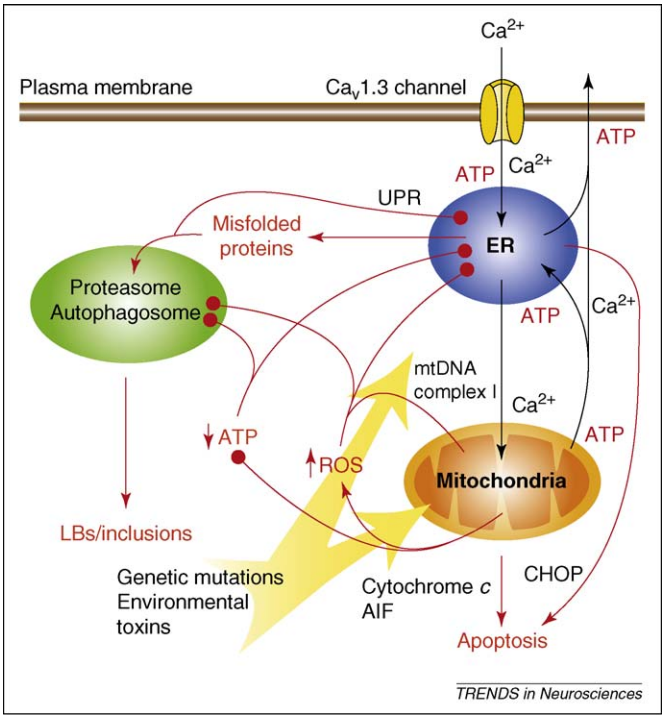


**Figure 2**. The role played by the ER and mitochondria in $Ca^{2+}$ homeostasis could contribute to Lewy body (LB) formation and premature death of SNc DA neurons. $Ca^{2+}$ entry through plasma membrane $Ca_v1.3$ $Ca^{2+}$ channels during activity is either pumped back across the plasma membrane or rapidly sequestered in the ER or mitochondria (Figure 1). Both processes require energy stored in the form of ATP (red 'ATP' labels denote ATP requirement). The metabolic demand created by these ATP-dependent steps in $Ca^{2+}$ homeostasis should increase oxidative phosphorylation in mitochondria and the production of damaging ROS. ROS damage mitochondrial proteins such as complex I and mtDNA, reducing the efficiency of oxidative phosphorylation (negative consequences are symbolized by red circles; positive or augmenting consequences are symbolized by red arrows). In extreme cases, the stress on mitochondria induces mPTP opening, swelling and the release of cytochrome *c* and other pro-apoptotic proteins such as apoptosis-inducing factor (AIF). In parallel, ROS are capable of damaging ER proteins, elevating the concentration of misfolded proteins that need to be degraded by proteasomes and autophagosomes. The unfolded protein response (UPR) triggered by this elevation in misfolded proteins should further reduce ER production of proteins and potentially lead to the release of pro-apoptotic factors such as C/EBP homologous protein (CHOP). The role of mitochondria in $Ca^{2+}$ homeostasis could further compromise their ability to generate ATP, leading to a functionally important drop in cytosolic ATP levels. Such a drop would compromise both ER and proteasome and autophagosome function, also promoting the formation of protein aggregates such as LBs. Genetic mutations (Box 1) or environmental toxins such as rotenone could further compromise mitochondrial or ER function, rendering them more vulnerable to $Ca^{2+}$-induced stress. By hastening the decline in ER and mitochondrial function and the accelerated loss of SNc DA neurons, these genetic and environmental factors could be seen as 'causing' PD.

## Is PD a manifestation of $Ca^{2+}$-accelerated aging?

One of the oldest and most popular theories of aging is that it is a direct consequence of accumulated mtDNA and organelle damage produced by ROS and related reactive molecules generated by the ETC in the course of oxidative phosphorylation [68,69]. A corollary of this hypothesis is that the rate of aging is directly related to metabolic rate. There is no obvious reason not to extend this organismal postulate to individual cells. The reliance of SNc DA neurons on a metabolically expensive strategy to generate autonomous activity that taxes mitochondria should mean that they age more rapidly than other types of neuron. The added homeostatic weight on mitochondria and the ER by $Ca^{2+}$ should exacerbate this metabolic stress.

Is PD simply a reflection of accelerated aging in neurons that rely too heavily upon $Ca^{2+}$ channels to do their business? Age is undoubtedly the single strongest risk factor for PD [70,71]. Stereological estimates of normal aging-related cell death in humans argue that SNc DA neurons are at a higher risk than other neurons in the absence of disease, because they are lost at a higher rate (5–10% per decade), than many other types of neurons

(some of which show no appreciable loss over a 6–7 decade span) [67]. In mammals with substantially shorter lifespans, loss of SNc DA neurons with age has not been seen reliably, but there is a clear decline in phenotypic markers with age and an increased susceptibility to toxins, arguing that they are on the same road traversed by human neurons [72–74]. Furthermore, the spatial pattern of the decline in phenotypic markers with age matches that seen in PD [75–77], arguing that they are closely related phenomena.

This 'wear and tear' theory of PD does not require a pathogenic agent. Moreover, it argues that there is no disease 'onset' other than the one created by the emergence of symptoms when the surviving SNc DA neurons are incapable of fully compensating for the loss of neighboring neurons [78]. It also predicts that we will all develop symptoms if we live long enough. Why then do some people become symptomatic in their 50 s, others in their 60 s or 70 s or not at all? Genetic and environmental factors certainly could account for this variation [28,70,79]. These factors could increase (or decrease) the rate at which vulnerable neurons age by compromising (or enhancing) ER or mitochondrial function. Furthermore, because the rate of cell loss should increase with accumulated age-dependent organelle damage, it is entirely possible that at some point an inflammatory threshold is crossed, triggering microglia activation and further neuron loss [80].

Can the $Ca^{2+}$-mediated cellular aging hypothesis account for the vulnerability of other cell types in PD? Certainly it is consistent with the diminished vulnerability of SNc DA neurons that express the $Ca^{2+}$-binding protein calbindin [81,82]. Other regions of the brain that have cell loss paralleling that of the SNc are the locus ceruleus (LC) and hypothalamic tuberomamillary nucleus [30,83]. The neurons of the LC and the tuberomamillary neurons are similar to SNc DA neurons in several respects. Like SNc DA neurons, both LC and tuberomamillary neurons are autonomous pacemakers that depend upon L-type $Ca^{2+}$ channels [84–86]. In contrast, DA neurons in the ventral tegmental area do not rely upon L-type $Ca^{2+}$ channels for pacemaking and are relatively intact in PD patients and in animal models of PD [9,40,81,87,88]. DA neurons in the olfactory bulb also are autonomous pacemakers and rely upon $Ca^{2+}$ channels (although not L-type channels) [88]. Olfactory deficits have been associated with PD [89]; however, there is no obvious loss of olfactory bulb DA neurons [90]. Although this would seem to run counter to the $Ca^{2+}$ hypothesis, this could simply be a consequence of the capacity of this region for adult neurogenesis [91].

## Can PD be prevented?

If PD is a consequence of $Ca^{2+}$-accelerated aging in SNc DA neurons (and in those neurons with a similar phenotype) then reducing $Ca^{2+}$ flux should delay the onset of PD symptoms and slow its progression. This might be possible with orally deliverable, dihydropyridine (DHP) L-type channel antagonists shown to be safe in humans [40]. Adult SNc DA neurons readily compensate for the antagonism of L-type $Ca_v1.3$ $Ca^{2+}$ channels and continue pacemaking at a normal rate. More importantly, although the impact on mitochondrial and ER stress can only be inferred at this point, reducing $Ca^{2+}$ influx during pacemaking dramatically diminishes the sensitivity of SNc DA neurons to toxins used to generate animal models of PD [40]. Furthermore, at neuroprotective doses of an L-type channel antagonist, mice have no obvious motor, learning or cognitive deficits, indicating that the patterned activity of SNc DA neurons is functionally unchanged [36,92].

Is there evidence that this strategy might work in humans to prevent or slow PD? Calcium channel antagonists (CCAs), including the DHPs used in animal studies, are commonly used in clinical practice, creating a potential database to be mined. A recent case-control study of hypertensive patients found a significant reduction in the observed risk of PD with CCA use, but not with medications that reduce blood pressure in other ways [93]. This finding is consistent with a retrospective examination of patients treated for hypertension with DHPs [94]. Given that many of the CCAs currently in use for hypertension are weak antagonists of $Ca_v1.3$ $Ca^{2+}$ channels or have low lipophilicity and are unlikely to cross the blood–brain barrier effectively [95–97], the apparent neuroprotective effect of CCAs as a group indicates that those drugs overcoming these obstacles might be very potent neuroprotective agents.

That said, these studies are not a substitute for a controlled clinical trial. In the absence of a selective $Ca_v1.3$ $Ca^{2+}$ channel antagonist, DHPs are the most attractive drug for such a trial. DHPs are more selective modulators of L-type channels than other CCAs approved for human use and many have good brain bioavailability [95]. However, most members of this drug class, including nimodipine (Nimotop) and nifedipine (Procardia, Adalat), are more potent negative modulators of $Ca_v1.2$ than $Ca_v1.3$ channels [98]. This is also true of isradipine (DynaCirc), but less so [99,100]. At the doses used to treat hypertension, isradipine has relatively minor side effects [101]. The question is whether it will prove neuroprotective at doses tolerated by the general population. Pharmacokinetic studies by our group have found that serum concentrations of isradipine achieved in mice that are protected ($\sim$2 ng/ml) against 1-methyl-4-phenyl-1,2,3,6-tetrahydropyridine and 6-hydroxydopamine toxicity are very close to those achieved in humans with a very well tolerated daily dose (10 mg/day, isradipine), indicating that neuroprotection is achievable.

It is also worth considering how CCAs compare with other drugs that are being tested in clinical neuroprotection trials for PD. Although early trials with creatine, coenzyme Q10 and other antioxidant supplements have been disappointing [102], they share the hypothesis that oxidative stress exacerbates the symptoms and progression of PD. Coenzyme Q10 is an electron acceptor for complexes I and II that seems to be compromised in PD patients [103] and is neuroprotective in animal models of PD [104]. Creatine is a substrate for ATP production that can both improve mitochondrial efficiency and reduce oxidative stress by buffering fluctuations in cellular energy production [105]. Both approaches are aimed at improving mitochondrial function rather than attacking the source of stress on mitochondria. This contrasts with the rationale for CCAs, in which the goal is to reduce the source of stress

responsible for mitochondrial and ER dysfunction. Nevertheless, the two approaches could prove complementary, pointing to a combination therapy.

## Conclusions

$Ca^{2+}$ dyshomeostasis has long been thought to be important in neurodegeneration, but it usually is envisioned as a late stage consequence of organelle damage inflicted by some other challenge. The unusual reliance of SNc DA neurons on voltage-dependent L-type $Ca^{2+}$ channels in autonomous pacemaking indicates that $Ca^{2+}$ entry and dyshomeostasis could be a cause of their selective vulnerability rather than simply a late stage consequence. This hypothesis is consistent with the centrality of the ER and mitochondria (which are key organelles in $Ca^{2+}$ homeostasis) in prevailing models of pathogenesis in PD. The additional stress placed upon these organelles by the demands associated with sustained $Ca^{2+}$ entry could accelerate their aging and enhance the vulnerability of SNc DA neurons to genetic and environmental challenges. Although plausible and consistent with regional deficits seen in normal aging and PD, the proposition that $Ca^{2+}$ entry during pacemaking compromises mitochondrial and ER function remains to be fully tested. The tools necessary to conduct this test are now becoming available. Nevertheless, given the plausibility of the link between $Ca^{2+}$ and the loss of SNc DA neurons, the absence of any proven neuroprotective therapy in PD and the availability of $Ca^{2+}$ channel antagonists that are well tolerated and approved for human use, it would seem that the human experiment should proceed now in the form of clinical neuroprotection trials.

### Acknowledgements

This work was supported by grants from the Hartman Foundation (www.hartmanfoundation.org), US Army Medical Research and Material Command and National Institutes of Health (www.nih.gov; NS047085).

### References

1 de Lau, L.M. *et al.* (2004) Incidence of parkinsonism and Parkinson disease in a general population: the Rotterdam Study. *Neurology* 63, 1240–1244
2 de Rijk, M.C. *et al.* (1997) Prevalence of parkinsonism and Parkinson's disease in Europe: the EUROPARKINSON Collaborative Study. European Community Concerted Action on the Epidemiology of Parkinson's disease. *J. Neurol. Neurosurg. Psychiatry* 62, 10–15
3 Dorsey, E.R. *et al.* (2007) Projected number of people with Parkinson disease in the most populous nations, 2005 through 2030. *Neurology* 68, 384–386
4 Hornykiewicz, O. (1966) Dopamine (3-hydroxytyramine) and brain function. *Pharmacol. Rev.* 18, 925–964
5 Riederer, P. and Wuketich, S. (1976) Time course of nigrostriatal degeneration in parkinson's disease. A detailed study of influential factors in human brain amine analysis. *J. Neural Transm.* 38, 277–301
6 Greenamyre, J.T. and Hastings, T.G. (2004) Biomedicine. Parkinson's – divergent causes, convergent mechanisms. *Science* 304, 1120–1122
7 Damier, P. *et al.* (1999) The substantia nigra of the human brain. II. Patterns of loss of dopamine-containing neurons in Parkinson's disease. *Brain* 122, 1437–1448
8 Ito, H. *et al.* (1992) Calbindin-D28k in the basal ganglia of patients with parkinsonism. *Ann. Neurol.* 32, 543–550
9 Kish, S.J. *et al.* (1988) Uneven pattern of dopamine loss in the striatum of patients with idiopathic Parkinson's disease. Pathophysiologic and clinical implications. *N. Engl. J. Med.* 318, 876–880
10 Matzuk, M.M. and Saper, C.B. (1985) Preservation of hypothalamic dopaminergic neurons in Parkinson's disease. *Ann. Neurol.* 18, 552–555
11 Saper, C.B. *et al.* (1991) Medullary catecholaminergic neurons in the normal human brain and in Parkinson's disease. *Ann. Neurol.* 29, 577–584
12 Fahn, S. (2005) Does levodopa slow or hasten the rate of progression of Parkinson's disease? *J. Neurol.* 252 (Suppl. 4), IV37–IV42
13 Schapira, A.H. (2008) Mitochondria in the aetiology and pathogenesis of Parkinson's disease. *Lancet Neurol.* 7, 97–109
14 Vila, M. *et al.* (2008) Mitochondrial alterations in Parkinson's disease: new clues. *J. Neurochem.* 107, 317–328
15 Henchcliffe, C. and Beal, M.F. (2008) Mitochondrial biology and oxidative stress in Parkinson disease pathogenesis. *Nat. Clin. Pract. Neurol.* 4, 600–609
16 Przedborski, S. *et al.* (2004) MPTP as a mitochondrial neurotoxic model of Parkinson's disease. *J. Bioenerg. Biomembr.* 36, 375–379
17 Betarbet, R. *et al.* (2000) Chronic systemic pesticide exposure reproduces features of Parkinson's disease. *Nat. Neurosci.* 3, 1301–1306
18 Mann, V.M. *et al.* (1994) Complex I, iron, and ferritin in Parkinson's disease substantia nigra. *Ann. Neurol.* 36, 876–881
19 Gu, M. *et al.* (1997) Mitochondrial respiratory chain function in multiple system atrophy. *Mov. Disord.* 12, 418–422
20 Keeney, P.M. *et al.* (2006) Parkinson's disease brain mitochondrial complex I has oxidatively damaged subunits and is functionally impaired and misassembled. *J. Neurosci.* 26, 5256–5264
21 Zhang, J. *et al.* (1999) Parkinson's disease is associated with oxidative damage to cytoplasmic DNA and RNA in substantia nigra neurons. *Am. J. Pathol.* 154, 1423–1429
22 Nicholls, D.G. and Ferguson, S.J. (2002) *Bioenergetics 3.* (1st edn), Academic Press
23 Soong, N.W. *et al.* (1992) Mosaicism for a specific somatic mitochondrial DNA mutation in adult human brain. *Nat. Genet.* 2, 318–323
24 Kraytsberg, Y. *et al.* (2006) Mitochondrial DNA deletions are abundant and cause functional impairment in aged human substantia nigra neurons. *Nat. Genet.* 38, 518–520
25 Bender, A. *et al.* (2006) High levels of mitochondrial DNA deletions in substantia nigra neurons in aging and Parkinson disease. *Nat. Genet.* 38, 515–517
26 Tretter, L. *et al.* (2004) Initiation of neuronal damage by complex I deficiency and oxidative stress in Parkinson's disease. *Neurochem. Res.* 29, 569–577
27 Jenner, P. (2001) Parkinson's disease, pesticides and mitochondrial dysfunction. *Trends Neurosci.* 24, 245–247
28 Moore, D.J. *et al.* (2005) Molecular pathophysiology of Parkinson's disease. *Annu. Rev. Neurosci.* 28, 57–87
29 Balch, W.E. *et al.* (2008) Adapting proteostasis for disease intervention. *Science* 319, 916–919
30 Del Tredici, K. and Braak, H. (2004) Idiopathic Parkinson's disease: staging an α-synucleinopathy with a predictable pathoanatomy. In *Molecular Mechanisms of Parkinson's Disease* (Kahle, P.J. and Haas, C., eds), pp. 1–32, Landes Bioscience
31 Ryu, E.J. *et al.* (2002) Endoplasmic reticulum stress and the unfolded protein response in cellular models of Parkinson's disease. *J. Neurosci.* 22, 10690–10698
32 Kaushik, S. and Cuervo, A.M. (2008) Chaperone-mediated autophagy. *Methods Mol. Biol.* 445, 227–244
33 Wang, H.Q. and Takahashi, R. (2007) Expanding insights on the involvement of endoplasmic reticulum stress in Parkinson's disease. *Antioxid. Redox Signal.* 9, 553–561
34 Grace, A.A. and Bunney, B.S. (1983) Intracellular and extracellular electrophysiology of nigral dopaminergic neurons – 2. Action potential generating mechanisms and morphological correlates. *Neuroscience* 10, 317–331
35 Romo, R. and Schultz, W. (1990) Dopamine neurons of the monkey midbrain: contingencies of responses to active touch during self-initiated arm movements. *J. Neurophysiol.* 63, 592–606
36 Bonci, A. *et al.* (1998) L-Type calcium channels mediate a slow excitatory synaptic transmission in rat midbrain dopaminergic neurons. *J. Neurosci.* 18, 6693–6703

37 Ping, H.X. and Shepard, P.D. (1996) Apamin-sensitive $Ca^{2+}$-activated $K^+$ channels regulate pacemaker activity in nigral dopamine neurons. *Neuroreport* 7, 809–814
38 Puopolo, M. *et al.* (2007) Roles of subthreshold calcium current and sodium current in spontaneous firing of mouse midbrain dopamine neurons. *J. Neurosci.* 27, 645–656
39 Wilson, C.J. and Callaway, J.C. (2000) Coupled oscillator model of the dopaminergic neuron of the substantia nigra. *J. Neurophysiol.* 83, 3084–3100
40 Chan, C.S. *et al.* (2007) 'Rejuvenation' protects neurons in mouse models of Parkinson's disease. *Nature* 447, 1081–1086
41 Striessnig, J. *et al.* (2006) Role of voltage-gated L-type $Ca^{2+}$ channel isoforms for brain function. *Biochem. Soc. Trans.* 34, 903–909
42 Sinnegger-Brauns, M.J. *et al.* (2008) Expression and 1,4-dihydropyridine-binding properties of brain L-type calcium channel isoforms. *Mol. Pharmacol.* 75, 407–414
43 Olson, P.A. *et al.* (2005) G-protein-coupled receptor modulation of striatal $Ca_V1.3$ L-type $Ca^{2+}$ channels is dependent on a Shank-binding domain. *J. Neurosci.* 25, 1050–1062
44 Rizzuto, R. (2001) Intracellular $Ca^{2+}$ pools in neuronal signalling. *Curr. Opin. Neurobiol.* 11, 306–311
45 Orrenius, S. *et al.* (2003) Regulation of cell death: the calcium-apoptosis link. *Nat. Rev. Mol. Cell Biol.* 4, 552–565
46 Berridge, M.J. *et al.* (2000) The versatility and universality of calcium signalling. *Nat. Rev. Mol. Cell Biol.* 1, 11–21
47 Berridge, M.J. (2002) The endoplasmic reticulum: a multifunctional signaling organelle. *Cell Calcium* 32, 235–249
48 Schwyn, R.C. and Fox, C.A. (1974) The primate substantia nigra: a Golgi and electron microscopic study. *J. Hirnforsch.* 15, 95–126
49 Choi, Y.M. *et al.* (2006) Regional interaction of endoplasmic reticulum $Ca^{2+}$ signals between soma and dendrites through rapid luminal $Ca^{2+}$ diffusion. *J. Neurosci.* 26, 12127–12136
50 Park, M.K. *et al.* (2000) The endoplasmic reticulum as one continuous $Ca^{2+}$ pool: visualization of rapid $Ca^{2+}$ movements and equilibration. *EMBO J.* 19, 5729–5739
51 Mogami, H. *et al.* (1997) $Ca^{2+}$ flow via tunnels in polarized cells: recharging of apical $Ca^{2+}$ stores by focal $Ca^{2+}$ entry through basal membrane patch. *Cell* 88, 49–55
52 Cui, G. *et al.* (2004) Spontaneous opening of T-type $Ca^{2+}$ channels contributes to the irregular firing of dopamine neurons in neonatal rats. *J. Neurosci.* 24, 11079–11087
53 Bardo, S. *et al.* (2006) The role of the endoplasmic reticulum $Ca^{2+}$ store in the plasticity of central neurons. *Trends Pharmacol. Sci.* 27, 78–84
54 Rose, C.R. and Konnerth, A. (2001) Stores not just for storage. intracellular calcium release and synaptic plasticity. *Neuron* 31, 519–522
55 Verkhratsky, A. (2005) Physiology and pathophysiology of the calcium store in the endoplasmic reticulum of neurons. *Physiol. Rev.* 85, 201–279
56 Park, M.K. *et al.* (2008) The endoplasmic reticulum as an integrator of multiple dendritic events. *Neuroscientist* 14, 68–77
57 Hetz, C.A. (2007) ER stress signaling and the BCL-2 family of proteins: from adaptation to irreversible cellular damage. *Antioxid. Redox Signal.* 9, 2345–2355
58 Toescu, E.C. (2005) Normal brain ageing: models and mechanisms. *Philos. Trans. R. Soc. Lond B. Biol. Sci.* 360, 2347–2354
59 Paschen, W. and Mengesdorf, T. (2005) Endoplasmic reticulum stress response and neurodegeneration. *Cell Calcium* 38, 409–415
60 LaFerla, F.M. (2002) Calcium dyshomeostasis and intracellular signalling in Alzheimer's disease. *Natl. Rev Neurosci.* 3, 862–872
61 Morikawa, H. *et al.* (2000) Inositol 1,4,5-triphosphate-evoked responses in midbrain dopamine neurons. *J. Neurosci.* 20, RC103
62 Rizzuto, R. and Pozzan, T. (2006) Microdomains of intracellular $Ca^{2+}$: molecular determinants and functional consequences. *Physiol. Rev.* 86, 369–408
63 Csordas, G. *et al.* (2006) Structural and functional features and significance of the physical linkage between ER and mitochondria. *J. Cell Biol.* 174, 915–921
64 Kirichok, Y. *et al.* (2004) The mitochondrial calcium uniporter is a highly selective ion channel. *Nature* 427, 360–364
65 McCormack, J.G. *et al.* (1990) Role of calcium ions in regulation of mammalian intramitochondrial metabolism. *Physiol. Rev.* 70, 391–425
66 Vergun, O. and Reynolds, I.J. (2005) Distinct characteristics of Ca2+-induced depolarization of isolated brain and liver mitochondria. *Biochim. Biophys. Acta* 1709, 127–137
67 Stark, A.K. and Pakkenberg, B. (2004) Histological changes of the dopaminergic nigrostriatal system in aging. *Cell Tissue Res.* 318, 81–92
68 Harman, D. (1972) The biologic clock: the mitochondria? *J. Am. Geriatr. Soc.* 20, 145–147
69 Wallace, D.C. (2005) A mitochondrial paradigm of metabolic and degenerative diseases, aging, and cancer: a dawn for evolutionary medicine. *Annu. Rev. Genet.* 39, 359–407
70 Calne, D.B. and Langston, J.W. (1983) Aetiology of Parkinson's disease. *Lancet* 2, 1457–1459
71 Gibb, W.R. and Lees, A.J. (1991) Anatomy, pigmentation, ventral and dorsal subpopulations of the substantia nigra, and differential cell death in Parkinson's disease. *J. Neurol. Neurosurg. Psychiatry* 54, 388–396
72 McCormack, A.L. *et al.* (2004) Aging of the nigrostriatal system in the squirrel monkey. *J. Comp. Neurol.* 471, 387–395
73 Ishikawa, T. *et al.* (1996) Comparative nigrostriatal dopaminergic imaging with iodine-123-β CIT-FP/SPECT and fluorine-18-FDOPA/PET. *J. Nucl. Med.* 37, 1760–1765
74 Backman, L. *et al.* (2000) Age-related cognitive deficits mediated by changes in the striatal dopamine system. *Am. J. Psychiatry* 157, 635–637
75 Collier, T.J. *et al.* (2007) Aging-related changes in the nigrostriatal dopamine system and the response to MPTP in nonhuman primates: diminished compensatory mechanisms as a prelude to parkinsonism. *Neurobiol. Dis.* 26, 56–65
76 Kanaan, N.M. *et al.* (2007) Age-related accumulation of Marinesco bodies and lipofuscin in rhesus monkey midbrain dopamine neurons: relevance to selective neuronal vulnerability. *J. Comp. Neurol.* 502, 683–700
77 Kanaan, N.M. *et al.* (2008) Age-related changes in dopamine transporters and accumulation of 3-nitrotyrosine in rhesus monkey midbrain dopamine neurons: relevance in selective neuronal vulnerability to degeneration. *Eur. J. Neurosci.* 27, 3205–3215
78 Zigmond, M.J. *et al.* (1990) Compensations after lesions of central dopaminergic neurons: some clinical and basic implications. *Trends Neurosci.* 13, 290–296
79 Sulzer, D. (2007) Multiple hit hypotheses for dopamine neuron loss in Parkinson's disease. *Trends Neurosci.* 30, 244–250
80 McGeer, P.L. and McGeer, E.G. (2008) Glial reactions in Parkinson's disease. *Mov. Disord.* 23, 474–483
81 German, D.C. *et al.* (1992) Midbrain dopaminergic cell loss in Parkinson's disease and MPTP-induced parkinsonism: sparing of calbindin-D28k-containing cells. *Ann. N. Y. Acad. Sci.* 648, 42–62
82 Yamada, T. *et al.* (1990) Relative sparing in Parkinson's disease of substantia nigra dopamine neurons containing calbindin-D28K. *Brain Res.* 526, 303–307
83 German, D.C. *et al.* (1992) Disease-specific patterns of locus coeruleus cell loss. *Ann. Neurol.* 32, 667–676
84 Williams, J.T. *et al.* (1984) Membrane properties of rat locus coeruleus neurones. *Neuroscience* 13, 137–156
85 Stevens, D.R. and Haas, H.L. (1996) Calcium-dependent prepotentials contribute to spontaneous activity in rat tuberomammillary neurons. *J. Physiol.* 493, 747–754
86 Taddese, A. and Bean, B.P. (2002) Subthreshold sodium current from rapidly inactivating sodium channels drives spontaneous firing of tuberomammillary neurons. *Neuron* 33, 587–600
87 Belzunegui, S. *et al.* (2007) The number of dopaminergic cells is increased in the olfactory bulb of monkeys chronically exposed to MPTP. *Synapse* 61, 1006–1012
88 Pignatelli, A. *et al.* (2005) Functional properties of dopaminergic neurones in the mouse olfactory bulb. *J. Physiol.* 564, 501–514
89 Postuma, R.B. *et al.* (2006) Potential early markers of Parkinson disease in idiopathic REM sleep behavior disorder. *Neurology* 66, 845–851
90 Huisman, E. *et al.* (2008) Gender-related changes in increase of dopaminergic neurons in the olfactory bulb of Parkinson's disease patients. *Mov. Disord.* 23, 1407–1413
91 Pignatelli, A. *et al.* (2009) A potential reservoir of immature dopaminergic replacement neurons in the adult mammalian olfactory bulb. *Pflugers Arch* 899–915

92 Grace, A.A. and Bunney, B.S. (1984) The control of firing pattern in nigral dopamine neurons: single spike firing. *J. Neurosci.* 4, 2866–2876
93 Becker, C. *et al.* (2008) Use of statins and the risk of Parkinson's disease: a retrospective case-control study in the UK. *Drug Saf.* 31, 399–407
94 Rodnitzky, R.L. (1999) Can calcium antagonists provide a neuroprotective effect in Parkinson's disease? *Drugs* 57, 845–849
95 Kupsch, A. *et al.* (1996) 1-Methyl-4-phenyl-1,2,3,6-tetrahydropyridine-induced neurotoxicity in non-human primates is antagonized by pretreatment with nimodipine at the nigral, but not at the striatal level. *Brain Res.* 741, 185–196
96 Mannhold, R. *et al.* (1995) Comparative evaluation of the predictive power of calculation procedures for molecular lipophilicity. *J. Pharm. Sci.* 84, 1410–1419
97 Eisenberg, M.J. *et al.* (2004) Calcium channel blockers: an update. *Am. J. Med.* 116, 35–43
98 Xu, W. and Lipscombe, D. (2001) Neuronal $Ca_V1.3\alpha_1$ L-type channels activate at relatively hyperpolarized membrane potentials and are incompletely inhibited by dihydropyridines. *J. Neurosci.* 21, 5944–5951
99 Koschak, A. *et al.* (2001) $_{\alpha}$1D (Cav1.3) subunits can form L-type $Ca^{2+}$ channels activating at negative voltages. *J. Biol. Chem.* 276, 22100–22106
100 Scholze, A. *et al.* (2001) Functional expression and characterization of a voltage-gated $Ca_V1.3$ ($\alpha_{1D}$) calcium channel subunit from an insulin-secreting cell line. *Molecular endocrinol.* 15, 1211–1221
101 Fitton, A. and Benfield, P. (1990) Isradipine. A review of its pharmacodynamic and pharmacokinetic properties, and therapeutic use in cardiovascular disease. *Drugs* 40, 31–74
102 Hung, A.Y. and Schwarzschild, M.A. (2007) Clinical trials for neuroprotection in Parkinson's disease: overcoming angst and futility? *Curr. Opin. Neurol.* 20, 477–483
103 Shults, C.W. *et al.* (1997) Coenzyme Q10 levels correlate with the activities of complexes I and II/III in mitochondria from parkinsonian and nonparkinsonian subjects. *Ann. Neurol.* 42, 261–264
104 Beal, M.F. *et al.* (1998) Coenzyme Q10 attenuates the 1-methyl-4-phenyl-1,2,3,tetrahydropyridine (MPTP) induced loss of striatal dopamine and dopaminergic axons in aged mice. *Brain Res.* 783, 109–114
105 Matthews, R.T. *et al.* (1999) Creatine and cyclocreatine attenuate MPTP neurotoxicity. *Exp. Neurol.* 157, 142–149
106 Andres-Mateos, E. *et al.* (2007) DJ-1 gene deletion reveals that DJ-1 is an atypical peroxiredoxin-like peroxidase. *Proc. Natl. Acad. Sci. U. S. A.* 104, 14807–14812
107 Greene, J.C. *et al.* (2003) Mitochondrial pathology and apoptotic muscle degeneration in *Drosophila parkin* mutants. *Proc. Natl. Acad. Sci. U. S. A.* 100, 4078–4083
108 Palacino, J.J. *et al.* (2004) Mitochondrial dysfunction and oxidative damage in parkin-deficient mice. *J. Biol. Chem.* 279, 18614–18622
109 Clark, I.E. *et al.* (2006) *Drosophila pink1* is required for mitochondrial function and interacts genetically with *parkin*. *Nature* 441, 1162–1166
110 Park, J. *et al.* (2006) Mitochondrial dysfunction in *Drosophila PINK1* mutants is complemented by *parkin*. *Nature* 441, 1157–1161
111 Exner, N. *et al.* (2007) Loss-of-function of human PINK1 results in mitochondrial pathology and can be rescued by parkin. *J. Neurosci.* 27, 12413–12418
112 Ishihara, L. *et al.* (2007) Screening for Lrrk2 G2019S and clinical comparison of Tunisian and North American Caucasian Parkinson's disease families. *Mov. Disord.* 22, 55–61
113 West, A.B. *et al.* (2005) Parkinson's disease-associated mutations in leucine-rich repeat kinase 2 augment kinase activity. *Proc. Natl. Acad. Sci. U. S. A.* 102, 16842–16847

Neurobiology of Disease

# Robust Pacemaking in Substantia Nigra Dopaminergic Neurons

**Jaime N. Guzman,* Javier Sánchez-Padilla,* C. Savio Chan, and D. James Surmeier**
Department of Physiology, Feinberg School of Medicine, Northwestern University, Chicago, Illinois 60611

**Dopaminergic neurons of the substantia nigra pars compacta are autonomous pacemakers. This activity is responsible for the sustained release of dopamine necessary for the proper functioning of target structures, such as the striatum. Somatodendritic L-type $Ca^{2+}$ channels have long been viewed as important, if not necessary, for this activity. The studies reported here challenge this viewpoint. Using a combination of optical and electrophysiological approaches in brain slices, it was found that antagonism of L-type $Ca^{2+}$ channel effectively stopped dendritic $Ca^{2+}$ oscillations but left autonomous pacemaking unchanged. Moreover, damping intracellular $Ca^{2+}$ oscillations with exogenous buffer had little effect on pacemaking rate. Although not necessary for pacemaking, L-type channels helped support pacemaking when challenged with cationic channel blockers. Simulations suggested that the insensitivity to antagonism of L-type channels reflected the multichannel nature of the pacemaking process. The robustness of pacemaking underscores its biological importance and provides a framework for understanding how therapeutics targeting L-type $Ca^{2+}$ channels might protect dopaminergic neurons in Parkinson's disease without compromising their function.**

## Introduction

Dopamine (DA)-releasing neurons of the substantia nigra pars compacta (SNc) are critical to a broad array of psychomotor functions, including action selection and reward-based learning (Schultz, 2007; Yin et al., 2008; Cohen and Frank, 2009). A key feature of these neurons is their steady, autonomous pacemaking. This self-generated activity maintains extracellular DA levels and the DA receptor signaling necessary for normal network operation in basal ganglia structures, such as the striatum (Albin et al., 1989; Gonon and Bloch, 1998). Although synaptic signals are capable of altering ongoing spike activity *in vivo* (Grace and Bunney, 1984; Tepper et al., 1998), the rate and regularity of the autonomous activity is remarkably robust in the face of a variety of pharmacological and molecular perturbations (Paladini et al., 2003; Chan et al., 2007).

The mechanisms underlying autonomous pacemaking have been the subject of investigation for more than a decade. At present, the dominant view is that, in adult SNc dopaminergic neurons, pacemaking is dependent on $Ca^{2+}$ channels that open at relatively hyperpolarized membrane potentials (Nedergaard et al., 1993; Mercuri et al., 1994; Amini et al., 1999; Wilson and Callaway, 2000; Puopolo et al., 2007). Based on the ability of dihydropyridines (DHPs) to slow or stop pacemaking, this channel has been assumed to be of the $Ca_v1$ or L-type (Nedergaard et al., 1993; Mercuri et al., 1994; Chan et al., 2007; Puopolo et al., 2007). However, the DHP concentrations necessary to achieve significant slowing or silencing in these acute physiological experiments are typically several orders of magnitude greater than those predicted by binding studies to be required for near complete channel antagonism (Koschak et al., 2001; Sinnegger-Brauns et al., 2009). In principle, there are several factors that might contribute to this mismatch. For example, the affinity of DHPs for L-type channels is state dependent, being approximately a thousand-fold lower at negative membrane potentials (Bean, 1984). Another major limitation is the difficulty in achieving binding equilibrium in brain slices. Lipophilic DHPs not only must diffuse tens of micrometers into the slice, they must partition into the membrane and diffuse to a binding site buried in the lipid bilayer (Lipkind and Fozzard, 2003). This makes equilibrium slow to achieve, taking as much as an hour (Herbette et al., 1989). Because electrophysiological recordings are typically stable for a much shorter period of time, high DHP concentrations have been used to achieve measurable levels of channel antagonism rapidly. This approach has a number of caveats, not the least of which is that, because DHPs have very high membrane partition coefficients (Herbette et al., 1989), their concentration can reach levels that begin to have nonspecific effects on other ion channels, complicating the interpretation of effects on complex phenomena, such as pacemaking.

Determining the role of L-type $Ca^{2+}$ channels in pacemaking is not only of theoretical importance but of clinical importance as well. $Ca^{2+}$ ions entering SNc DA neurons through L-type $Ca^{2+}$ channels during pacemaking elevates cellular vulnerability to toxins used to create animal models of Parkinson's disease (PD) (Chan et al., 2007). The potential linkage of these channels to PD has been strengthened by epidemiological studies showing a decreased disease risk in humans treated for hypertension with

Received May 30, 2009; revised July 13, 2009; accepted July 27, 2009.

This work was supported by the Hartman Foundation, the Falk Trust, United States Army Medical Research and Material Command Grant W81 XWH-071-0170, and National Institutes of Health Grant NS047085. We thank Karen Saporito, Sasha Ulrich, David Wokosin, and Ema Ilijic for their technical support and scientific contributions.

*J.N.G. and J.S.-P. contributed equally to this work.

Correspondence should be addressed to Dr. D. James Surmeier, Department of Physiology, Feinberg School of Medicine, Northwestern University, 303 East Chicago Avenue, Chicago, IL 60611. E-mail: j-surmeier@northwestern.edu.

DOI:10.1523/JNEUROSCI.2519-09.2009

 0270-6474/09/2911011-09$15.00/0

DHPs (Becker et al., 2008). However, if L-type channels are critical to pacemaking, this therapeutic benefit must come at a functional cost, such as a drop in pacemaking rate and DA in target structures. Using optical and electrophysiological approaches to assay acute L-type channel antagonism, we show that, although these channels contribute to the robustness of pacemaking, they are not necessary.

## Materials and Methods

*Electrophysiological recordings.* Acute midbrain coronal slices (220 $\mu$m thick) were obtained from wild-type male C57BL/6 mice (Charles River) between postnatal ages 21 and 32 d, unless specified otherwise. The handling of mice and all procedures performed on them were approved by the institutional Animal Care and Use Committee and were in accordance with the National Institutes of Health *Guide to the Care and Use of Laboratory Animals* and Society for Neuroscience guidelines. Mice were anesthetized with a ketamine/xylazine mixture, followed by a transcardial perfusion with ice-cold, oxygenated artificial CSF (ACSF) containing the following (in mM): 125 NaCl, 2.5 KCl, 25 $NaHCO_3$, 1.25 $NaH_2PO_4$, 2 $CaCl_2$, 1 $MgCl_2$, and 25 dextrose, pH 7.3 (osmolality 315–320 mOsm/L). After perfusion, mice were decapitated and brains were removed rapidly, followed by sectioning in ice-cold oxygenated ACSF using a vibratome (VT1000S; Leica Microsystems). Midbrain slices recovered in ACSF at 34°C for 30 min before electrophysiological recordings. Slices were transferred to a small-volume (<0.5 ml) recording chamber that was mounted on a fixed-stage, upright microscope (BX51; Olympus America) equipped with infrared differential interference contrast [0.9 numerical aperture (NA)] with de Sénarmont compensation (Olympus). Experiments were performed at 33–34°C, unless specified otherwise. The recording chamber was superfused with carbogen-saturated ACSF with a flow rate of 2–3 ml/min running through an in-line heater (SH-27B with TC-324B controller; Warner Instruments). Neuronal somata and proximal dendrites were visualized by video microscopy at high magnification (60×, 0.9 NA water-immersion objective; Olympus). Cell-attached and whole-cell patch-clamp recordings were performed in DA neurons from the mid-to-ventral tier of the SNc. Recording patch electrodes (resistance of 3–4 M$\Omega$) were prepared with a Sutter Instruments horizontal puller using borosilicate glass with filament. For all voltage- and current-clamp recordings, patch electrodes were filled with internal solution containing the following (in mM): 135 K-$MeSO_4$, 5 KCl, 5 HEPES, 0.05 EGTA, 10 phosphocreatine-di(tris), 2 ATP-Mg, and 0.5 GTP-Na, the pH adjusted to 7.3 (osmolality adjusted to 290–300 mOsm/L). The liquid junction potential in our recording ACSF was 7 mV and not corrected for. Conventional tight-seal (>3 G$\Omega$) whole-cell patch-clamp and cell-attached recordings were made on visually identified neurons based on (1) size and somatodendritic morphology, (2) regular spiking between 1 and 4 Hz, (3) presence of a voltage sag during delivery of a hyperpolarizing pulse (−250 pA current injection), and (4) the presence of the HCN current recorded in voltage clamp (data not shown). For $Na^+$ current recordings, voltage control and space clamp was improved by lowering the external concentration of $Na^+$ to 20 mM and adding 50 $\mu$M $Cd^{2+}$ to the perfusate; patch electrodes were filled with a cesium-based internal containing the following (in mM): 120 Cs-$MeSO_3$, 15 CsCl, 8 NaCl, 10 HEPES, 0.2 EGTA, 3 ATP-Mg, 0.3 GTP-Na, and 10 tetraethylammonium-Cl, pH 7.3 (osmolality 280 mOsm/L). Tetrodotoxin (TTX)-sensitive sodium currents were recorded in voltage clamp with ramps from −70 to −40 mV for 500 ms (ramp speed of 0.06 mV/ms), and peak currents were measured. Signals were filtered at 1–4 kHz and digitized at 5–20 kHz with a Digidata 1322A (Molecular Devices). For current-clamp recordings, the amplifier bridge circuit was adjusted to compensate for electrode resistance and monitored. Electrode capacitance was also compensated. If series resistance increased >20% during recording, the data were discarded.

*Two-photon laser scanning microscopy.* For dendritic $Ca^{2+}$ measurements, SNc DA neurons in tissue slices (as described above) were loaded with Alexa Fluor 594 (50 $\mu$M) and Fluo-4 (200 $\mu$M) through the patch pipette. All experiments were performed at 32–34°C. Images were acquired with a 60×/0.9 NA water-immersion lens. Dyes were allowed to equilibrate for at least 15 min before imaging. The two-photon excitation source was a Chameleon-ultra2 tunable laser system (680 to 1080 nm) using titanium:sapphire gain medium with all-solid-state active components and a computer-optimized algorithm to ensure reproducible excitation wavelength, average power, and peak power (Coherent Laser Group). Optical signals were acquired using 810 nm excitation beam (80-MHz pulse repetition frequency and ~250 fs pulse duration) to simultaneously excite Alexa and Fluor-4 dyes. Laser power attenuation was achieved with two Pockel cell electro-optic modulators (models 350-80; Con Optics). The two cells are aligned in series to provide enhanced modulation range for fine control of the excitation dose (0.1% steps over four decades). The laser-scanned images were acquired with a Bio-Rad Radiance MPD system. The fluorescence emission was collected by external or non-descanned photomultiplier tubes (PMTs). The green fluorescence (500–550 nm) was detected by a bialkali-cathode PMT, and the red fluorescence (580–640 nm) was collected by a multi-alkali-cathode (S-20) PMT. The system digitizes the current from detected photons to 12 bits. The laser light transmitted through the sample was collected by the condenser lens and sent to another PMT to provide a bright-field transmission image in registration with the fluorescent images. Measurements were taken in a sample plane along dendritic segments (100–150 mm from the soma). Line scan signals were acquired (as described above) at 6 ms per line and 512 pixels per line with 0.18 $\mu$m pixels and 10 $\mu$s pixel dwell time. The time between the control and isradipine treatment measurements was 5–7 min.

*Statistical analysis.* Electrophysiological data collected were analyzed using ClampFit 10.1 (Molecular Devices), Igor Pro 6.0 (Wavemetrics), or Matlab (MathWorks). The stimulation, display, and analysis software for the two-photon imaging data was analyzed using a custom-written shareware package, WinFluor, PicViewer, and PowerCAL kindly provided by John Dempster (Strathclyde University, Glasgow, UK). Data were summarized either using box plots for small sample sizes or with parametric statistics (mean ± SE) for larger samples. Statistical analysis was done with SigmaStat 3.5 (Systat Software) using nonparametric testing Mann–Whitney rank sum test for comparing between two groups or Kruskal–Wallis ANOVA with Dunnett's *post hoc* for multiple group comparison. Before–after statistical analyses were performed using the Wilcoxon's signed rank test. Probability threshold for statistical significance was $p < 0.05$.

*Pharmacological reagents and channel ligands.* Reagents were purchased from Sigma, except K-$MeSO_4$ (MP Biomedicals), GTP-Na (Roche Diagnostics), isradipine, ZD 7288 (4-ethylphenylamino-1,2-dimethyl-6-methylaminopyrimidinium chloride) (Tocris Bioscience), tetrodotoxin and $\alpha$-dendrotoxin (Alomone Labs), and BAPTA tetrasodium salt, Alexa594, Fura-2, and Fluo-4 (Invitrogen). Drugs stocks solutions were prepared in deionized water, DMSO, or methanol; on the day of experiment, stocks were diluted to final concentrations in ACSF to achieve a final solvent concentration of <0.01% v/v.

*Modeling.* Simulations were performed with NEURON, version 5.9 (Hines and Carnevale, 2001). The model neuron was constructed of a cylindrical soma (lateral, 15 $\mu$m; dorsal, 15 $\mu$m) with axial resistivity of 70 $\Omega$/cm and membrane capacitance of 1 $\mu$F/cm$^2$; the temperature was 35°C, and all conductances had $Q_{10}$ values of 3–4. The density of the simulated channels (siemens per square centimeter) inserted into the membrane were as follows: $Na_v1$ (3.5e-2), $K_v1$ (3e-5), $K_v2$ (2.5e-3), $K_v4_{fast}$ (8.5e-5), $K_v4_{slow}$ (2e-5), $K_v7$ (7e-7), BK (1e-3), SK (1e-5), HCN (1.25e-4), $Ca_v1.3$ (5e-5), $Ca_v2$ (1e-5), and leak (3.5e-6); $E_{na} = 50$ mV, $E_k = -90$ mV, and $E_{leak/HCN} = -20$ mV. Kinetics and voltage dependence of channel gating were adjusted to fit experimentally derived values in either SNc DA neurons or other basal ganglia neurons (Mercer et al., 2007); densities were adjusted to fit experimental results and to achieve pacemaking in a normal range. Mod files for $Ca^{2+}$ diffusion, buffering, and pumping were adapted to fit the kinetics observed experimentally using Fluo-4. All of the NEURON mod files used in simulation will be posted on the NeuronDB website (http://senselab.med.yale.edu/neurondb) or are available on request.

Simulations of the modulated DHP receptor were performed with Matlab using the framework proposed by Bean (1984). The channel was assumed to have two affinity states: a high-affinity state at depolarized (inactivated) membrane potentials and a low-affinity state at hyperpo-

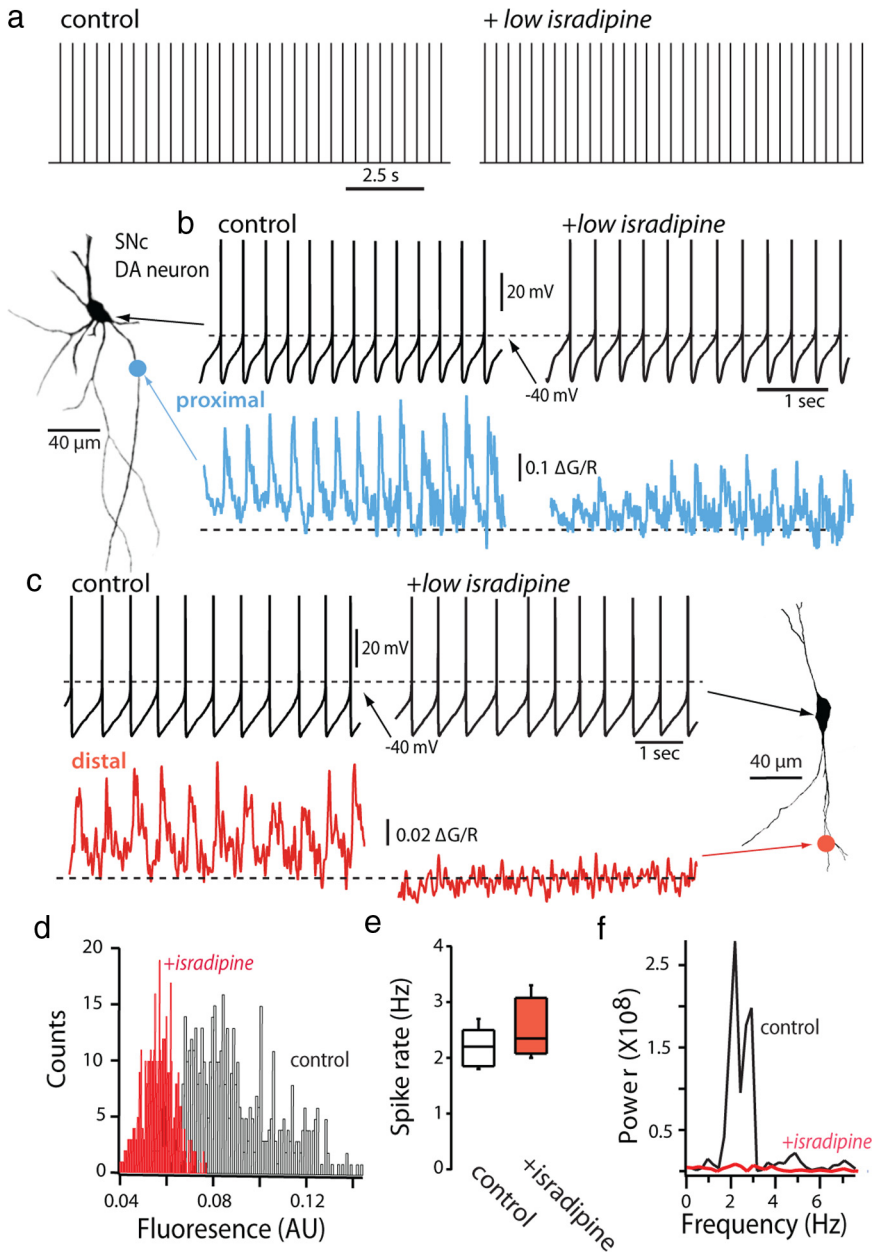


**Figure 1.** Low concentrations of DHPs suppress dendritic $Ca^{2+}$ oscillations but do not slow pacemaking. ***a***, Digitized cell-attached patch recordings from an SNc DA neuron before and after application of isradipine (5 $\mu$M). The median discharge rate before isradipine application was 2.2 and 2.4 Hz after ( $p > 0.05$; $n = 10$). ***b***, Whole-cell recording from the cell shown to the left (projection image) before and after isradipine (5 $\mu$M) application; there was no significant change in discharge rate in this cell or in 10 others. At the bottom, two-photon laser scanning microscopy measurements of Fluo-4 fluorescence (G) at a proximal dendritic location (~40 $\mu$m from the soma) normalized by the fluorescence of the red Alexa dye used to image the cell. ***c***, Somatic recording during imaging at a more distal dendritic location (~120–200 $\mu$m from the soma). Note the complete elimination of the spike-associated dendritic $Ca^{2+}$ transient at the distal imaging site. Similar results were obtained in six other neurons. ***d***, All points histogram of fluorescence at the distal location of the cell in ***c*** showing that the median fluorescence was reduced by isradipine. Similar results were obtained in six cells. AU, Arbitrary units. ***e***, Summary showing that, in whole-cell recordings in which imaging was done, isradipine did not change the discharge rate ( $p > 0.05$; $n = 10$). ***f***, Spectral analysis of the fluorescence signal readily detected oscillations at the pacemaking frequency; power at this frequency was eliminated by isradipine. Similar results were obtained in six cells.

larized (resting) membrane potentials. The dissociation constant for high-affinity state was assumed to be equal to that found in equilibrium binding studies, whereas the dissociation constant for low-affinity state was assumed to be a thousand-fold higher (Bean, 1984). The macroscopic balance between these states was assumed to be governed by voltage-dependent inactivation of the channel (Bean, 1984); the relationship between steady-state inactivation and voltage for $Ca_v1.3$ channels was taken from the work of Koschak et al. (2001).

## Results

### Selective antagonism of L-type $Ca^{2+}$ channels does not slow or stop pacemaking

To speed drug delivery to cells buried (30–75 $\mu$m below the surface) in a slice, 5 $\mu$M isradipine was applied, a concentrations 25–50 times that calculated to achieve near complete blockade of $Ca_v1.3$ channels at the depolarized membrane potentials traversed by SNc DA neurons (Bean, 1984). In cell-attached patch recordings (to minimize rundown), application of 5 $\mu$M isradipine for 10 min failed to slow pacemaking (Fig. 1*a*,*b*). This was not because isradipine had not antagonized L-type $Ca^{2+}$ channels. The antagonism could be clearly seen in whole-cell recordings of SNc DA neurons in which oscillations in dendritic $Ca^{2+}$ concentration were monitored using the $Ca^{2+}$ dye Fluo-4 (200 $\mu$M). In proximal dendrites (less than ~70 $\mu$m from the soma), isradipine clearly reduced the oscillations in $Ca^{2+}$ concentration (Fig. 1*b*). In the more distal (>80 $\mu$m from the soma) dendrites, 5 $\mu$M isradipine at this time point eliminated any detectable oscillation in $Ca^{2+}$ concentration and lowered modal fluorescence (Fig. 1*c*,*d*). Again, at the time point at which these measurements were made, there was no change in spike rate (Fig. 1*e*). Spectral analysis of the fluorescence signal in these distal dendrites consistently failed to detect power at the pacemaking frequency (Fig. 1*f*).

Another observation that has been taken as evidence of the centrality of L-type channels in pacemaking is that, after block of voltage-dependent $Na^+$ channels with TTX, the membrane potential continues to oscillate at near the pacemaking frequency (Yung et al., 1991; Nedergaard et al., 1993). These slow oscillatory potentials (SOPs) are widely held to drive pacemaking and trigger $Na^+$ spikes. However, like the oscillations in dendritic $Ca^{2+}$ concentration, the SOPs were eliminated by application of low micromolar concentrations of isradipine (Fig. 2*a*), concentrations that did not change pacemaking rate when $Na^+$ channels were left unblocked (Fig. 1*a*). To better test the inferences drawn above, slices were incubated in 200 nM isradipine for 60 min and then patched. If the rate-limiting step in DHP antagonism is diffusion within the lipid bilayer, then at this time point the number of bound channels should be within 10% of the equilibrium value (Herbette et al., 1989); assuming a modal membrane potential of −60 mV (a

conservative estimate), >90% of the $Ca_v1.3$ channels should be antagonized at this point. As predicted from the work with exposure to higher isradipine concentrations, there was no detectable change in pacemaking rate or regularity of SNc DA neurons sampled with cell-attached recordings from slices treated in this way (Fig. 2*b*,*d*). However, invariably, these cells lacked TTX-insensitive SOPs (Fig. 2*c*), arguing that $Ca_v1.3$ $Ca^{2+}$ channels were effectively antagonized. Spectral analysis of the membrane potential in these cells occasionally detected some residual power near the pacemaking rate with exposure to 200 nM isradipine but never with higher concentrations (Fig. 2*e*).

The SOPs seen in the presence of TTX reflect the interplay between dendritic L-type $Ca^{2+}$ channels and small conductance, $Ca^{2+}$-activated $K^+$ (SK) channels (Ping and Shepard, 1996; Wilson and Callaway, 2000). If this interplay was necessary for pacemaking, then disrupting the efficient activation of SK channels by chelating intracellular $Ca^{2+}$ should suppress pacemaking. However, whole-cell dialysis with BAPTA (5 mM) did not disrupt pacemaking but rather led to a slow acceleration of pacemaking (Fig. 3*a*), despite its elimination of the SOP seen in the presence of TTX (Fig. 2*b*) and its predicted effect on the trajectory of the spike afterhyperpolarization (Fig. 3*c*). Finally, the temporal properties of the SOPs, which clearly depend on L-type channels, were not consistent with a causal role in pacemaking. First, the frequency of spiking during pacemaking was not strongly correlated with the SOP frequency in the same cell after TTX application (Fig. 3*d*). Second, the coefficient of variation in interval duration during spiking was an order of magnitude smaller than that of the SOP (median CV spiking, 1.9e-4; median CV oscillation, 3.2e-2; $n = 9$; $p < 0.05$), and examination of successive intervals consistently showed random scatter in the SOP interval, even when the interspike interval in the same cell was very regular (Fig. 3*e*).

The insensitivity of pacemaking to DHPs seen in our work differs from that seen in younger, acutely isolated SNc DA neurons from mice (Puopolo et al., 2007). One possible explanation is that the work with acutely isolated neurons was performed at room temperature, some 10°C cooler than the experiments described here. To test this hypothesis, SNc DA neurons in slices were recorded at 23–25°C. At this temperature, pacemaking rate in cell-attached recordings was ap-

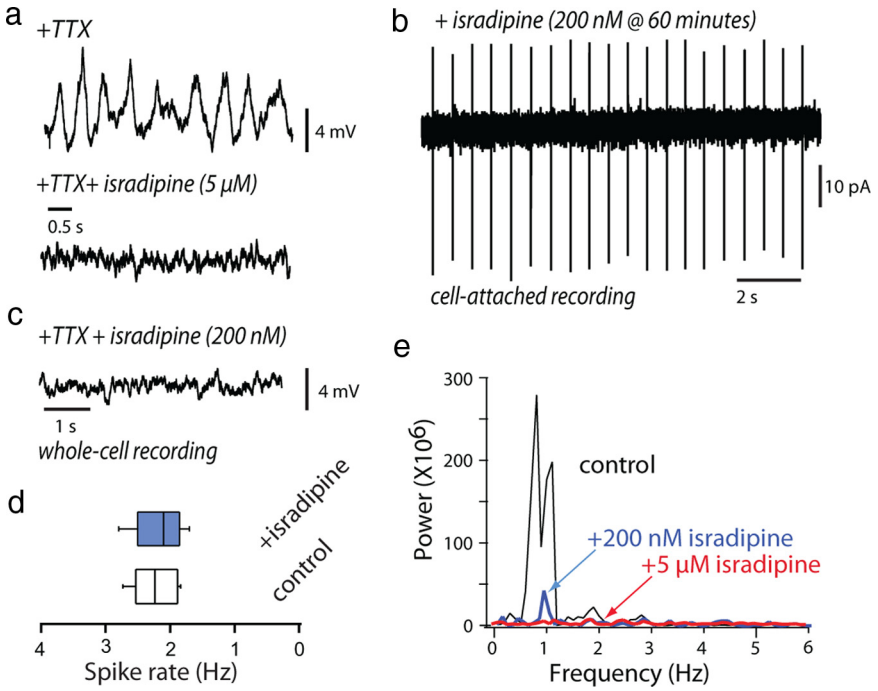


**Figure 2.** Submicromolar levels of DHPs are sufficient to block SOPs without compromising pacemaking activity. ***a***, Representative SOP traces (after blockade of sodium channels with 1 μM TTX) in the presence or absence of isradipine (5 μM). Micromolar concentrations of isradipine (5 μM) blocked the TTX-insensitive SOPs ($n = 10$ cells). ***b***, Submicromolar concentrations of DHPs (200 nM isradipine) had no effect in pacemaking firing rate ( $p > 0.05$; $n = 5$ cells). ***c***, Representative current-clamp trace showing no SOPs of a DA neuron pretreated with 200 nM isradipine for 1 h ($n = 5$ cells). ***d***, Summary box plots showing that 200 nM isradipine had no effect in spike rate. ***e***, Spectral analysis of the fluorescence showing a significant reduction in the power of the frequency detected in control, highly reduced power in the presence of 200 nM isradipine and complete elimination of frequency by 5 μM isradipine.

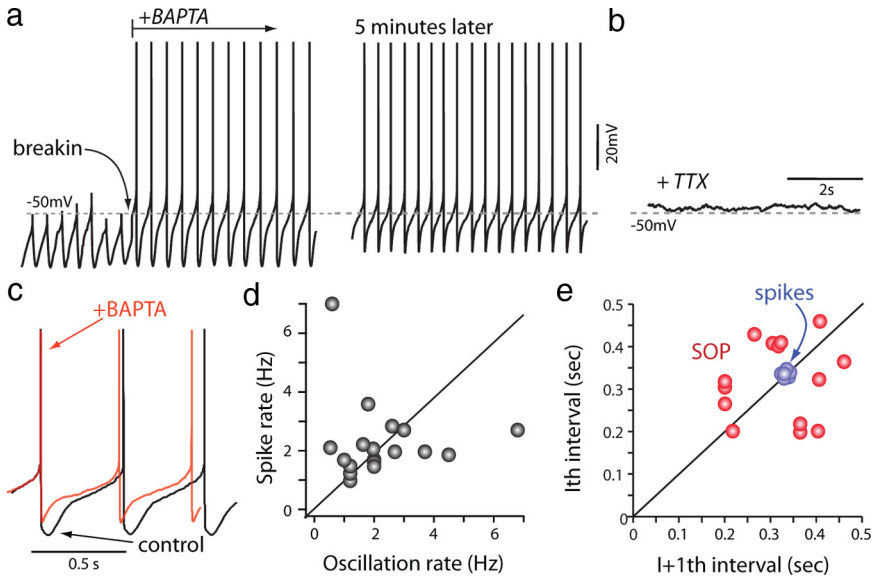


**Figure 3.** SOPs are absent after chelation of intracellular calcium. ***a***, Recording from an SNc DA neuron with an electrode containing 5 mM BAPTA. Before break-in, the pacemaking rate could be seen; after break-in, the rate slowly increased and the afterhyperpolarization became less pronounced, as shown in ***d***. Similar results were obtained in six cells. ***b***, Application of TTX demonstrated the absence of SOPs in the presence of BAPTA. ($n = 4$). ***c***, Voltage traces from ***b*** early (black trace) and later (red trace) in the dialysis with BAPTA showing the change in the afterhyperpolarization. ***d***, The discharge rate before application of TTX is plotted against the frequency of SOP oscillation. Note the scatter around the line with a slope of 1 ($n = 19$). ***e***, Plots of successive spike intervals or successive SOP intervals (measured from the point at which the voltage reached the median voltage of the oscillation). A sample of nine cells is plotted. Note the tight clustering of the spike data and the dispersion of the SOP data.

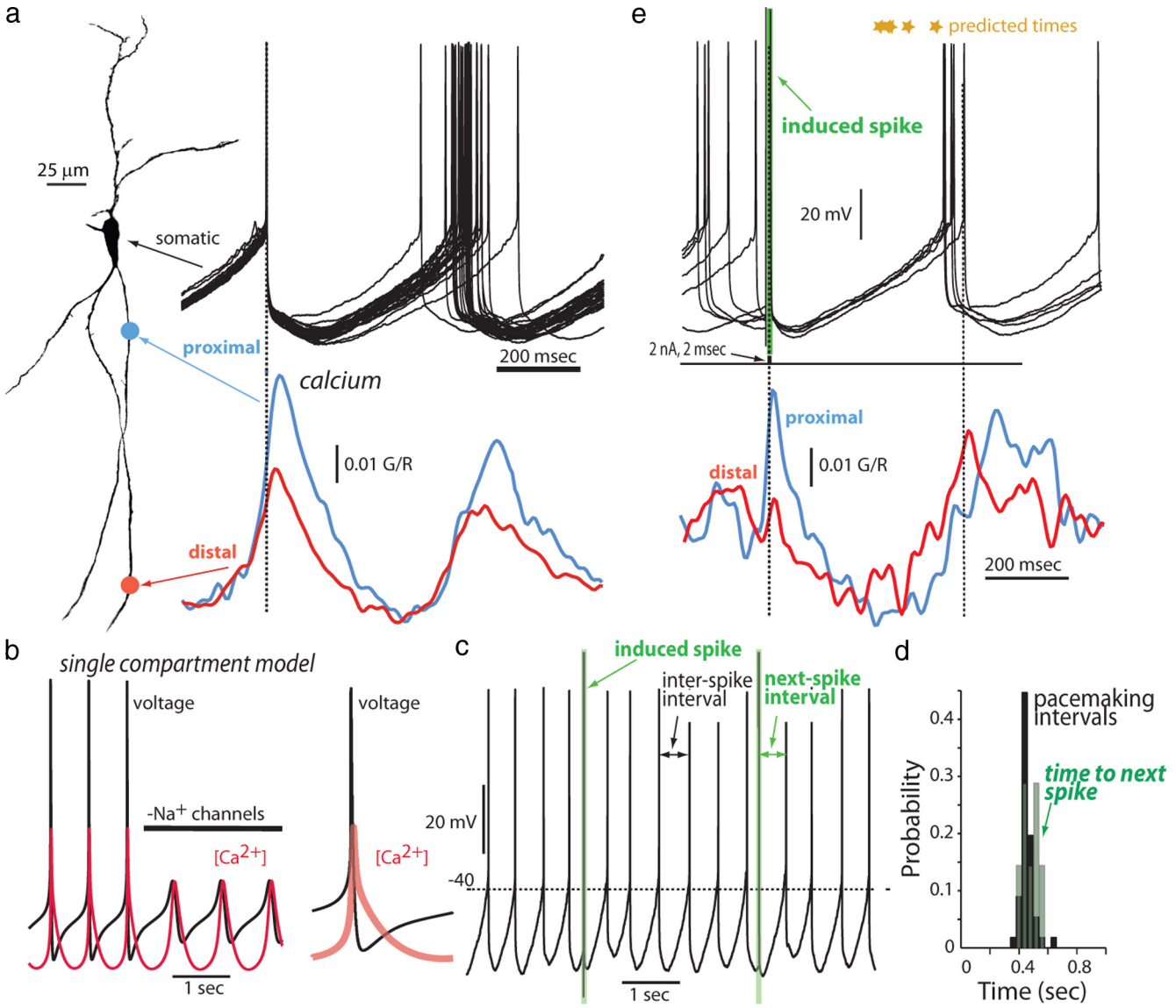


**Figure 4.** Dendritic $Ca^{2+}$ oscillations are phase locked to somatic spiking. ***a***, Projection image of an SNc DA neuron recorded from with a somatic patch electrode containing Alexa 594 (50 $\mu$M) and the $Ca^{2+}$ dye Fluo-4 (200 $\mu$M). To the right are somatic voltage recordings during pacemaking. At the bottom are averages of the fluorescence changes (G/R) at two dendritic locations shown by blue (proximal) and red (distal) dots. The averages were computed by aligning segments of the fluorescence records of 10 successive spikes; because the timing of the next spike varied, the timing of the fluorescence change after the initial spike in the average is only approximate and was used to gauge the phase relationship of the $Ca^{2+}$ oscillation. ***b***, A simulation using a single compartment model showing the relationship between the voltage (black trace) and the rise in intracellular $Ca^{2+}$ concentration (red) before and after block of $Na^{+}$ channels; note the similarity between these records and the data in ***a*** where $Ca^{2+}$ concentration rises just before the spike and peaks after the spike, falling during the afterhyperpolarization. ***c***, Recording from an SNc DA neuron in which ectopic spikes were introduced by brief (2 ms) current pulses; the green bar shows the timing of the ectopic spikes. ***d***, Histogram of the intervals during normal pacemaking (black filled) and the intervals after an ectopic spike (green filled) showing that it generated an interval typical of normal pacemaking, regardless of its phase relationship to the ongoing spiking. Similar behavior was seen in all four cells examined in this way. ***e***, At the top, somatic voltage records from one of these experiments showing the ectopic spike; at the bottom, fluorescence records (G/R) at the same locations shown in ***a***, but now aligned with the ectopic spike. Note that, at the proximal location, the ectopic spike evoked a $Ca^{2+}$ transient but not at the distal location; nevertheless, the oscillation in the $Ca^{2+}$ fluorescence was reset to coincide with the next spike in the series.

proximately half that seen near body temperature, in agreement with previous work (Guatteo et al., 2005). However, application of isradipine (5 $\mu$M) for 10–15 min failed to significantly slow the discharge rate at 25°C (control median, 0.67 Hz; plus isradipine, 0.78 Hz; $n = 4$; $p > 0.05$) (supplemental Fig. S1, available at www.jneurosci.org as supplemental material). Again, this was not because isradipine had failed to antagonize L-type channels, because the SOPs were absent when the membrane patch was disrupted to monitor transmembrane voltage (supplemental Fig. S1, available at www.jneurosci.org as supplemental material). One interpretation of these results is that the dendrites or axon initial segment (AIS), which are sheared off during acute isolation, contribute to pacemaking, rendering it sensitive to antagonism of L-type $Ca^{2+}$ channels. Underscoring the importance of these regions to the pacemaking process, SNc DA neurons in tissue slices also were insensitive to TRP channel antagonists 2-APB (20 $\mu$M; $n = 4$; $p > 0.05$) and SKF 96365 [1-2-(4-methoxyphenyl)-2-[3-(4-methoxyphenyl)propoxy]ethyl-1*H*-imidazole] (20 $\mu$M; $n = 4$; $p > 0.05$), in contrast to the situation reported in acutely isolated DA neurons (Kim et al., 2007).

### Somatic and dendritic compartments are electrically coupled

The prevailing $Ca^{2+}$ channel-dependent model of pacemaking hypothesizes that dendritic and somatic $Ca^{2+}$ oscillations are

coupled, synchronizing the somatodendritic membrane potential and driving spike generation (Wilson and Callaway, 2000). A key feature of the coupled oscillator model is strong electrical coupling between somatic and dendritic compartments, leading to synchronization of the membrane potential. This means that oscillations in $Ca^{2+}$ concentration should be phase locked in dendritic and somatic compartments. To test these two aspects of the model, line scans assessing changes in $Ca^{2+}$ concentration were performed at both proximal and distal dendritic regions of SNc DA neurons during pacemaking; averages of the $Ca^{2+}$-induced fluorescence just before and after the spike were then calculated. In agreement with this aspect of the model, the proximal and distal dendritic $Ca^{2+}$ signals were tightly phase locked in all neurons examined ($n = 4$), rising with the depolarization that preceded the spike and peaking just after the spike (Fig. 4*a*). Computer simulations with a single compartment model of an SNc DA neuron containing low-threshold $Ca_v1.3$ $Ca^{2+}$ channels yielded a very similar relationship between intracellular $Ca^{2+}$ concentration and membrane potential (Fig. 4*b*), arguing that the slow depolarization preceding the spike was driving $Ca^{2+}$ channel opening throughout the dendritic tree.

Although the dendritic tree might be electrotonically compact for slowly changing signals, like those in the interspike period, there should be greater attenuation of more rapidly changing voltages unless there are active processes involved (Holmes and Rall, 1992). Previous work has shown that spikes originate in the AIS of SNc DA neurons and that, in the absence of pacemaking, these action potentials are actively propagated into distal dendritic regions (Häusser et al., 1995). However, action potential propagation is strongly influenced by even small changes in membrane potential (Gentet and Williams, 2007), making it uncertain whether there is back-propagation during pacemaking. If conducted into the dendrites, these spikes should reset dendritic oscillations that rely on voltage-dependent $Ca^{2+}$ channels. To test this possibility, ectopic spikes were generated in the somatic region by a brief current pulse and the effects on somatic and dendritic oscillations monitored (Fig. 4*c*). In all of the neurons studied ($n = 4$), ectopic spikes occurring in the first half of the pacemaking cycle phase delayed the next spike, suggesting that the pacemaking mechanism had been reset (Fig. 4*d*). In some cells (like the one illustrated in Fig. 4), the spike only propagated into the proximal dendritic regions as judged by the change in $Ca^{2+}$-dependent fluorescence (Fig. 4*e*), suggesting that resetting the somatic component of the pacemaker was sufficient to reset the entire pacemaking process. These results are consistent with strong somatodendritic coupling posited in previous models but argue that the $Na^+$ channel-dependent spike itself is a key part of the pacemaking mechanism, not simply an epiphenomenon riding on top of the SOP, and that this proximally generated event determines pacemaking rate. This conclusion is consistent with the work presented above, showing that pacemaking continues unaltered in frequency or regularity in the absence of dendritic $Ca^{2+}$ oscillations and the SOP.

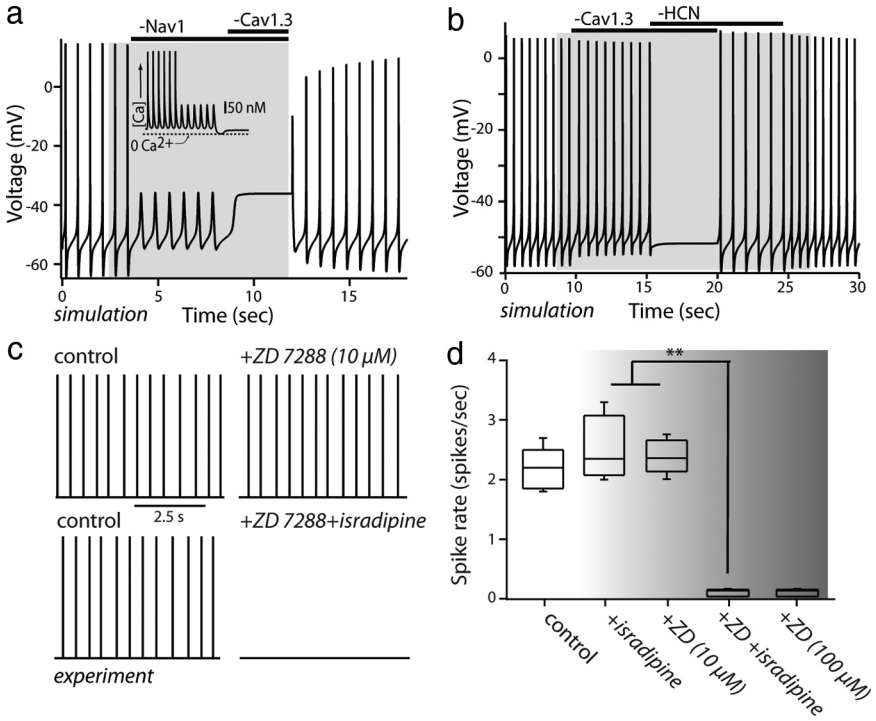


**Figure 5.** Simulations of pacemaking behavior and sensitivity to channel antagonism. ***a***, Voltage measurements from a single compartment simulation of an SNc DA neuron before and after removal of $Na^+$ channels, showing SOP-like behavior, and then after the additional removal of $Ca_v1.3$ $Ca^{2+}$ channels, showing cessation of the SOP. Restoring the channels led to restoration of pacemaking. Inset is intracellular $Ca^{2+}$ concentrations in the model before and after removal of $Na^+$ channels. Timing of the changes is shown in the bars at the top. ***b***, Voltage measurements of a simulation in which there was successive removal of first $Ca_v1.3$ and then combined removal of HCN and $Ca_v1.3$ channels. Note that pacemaking stopped only with the removal of both channels. ***c***, Digitized cell-attached patch recordings before and after application of ZD 7288 (10 $\mu$M) showing no significant change in discharge rate (see summary in ***d***). At the bottom, digitized cell-attached patch recordings before and after application of ZD 7288 (10 $\mu$M) and isradipine (5 $\mu$M) showing silencing of the cell. ***d***, Summary of experiments as in ***c***. The fall in discharge rates with coapplication of ZD 7288 (10 $\mu$M) and isradipine (5 $\mu$M) or with application of high concentrations of ZD 7288 (100 $\mu$M) alone was significant (**$p < 0.01$). Sample sizes were control ($n = 6$), isradipine (5 $\mu$M; $n = 7$), low ZD 7288 (10 $\mu$M; $n = 8$), low isradipine plus low ZD 7288 ($n = 5$), and high ZD 7288 (100 $\mu$M; $n = 4$).

### A computational model accounts for the insensitivity to DHPs

In an attempt to gain a better conceptual foothold on the mechanisms controlling pacemaking, a computational model was created using NEURON. The model consisted of a single "somatic" compartment; biophysically accurate models of channels thought to govern pacemaking were incorporated at densities resembling those seen experimentally (see Materials and Methods). The model generated regular, autonomous spiking at 1–2 Hz (Fig. 5*a*). As observed experimentally (Puopolo et al., 2007), the $Ca_v1.3$ $Ca^{2+}$ current was significantly larger than the $Na_v1$ $Na^+$ current in the interspike interval (supplemental Fig. S2, available at www.jneurosci.org as supplemental material); however, both currents were significantly smaller than those generated by "leak" channels, as in previous simulations (Amini et al., 1999). Reducing the $Na_v1$ channel density to zero prevented spiking but did not stop subthreshold oscillations, but subsequent block of $Ca_v1.3$ channels did, stabilizing the membrane potential near −40 mV.

Having verified that the basic behavior of the model resembled that seen experimentally, the interaction between $Ca_v1.3$

channels and other cationic channels in regulating pacemaking was explored. Eliminating $Ca_v1.3$ channels had little effect on pacemaking rate, despite clear effects on the voltage trajectory (Fig. 5*b*). Similarly, completely eliminating HCN channels had little effect on pacemaking rate. In both cases, the loss of inward current was compensated for by alterations in other conductances (supplemental Fig. S2, available at www.jneurosci.org as supplemental material). The combined removal of HCN and $Ca_v1.3$ channels, however, stopped spiking (Fig. 5*b*).

These results suggest that pacemaking is a robust, cooperative process, capable of withstanding perturbations in the availability of any one channel. To test this idea, recordings were made from SNc DA neurons, and combinations of channels were antagonized pharmacologically. Selective block of HCN channels with saturating concentrations of ZD 7288 (10 $\mu$M) had little or no effect on pacemaking rate (Fig. 5*c*,*d*). However, as predicted by the simulations, blocking HCN channels rendered pacemaking sensitive to antagonism of L-type $Ca^{2+}$ channels, because application of isradipine (5 $\mu$M) in the presence of ZD 7288 (10 $\mu$M) silenced every SNc DA neuron tested ($n = 5$) (Fig. 5*c*,*d*). It is worth noting that higher concentrations of ZD 7288 (50–100 $\mu$M) antagonized non-HCN channels (Zolles et al., 2006) and stopped pacemaking on their own (Fig. 5*d*).

### High concentrations of DHPs stop pacemaking by affecting other channel types

Why do high concentrations of DHPs, like isradipine, reliably slow or stop pacemaking in SNc DA neurons (Nedergaard et al., 1993; Mercuri et al., 1994; Ping and Shepard, 1996; Chan et al., 2007)? The work presented thus far argues that significant slowing or silencing is not attributable to antagonism of $Ca_v1.3$ $Ca^{2+}$ channels and must be attributable to reductions in other inward currents that help support pacemaking. There are three potential targets: $Na_v1$ $Na^+$, HCN, and cation leak channels. Point-clamp experiments using slow, depolarizing voltage ramps revealed that 20 $\mu$M isradipine modestly but consistently reduced peak $Na^+$ currents in SNc DA neurons (median reduction, 27%; $n = 4$; $p < 0.05$). In contrast, isradipine did not reduce the amplitude of the voltage sag produced by hyperpolarizing current steps (median reduction, 0.04%; $n = 6$; $p > 0.05$). However, input conductance measured by small hyperpolarizing steps from −60 mV was significantly reduced by isradipine, suggesting that cationic leak channels were being partially blocked (median reduction, 31%; $n = 9$; $p < 0.05$). Reducing $Na^+$ and leak channel density together by 20% consistently silenced pacemaking in the model, making this explanation plausible (Fig. 6*a*).

With sustained application of silencing concentrations of isradipine, pacemaking restarts after several hours (Chan et al., 2007). It could be restarted immediately by application of $K_v1$ channel antagonists (Fig. 6*b*,*c*), suggesting that the delayed restarting seen previously depends on functional downregulation of these channels. The model captured this recovery, because the silencing produced by partial block of $Na^+$ and leak channels was reversed by block of $K_v1$ channels (Fig. 6*a*). More importantly, this result reinforces the proposition that pacemaking reflects the interaction of a network of ion channels that is capable of withstanding perturbations in individual components.

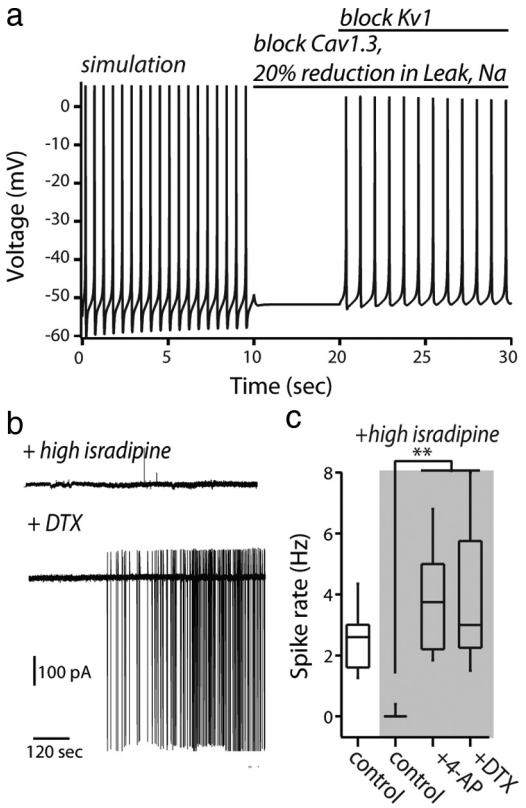


**Figure 6.** Pacemaking in DA neurons silenced with high DHP is restored by blocking $K_v1$ channels. ***a***, NEURON simulation model of pacemaking firing previous and after blockade of $Ca_v1.3$, 20% reduction in sodium current, and 20% reduction in leak currents. Combined partial blockade of these inward currents silenced pacemaking as in the experimental conditions described below (***b***, ***c***). Spiking activity was restored on blockade of $K_v1$ channels. ***b***, Cell-attached patch recording from an SNc DA neuron that had been silenced by isradipine (20 $\mu$M) and then restarted by bath application of $\alpha$-dendrotoxin (DTX; 100 nM). ***c***, Summary of similar experiments showing discharge rates in control ($n = 8$), isradipine exposed ($n = 6$), and then cells exposed to either $\alpha$-dendrotoxin (100 nM; $n = 6$) or 4-aminopyridine (100 $\mu$M; $n = 6$); the change in discharge rate after exposure to either toxin was significant (**$p < 0.01$) when compared with the isradipine-induced silenced state.

## Discussion

Our principal conclusion is that, although L-type $Ca^{2+}$ channels contribute to the oscillatory behavior of SNc DA neurons, they are not necessary for autonomous pacemaking (Nedergaard et al., 1993; Mercuri et al., 1994; Wilson and Callaway, 2000; Puopolo et al., 2007). Our work shows that there is an interactive network of ion channels in SNc DA neurons that is capable of sustaining pacemaking even when parts of it, like L-type $Ca^{2+}$ channels, are antagonized. This finding adds another dimension to an array of other observations showing that the rate of autonomous spiking in SNc DA neurons is insensitive to a variety of extrinsic and intrinsic perturbations (Paladini et al., 2003; Chan et al., 2007), a testament to the importance of pacemaking in the maintenance of DA in target structures involved in movement, learning, and cognition.

### Pacemaking in SNc DA neurons is robust

The view that somatodendritic L-type $Ca^{2+}$ channels contribute to pacemaking in SNc DA neurons has a long history. Initially, it was found that, in the presence of the $Na^+$ channel blocker TTX, the membrane potential of SNc DA neurons continued to oscillate at near the pacemaking frequency (Yung et al., 1991; Nedergaard et al., 1993). This SOP was sensitive to blockade of $Ca^{2+}$ channels and, more importantly, to DHPs that antagonize L-type $Ca^{2+}$ channels (Nedergaard et al., 1993; Mercuri et al., 1994). The hyperpolarizing phase of this oscillation is brought about by activation of $Ca^{2+}$-activated SK $K^+$ channels (Ping and Shepard, 1996). The ability of DHPs to suppress the SOPs has been repeated by several

groups (Nedergaard et al., 1993; Chan et al., 2007). It was natural to infer from the temporal similarity of the oscillatory potential and pacemaking that the two processes were causally linked. This inference was supported by the ability of DHPs to slow or stop the regular spiking of SNc DA neurons (Nedergaard et al., 1993; Mercuri et al., 1994). However, in previous experiments, silencing typically required DHP concentrations in the low micromolar range, several orders of magnitude above the $K_D$ of DHPs for the $Ca_v1.3$ L-type $Ca^{2+}$ channels that drive the SOP.

Our work argues that the ability of DHPs at these high concentrations to slow or stop pacemaking has little to do with L-type $Ca^{2+}$ channels. There are five key pieces of experimental evidence on this point. First, $Ca^{2+}$ imaging studies showed that intracellular fluctuations in $Ca^{2+}$ concentration attributable to opening of L-type $Ca^{2+}$ channels were significantly attenuated or eliminated by application of the DHP isradipine at concentrations that did not alter pacemaking rate. Second, concentrations of isradipine that blocked SOPs did not alter pacemaking rate. Third, SOPs were less regular and often slower than pacemaking. Fourth, chelation of intracellular $Ca^{2+}$ did not stop or slow pacemaking but rather accelerated it. Last, the ability of an ectopic somatic spike to reset the $Ca^{2+}$ oscillation throughout the dendritic tree, even when there was no evidence that the spike invaded the distal dendrites, argues that $Na^+$-dependent spikes originating in the AIS (Häusser et al., 1995) pace the somatodendritic oscillations, determining their rate and regularity, not the other way around.

Simulations that incorporated realistic descriptions of the ion channels known to participate in pacemaking provided an explanation for much of the experimental data. Not only did the model generate autonomous spiking of the right rate and regularity, it also produced SOPs when $Na^+$ channels were blocked that strongly resembled those seen experimentally. The model also sustained pacemaking in the absence of L-type $Ca^{2+}$ channels, showing how the compensatory changes in other conductances served to maintain the discharge rate. Thus, the channels expressed by SNc DA neurons form an interactive network that is capable of maintaining pacemaking in the face of perturbations in the channel availability. This level of robustness should provide a means of withstanding fluctuations in channel availability as a consequence of neuromodulatory challenge or synaptically driven activity.

That said, the robustness of the model and real SNc DA neurons was limited. Combined antagonism of $Ca_v1.3$ and HCN channels stopped pacemaking, although antagonism of either alone had little or no effect, just as observed experimentally. The sensitivity of SNc DA neurons to the combined disruption of a mixed population of ion channels helps explain the effects of high DHP concentrations on pacemaking. At DHP concentrations that consistently induced silencing, isradipine reduced not only L-type $Ca^{2+}$ channel currents but $Na^+$ channel currents and leak channel currents as well. Simulations showed how this combined antagonism could account for cessation of pacemaking. This also means that experimental interventions that compromise the pacemaking mechanism could lead to a spurious elevation in the sensitivity to DHPs. Our assessment of DHP sensitivity relied primarily on cell-attached patch recordings that did not alter the intracellular environment the way whole-cell or sharp electrode recordings can. In cell-attached patch recordings, there was not a graded slowing of pacemaking with increasing DHP concentration; rather, at a well defined time point after bath application, cells continued at a normal rate, became irregular, or stopped entirely (as also described by Nedergaard et al., 1993). In our hands, this transition occurred at DHP concentrations at which other channels besides L-type $Ca^{2+}$ channels were being blocked. This was also true in our simulations. As a consequence, the slowing of pacemaking at lower DHP concentrations described by Mercuri et al. (1994) or anecdotally by Nedergaard et al. (1993) in brain slices can only be explained (within our framework) by positing that either (1) their sharp electrode recordings disrupted the capacity of these collateral ionic mechanisms to compensate for the loss of L-type channels or (2) because of lipid phase partitioning [DHP partition coefficients >1000 (Herbette et al., 1989)] and extended drug exposure, DHP concentration in the membrane had risen to levels at which non-L-type channels were being affected, despite the fact that bath concentrations were below 10 $\mu$M. The difficulty of this pharmacokinetic problem was one of the primary motivations for our use of $Ca^{2+}$ imaging to monitor fluctuations in dendritic $Ca^{2+}$ concentration during drug application, giving us a much more direct way of monitoring effective membrane concentrations of bath-applied DHPs. Although potentially an issue in brain slices, pharmacokinetics is not a major concern with acutely isolated neurons, but there are other issues. In their biophysical study, Puopolo et al. (2007) reported that low micromolar, selective concentrations of nimodipine had variable effects on pacemaking of acutely isolated DA neurons recorded with whole-cell methods, sometimes slowing or stopping pacemaking, sometimes having no effect. This variability is most readily attributed to the one variable that is poorly controlled with this approach, the degree to which dendritic and axonal arbors are truncated. Although not necessary, these are regions that very likely contribute in a material way to the robustness of pacemaking (Tepper et al., 1987; Grace and Onn, 1989; Häusser et al., 1995; Amini et al., 1999; Wilson and Callaway, 2000).

### What does this mean for a potential neuroprotective therapy in PD?

The robustness of pacemaking in SNc DA neurons has implications for neuroprotective therapies. $Ca^{2+}$ entry through L-type $Ca^{2+}$ channels renders SNc DA neurons vulnerable to a range of toxins used to create animal models of PD (Chan et al., 2007). Moreover, DHP use in humans is associated with a decreased incidence of PD (Becker et al., 2008). Isradipine is now being tested in clinical trials for its ability to modify PD progression. At the doses to be used in this study, isradipine achieves stable serum concentrations of ~2 ng/ml, which is close to the serum concentration that is neuroprotective in animal models of PD (our unpublished observations). If we assume that brain and serum concentrations are similar (Kupsch et al., 1996), isradipine should be ~5 nM in the extracellular space bathing SNc DA neurons, which should antagonize between 70 and 80% of their $Ca_v1.3$ $Ca^{2+}$ channels, assuming a modal membrane potential of −50 mV (Bean, 1984; Sinnegger-Brauns et al., 2009). Our results show that the neuroprotection afforded by this antagonism should not come at the cost of a reduction in basal pacemaking rate in SNc DA neurons.

## References

Albin RL, Young AB, Penney JB (1989) The functional anatomy of basal ganglia disorders. Trends Neurosci 12:366–375.

Amini B, Clark JW Jr, Canavier CC (1999) Calcium dynamics underlying pacemaker-like and burst firing oscillations in midbrain dopaminergic neurons: a computational study. J Neurophysiol 82:2249–2261.

Bean BP (1984) Nitrendipine block of cardiac calcium channels: high-affinity binding to the inactivated state. Proc Natl Acad Sci U S A 81:6388–6392.

Becker C, Jick SS, Meier CR (2008) Use of antihypertensives and the risk of Parkinson disease. Neurology 70:1438–1444.

Chan CS, Guzman JN, Ilijic E, Mercer JN, Rick C, Tkatch T, Meredith GE, Surmeier DJ (2007) "Rejuvenation" protects neurons in mouse models of Parkinson's disease. Nature 447:1081–1086.

Cohen MX, Frank MJ (2009) Neurocomputational models of basal ganglia function in learning, memory and choice. Behav Brain Res 199:141–156.

Gentet LJ, Williams SR (2007) Dopamine gates action potential backpropagation in midbrain dopaminergic neurons. J Neurosci 27:1892–1901.

Gonon F, Bloch B (1998) Kinetics and geometry of the excitatory dopaminergic transmission in the rat striatum in vivo. Adv Pharmacol 42:140–144.

Grace AA, Bunney BS (1984) The control of firing pattern in nigral dopamine neurons: single spike firing. J Neurosci 4:2866–2876.

Grace AA, Onn SP (1989) Morphology and electrophysiological properties of immunocytochemically identified rat dopamine neurons recorded *in vitro*. J Neurosci 9:3463–3481.

Guatteo E, Chung KK, Bowala TK, Bernardi G, Mercuri NB, Lipski J (2005) Temperature sensitivity of dopaminergic neurons of the substantia nigra pars compacta: involvement of transient receptor potential channels. J Neurophysiol 94:3069–3080.

Häusser M, Stuart G, Racca C, Sakmann B (1995) Axonal initiation and active dendritic propagation of action potentials in substantia nigra neurons. Neuron 15:637–647.

Herbette LG, Vant Erve YM, Rhodes DG (1989) Interaction of 1,4 dihydropyridine calcium channel antagonists with biological membranes: lipid bilayer partitioning could occur before drug binding to receptors. J Mol Cell Cardiol 21:187–201.

Hines ML, Carnevale NT (2001) NEURON: a tool for neuroscientists. Neuroscientist 7:123–135.

Holmes WR, Rall W (1992) Estimating the electrotonic structure of neurons with compartmental models. J Neurophysiol 68:1438–1452.

Kim SH, Choi YM, Jang JY, Chung S, Kang YK, Park MK (2007) Nonselective cation channels are essential for maintaining intracellular $Ca^{2+}$ levels and spontaneous firing activity in the midbrain dopamine neurons. Pflugers Arch 455:309–321.

Koschak A, Reimer D, Huber I, Grabner M, Glossmann H, Engel J, Striessnig J (2001) alpha 1D (Cav1.3) subunits can form l-type $Ca^{2+}$ channels activating at negative voltages. J Biol Chem 276:22100–22106.

Kupsch A, Sautter J, Schwarz J, Riederer P, Gerlach M, Oertel WH (1996) 1-Methyl-4-phenyl-1,2,3,6-tetrahydropyridine-induced neurotoxicity in non-human primates is antagonized by pretreatment with nimodipine at the nigral, but not at the striatal level. Brain Res 741:185–196.

Lipkind GM, Fozzard HA (2003) Molecular modeling of interactions of dihydropyridines and phenylalkylamines with the inner pore of the L-type $Ca^{2+}$ channel. Mol Pharmacol 63:499–511.

Mercer JN, Chan CS, Tkatch T, Held J, Surmeier DJ (2007) $Na_v1.6$ sodium channels are critical to pacemaking and fast spiking in globus pallidus neurons. J Neurosci 27:13552–13566.

Mercuri NB, Bonci A, Calabresi P, Stratta F, Stefani A, Bernardi G (1994) Effects of dihydropyridine calcium antagonists on rat midbrain dopaminergic neurones. Br J Pharmacol 113:831–838.

Nedergaard S, Flatman JA, Engberg I (1993) Nifedipine- and omega-conotoxin-sensitive $Ca^{2+}$ conductances in guinea-pig substantia nigra pars compacta neurones. J Physiol 466:727–747.

Paladini CA, Robinson S, Morikawa H, Williams JT, Palmiter RD (2003) Dopamine controls the firing pattern of dopamine neurons via a network feedback mechanism. Proc Natl Acad Sci U S A 100:2866–2871.

Ping HX, Shepard PD (1996) Apamin-sensitive $Ca^{2+}$-activated $K^+$ channels regulate pacemaker activity in nigral dopamine neurons. Neuroreport 7:809–814.

Puopolo M, Raviola E, Bean BP (2007) Roles of subthreshold calcium current and sodium current in spontaneous firing of mouse midbrain dopamine neurons. J Neurosci 27:645–656.

Schultz W (2007) Multiple dopamine functions at different time courses. Annu Rev Neurosci 30:259–288.

Sinnegger-Brauns MJ, Huber IG, Koschak A, Wild C, Obermair GJ, Einzinger U, Hoda JC, Sartori SB, Striessnig J (2009) Expression and 1,4-dihydropyridine-binding properties of brain L-type calcium channel isoforms. Mol Pharmacol 75:407–414.

Tepper JM, Sawyer SF, Groves PM (1987) Electrophysiologically identified nigral dopaminergic neurons intracellularly labeled with HRP: light-microscopic analysis. J Neurosci 7:2794–2806.

Tepper JM, Paladini CA, Celada P (1998) GABAergic control of the firing pattern of substantia nigra dopaminergic neurons. Adv Pharmacol 42:694–699.

Wilson CJ, Callaway JC (2000) Coupled oscillator model of the dopaminergic neuron of the substantia nigra. J Neurophysiol 83:3084–3100.

Yin HH, Ostlund SB, Balleine BW (2008) Reward-guided learning beyond dopamine in the nucleus accumbens: the integrative functions of cortico-basal ganglia networks. Eur J Neurosci 28:1437–1448.

Yung WH, Häusser MA, Jack JJ (1991) Electrophysiology of dopaminergic and non-dopaminergic neurones of the guinea-pig substantia nigra pars compacta in vitro. J Physiol 436:643–667.

Zolles G, Klöcker N, Wenzel D, Weisser-Thomas J, Fleischmann BK, Roeper J, Fakler B (2006) Pacemaking by HCN channels requires interaction with phosphoinositides. Neuron 52:1027–1036.

# Mitochondrial oxidant stress arising from calcium entry during pacemaking in substantia nigra dopaminergic neurons is attenuated by DJ-1

Jaime N. Guzman[1], Javier Sanchez-Padilla[1], David Wokosin[1], Jyothisri Kondapalli[2], Ema Ilijic[1], Paul T. Schumacker[2] and D. James Surmeier[1*]

Departments of Physiology[1] and Pediatrics[2], Feinberg School of Medicine, Northwestern University, Chicago, IL 60611 USA

*Corresponding author: D. James Surmeier, Department of Physiology, Feinberg School of Medicine, Northwestern University, 303 E. Chicago Ave. Chicago, IL 60611 USA, j-surmeier@northwestern.edu, 312-503-4904 (voice).

Parkinson's disease (PD) is a pervasive, aging-related neurodegenerative disease whose cardinal motor symptoms reflect the loss of a small group of neurons – dopaminergic neurons in the substantia nigra pars compacta (SNc) [1]. Mitochondrial oxidant stress is widely viewed as responsible for this loss [2], but why these particular neurons should be stressed is a mystery. Using transgenic mice that expressed a redox-sensitive variant of green fluorescent protein targeted to the mitochondrial matrix, it was discovered that the unusual engagement of plasma membrane L-type calcium channels during normal autonomous pacemaking created an oxidant stress that was specific to vulnerable SNc dopaminergic neurons. This stress engaged defenses that induced transient, mild mitochrondrial depolarization or uncoupling. The mild uncoupling was not affected by deletion of cyclophilin D, a component of the permeability transition pore, but was attenuated by genipin, an antagonist of cloned uncoupling proteins. Knocking out DJ-1, a gene associated with an early onset form of PD, compromised calcium-induced uncoupling and increased oxidation of matrix proteins specifically in SNc dopaminergic neurons. Because calcium entry through L-type channels is not essential for the normal function of SNc dopaminergic neurons and can be effectively antagonized with drugs approved for human use, these results point to a novel neuroprotective strategy for both idiopathic and familial forms of PD.

The selective vulnerability of SNc dopaminergic neurons in PD has been the subject of speculation for decades. Dopamine itself has long been suspected to be a culprit, as its oxidation leads to the generation of reactive hydroxyquinones capable of damaging proteins and dexoxyribonucleic acid (DNA) [3]. However, the recognition that boosting intracellular dopamine levels with levodopa does not accelerate disease progression [4] and that cell loss in PD is not strictly limited to neurons synthesizing dopamine [5] has motivated a search for alternative mechanisms.

Recently, it has been shown that calcium entry through voltage-dependent L-type channels during autonomous pacemaking rendered SNc dopaminergic neurons more vulnerable to mitochondrial toxins used to create animal models of PD [6]. Unlike the situation in most neurons where calcium entry is limited to the brief period during a spike, calcium entry in SNc dopaminergic neurons occurs throughout the pacemaking cycle [7] and leads to sustained oscillations in cytosolic calcium concentration, contrasting them with neighboring dopaminergic neurons in the ventral tegmental area (VTA) that are much less affected in PD (Fig. 1a,b). This influx is not necessary for pacemaking, as treatment with channel-specific concentrations of the dihydropyridine L-type channel antagonist isradipine eliminate cytosolic calcium oscillations, but leave pacemaking intact [8] (Fig. 1a).

Because cytosolic calcium must be extruded or sequestered by adenosine triphosphate (ATP)-dependent processes, its entry during pacemaking creates a metabolic burden for dopaminergic neurons. This demand for ATP is met primarily by mitochondria through oxidative phosphorylation (OXPHOS). Increasing OXPHOS inevitably comes at the cost of increasing the generation of superoxide and other reactive oxygen species (ROS) [9]. However, given the metabolic defenses against superoxide, whether this burden creates a measurable oxidant stress in SNc neurons in situ is an open question. To provide an answer, transgenic mice expressing a redox-sensitive variant of green fluorescent protein (roGFP) with a mitochondrial matrix targeting sequence (mito-roGFP) were generated [10,11]. To limit expression to monoaminergic neurons, mito-roGFP was expressed under control of the tyrosine hydroxylase promoter (Fig. 1c). Dopaminergic neurons in the SNc and the adjacent VTA from these mice

robustly expressed mito-roGFP that co-localized with mitochondrial markers (Fig. 1c-e), providing a reversible, quantitative means of monitoring oxidation of mitochondrial matrix proteins in living brain slices using two photon laser scanning microscopy (2PLSM). In VTA dopaminergic neurons, where pacemaking is not accompanied by large oscillations in intracellular calcium concentration, the basal oxidation of mito-roGFP was very low (Fig.1f). In contrast, the oxidation of mito-roGFP was significantly higher in SNc dopaminergic neurons (Fig.1f,g). Antagonizing L-type channels with isradipine dramatically lowered the extent of mito-roGFP oxidation (Fig.1g,h), as did slowing pacemaking and calcium entry by lowering the temperature of the slice (Fig. 1h) [6]. Blocking calcium entry into mitochondria with Ru360, an antagonist of the calcium uniporter [12], also significantly diminished mitochondrial oxidation (Fig. 1h). As Ru360 had no effect on pacemaking or cytosolic calcium oscillations (data not shown), this finding suggests that calcium helps to stimulate OXPHOS by entering mitochondria and up-regulating the activity of enzymes in the citric acid cycle that generate reducing equivalents for the electron transport chain [13]. Thus, calcium entry during pacemaking significantly elevated mitochondrial oxidation selectively in SNc dopaminergic neurons.

One of the proteins that participates in the mitochondrial defense against oxidant stress is DJ-1. Loss-of-function mutations in DJ-1 are linked to an autosomal recessive, early onset form of PD [14]. Although DJ-1 is not an anti-oxidant enzyme itself, it is redox-sensitive and appears to participate in signaling cascades made active by mitochondrial superoxide generation [15]. Through an unknown mechanism, DJ-1-dependent signaling decreases oxidation of isolated mitochondria and increases the resistance to electron transport chain toxins. To test whether the loss of functional DJ-1 would affect the mitochondrial oxidative state of active SNc dopaminergic neurons in situ, DJ-1 knockout mice were crossed with the TH-mito-roGFP mice, their brains sliced and examined using 2PLSM. SNc dopaminergic neurons in these slices had normal pacemaking and associated oscillations in intracellular calcium concentration (Fig. 2a). Despite this similarity, the oxidation of mito-roGFP was significantly higher in neurons lacking DJ-1 than in those with it. Basal mito-roGFP oxidation was nearly complete at physiological temperatures in these experiments, so cells were re-examined at room temperature. These studies

confirmed the robust difference in oxidation between wild-type and DJ-1 knockout neurons seen at higher temperature (Fig. 2b,c). Moreover, the impact of deleting DJ-1 on mitochondrial oxidant stress was virtually abolished by antagonism of plasma membrane L-type calcium channels (Fig. 2b,c). In contrast, the mitochondria in neighboring VTA dopaminergic neurons, which do not have the same oscillations in cytosolic calcium, were unaffected by DJ-1 deletion (Fig. 2d). These findings suggest that DJ-1 is engaged in the response to mitochondrial superoxide production and oxidant stress arising from calcium entry during pacemaking.

A clue about the role played by DJ-1 in attenuating oxidant stress came from measurements of the inner mitochondrial membrane (IMM) potential with the cationic dye tetramethyl rhodamine methylester (TMRM) (Fig. 3a; Supplemental movie) [13]. In VTA dopaminergic neurons, TMRM fluorescence was robust and stable for long periods (Fig. 3b). In contrast, mitochondrial TMRM fluorescence in neighboring SNc dopaminergic neurons repeatedly fell and then rose back to peak values, indicating that mitochondria were transiently depolarizing (Fig. 3b; Supplementary movie). This 'flickering' was stable for long periods (>60 minutes), arguing that it was not a consequence of an acute stress. To calibrate the TMRM signal, fluorescence was monitored after application of the ATP synthase inhibitor oligomycin to fully polarize mitochondria. These studies indicated that there was little or no quenching at the TMRM concentrations used in these assays; moreover, they excluded a role for ATP synthase in the origins of the flickering. To estimate the relative change in mitochondrial potential during the flickering, a Nernst equation relating IMM potential to the ratio of mitochondrial to nuclear TMRM fluorescence was used [16]. This analysis indicated that the flickering in mitochondrial potential was only about 15-20% of the maximum potential, corresponding to a mild IMM depolarization of 20-30 mV.

Antagonizing plasma membrane L-type calcium channels with isradipine dramatically reduced the rate of flickering (Fig. 3c; Supplemental movie), as did blocking calcium entry into the mitochondria with Ru360 (Fig. 3c). However, flickering was also attenuated by scavenging ROS with the cell-permeable antioxidant N-(2-mercaptopropionyl)-glycine (MPG) (Fig. 3d), implicating oxidant stress created by calcium entry, rather than calcium per se, was responsible

for the mitochondrial flickering. Superoxide generation is known to trigger the opening of two types of ion channel that depolarize the IMM. One of these is the permeability transition pore (PTP) [17]. However, TMRM flickering in SNc dopaminergic neurons lacking cyclophilin D – a key modulator of the PTP [18] – was intact (Fig. 3e), arguing against a role for the PTP. Cyclosporin A, an immunosuppressant that is known to antagonize the PTP [19], decreased IMM flickering, but it also slowed or stopped pacemaking (and calcium influx), making it an unreliable diagnostic tool (data not shown). The uncoupling proteins (UCPs) are another class of mitochondrial ion channel whose open probability is increased by superoxide [20]. By creating a leak across the IMM, UCPs uncouple OXPHOS from ATP synthesis. UCP opening decreases the IMM potential modestly [21], making it a plausible mediator of the 10-20% drop in IMM potential inferred from the TMRM measurements. Five UCPs have been cloned, three of which are robustly expressed in the SNc (UCP2,4,5) [20,22]. Application of the UCP antagonist genipin [23] significantly decreased the frequency and amplitude of mitochondrial flickering (Fig. 3e). Because UCP2 increases the resistance of SNc dopaminergic to toxins [22], mitochondrial behavior was examined in neurons from UCP2 knockout mice. Mitochondrial flickering was normal in these neurons, implicating UCP4 or UCP5 in the phenomenon (data not shown).

UCP activation diminishes superoxide generation, creating a protective, negative feedback system to complement enzymatic defenses against ROS [24,25]. Although it has not been described previously, the observed flickering or the apparent switching of the UCPs on-and-off is precisely what would be expected of a negative feedback system with a threshold (e.g., a furnace connected to a thermostat). Because the kinetics of mito-roGFP are slow compared to those of TMRM, it was not possible to determine whether mitochondrial potential was tracking superoxide generation. But if this interpretation is correct, then disrupting UCP activation with genipin should increase the oxidation of mitochondrial proteins. Indeed, genipin significantly elevated oxidation of mito-roGFP in SNc dopaminergic neurons, whereas it had no effect on mitochondrial oxidation in VTA dopaminergic neurons where the UCP defense was not engaged (Fig. 3f). In SNc dopaminergic neurons from DJ-1 knockouts, mitochondrial flickering was significantly impaired (Fig. 3g), suggesting that DJ-1 helps link superoxide generation to UCP

activation. The disruption of this protective feedback mechanism therefore provides a ready explanation for the elevation in mitochondrial oxidation in DJ-1 knockouts and its reversal with removal of the metabolic load created by L-type calcium channels.

Collectively, our studies demonstrate that calcium influx during normal, autonomous pacemaking in SNc dopaminergic neurons significantly elevates mitochondrial oxidant stress, engaging a DJ-1-dependent defense mechanism involving UCPs. Mitochondrial oxidant stress has long been thought to be central to the etiology of PD [2]. However, there has been no explanation for why this stress should be greater in a small population of mesencephalic neurons. Our results fill this key gap in our understanding (Fig. 4). This basal oxidant stress is amplified by deletion of DJ-1, a gene associated with an early onset, familial form of PD. Without this basal stress, deletion of DJ-1 had no measurable effect, as demonstrated by the normality of DJ-1 deficient VTA dopaminergic neurons and near complete removal of oxidant stress in DJ-1 deficient SNc dopaminergic neurons by antagonizing L-type calcium channels. The suggestion that DJ-1 enhances the activation of UCPs in response to superoxide production agrees with studies pointing to a redox signaling role for DJ-1 [15]. However, whether DJ-1 directly participates in mitochondrial signaling or is indirectly involved, for example, by regulating the expression UCPs in response to sustained oxidant stress, remains to be determined.

The high basal mitochondrial oxidant stress in SNc dopaminergic neurons helps to explain why age is the principal risk factor in PD. Although aging is complex, declining mitochondrial competence is widely viewed a key part of this process [26]. In humans, SNc dopaminergic neurons accumulate more mitochondrial DNA (mtDNA) mutations with age than neurons in other brain regions [27,28]. These mutations, which are attributable to superoxide exposure, diminish mitochondrial competence and promote phenotypic decline, proteostatic impairments and eventual neuronal death [29,30]. Mice in which the respiratory capacity of mitochondria has been compromised in SNc dopaminergic neurons, rapidly develop a PD phenotype replete with intracellular inclusions and neuronal loss [31]. Furthermore, in primates and humans, there are clear signs of accelerated phenotypic decline in the SNc with normal aging [32,33]. Against this backdrop, it not surprising that genetic mutations or environmental toxins that further

compromise mitochondrial function would accelerate this decline and reduce the age at which cell loss crosses the symptomatic threshold [2,34,35]. Lastly, the proposition that physiological phenotype is a major risk factor provides a framework for understanding the broader neuronal pathology in PD [36].

Because the L-type calcium channels underlying oxidant stress can be effectively antagonized by dihydropyridines that have a long history of safe use in humans [37], our results point clearly to a novel neuroprotective strategy for idiopathic and familial forms of PD. The proposition that dihydropyridines are neuroprotective is supported by retrospective epidemiological studies, showing that patients using them for hypertension have a lower incidence of PD [38,39]. Nevertheless, a prospective clinical trial will be required to unequivocally determine their therapeutic value in slowing or stopping the progression of PD.

## Methods Summary

Mice between postnatal ages P21 and P30 were used for these studies. Mice were handled according to the guidelines established by the Northwestern University Animal Care and Use Committee, the National Institutes of Health and the Society for Neuroscience. Slices containing the mesencephalon were transferred to a submersion-style recording chamber; SNc and VTA neurons were initially visualized with an infrared-differential interference contrast (IR-DIC) video microscopy system (for patch clamp recording) and subsequently imaged with 2PLSM using a Ti:sapphire pulsed laser tuned to 810 nm for dendritic measurements of calcium transients, 830 nm for TMRM imaging of mitochondrial membrane potential, and 920 nm for imaging of mitochondrial roGFP signal. Fluorescence emission for mitochondrial imaging was collected with fixed location and dimensional region of interests by non-descanned photomultiplier tubes. For calcium imaging experiments, VTA or SNc neurons were filled with 50 μM Alexa594 and 200 μM Fluo-4 with a patch electrode and dendritic calcium transients were imaged as described previously [8]. In TMRM experiments, mitochondrial membrane potential was calculated using a Nerst equation describing the distribution of the dye [16] (See Full Methods). Transgenic mice were generated with conventional approaches with a construct containing the tyrosine hydroxylase promoter and a matrix mitochondria targeting DNA sequence (obtained

from cytochrome oxidase subunit 4). Relative oxidation of mito-roGFP was determined from fluorescence measurements after fully reducing mitochondria with dithiothreitol and fully oxidizing with aldrithiol. Primers and reaction protocols for single-cell reverse transcription-polymerase chain reaction (scRT-PCR) have been described previously [6]. Statistical analysis of data was performed with non-parametric tests: Mann-Whitney Rank Sum Test for comparing between two groups or Kruskal Wallis analysis of variance (ANOVA) with Dunnet's post hoc for multiple group comparison. Paired statistical analyses were performed using the Wilcoxon Signed Rank Test. Probability (P) threshold for statistical significance was 0.05.


1 Albin, R. L., Young, A. B. & Penney, J. B. The functional anatomy of disorders of the basal ganglia. Trends Neurosci 18, 63-64, (1995).

2 Schapira, A. H. Mitochondria in the aetiology and pathogenesis of Parkinson's disease. Lancet Neurol 7, 97-109, (2008).

3 Sulzer, D. Multiple hit hypotheses for dopamine neuron loss in Parkinson's disease. Trends Neurosci 30, 244-250, (2007).

4 Fahn, S. Does levodopa slow or hasten the rate of progression of Parkinson's disease? J Neurol 252 Suppl 4, IV37-IV42, (2005).

5 Braak, H. et al. Pathology associated with sporadic Parkinson's disease--where does it end? J Neural Transm Suppl, 89-97, (2006).

6 Chan, C. S. et al. 'Rejuvenation' protects neurons in mouse models of Parkinson's disease. Nature 447, 1081-1086, (2007).

7 Puopolo, M., Raviola, E. & Bean, B. P. Roles of subthreshold calcium current and sodium current in spontaneous firing of mouse midbrain dopamine neurons. J Neurosci 27, 645-656, (2007).

8 Guzman, J. N., Sanchez-Padilla, J., Chan, C. S. & Surmeier, D. J. Robust pacemaking in substantia nigra dopaminergic neurons. J Neurosci 29, 11011-11019, (2009).

9 Lambert, A. J. & Brand, M. D. Reactive oxygen species production by mitochondria. Methods Mol Biol 554, 165-181, (2009).

10 Dooley, C. T. et al. Imaging dynamic redox changes in mammalian cells with green fluorescent protein indicators. J Biol Chem 279, 22284-22293, (2004).

11 Hanson, G. T. et al. Investigating mitochondrial redox potential with redox-sensitive green fluorescent protein indicators. J Biol Chem 279, 13044-13053, (2004).

12 Matlib, M. A. et al. Oxygen-bridged dinuclear ruthenium amine complex specifically inhibits Ca2+ uptake into mitochondria in vitro and in situ in single cardiac myocytes. J Biol Chem 273, 10223-10231, (1998).

13 Nicholls, D. G. & Ferguson, S. J. Bioenergetics 3. [3rd edn, (Academic Press, 2002).

14 Moore, D. J., West, A. B., Dawson, V. L. & Dawson, T. M. Molecular pathophysiology of Parkinson's disease. Annu Rev Neurosci 28, 57-87, (2005).

15 Kahle, P. J., Waak, J. & Gasser, T. DJ-1 and prevention of oxidative stress in Parkinson's disease and other age-related disorders. Free Radic Biol Med, (2009).

16 Ehrenberg, B., Montana, V., Wei, M. D., Wuskell, J. P. & Loew, L. M. Membrane potential can be determined in individual cells from the nernstian distribution of cationic dyes. Biophys J 53, 785-794, (1988).
17 Rasola, A. & Bernardi, P. The mitochondrial permeability transition pore and its involvement in cell death and in disease pathogenesis. Apoptosis 12, 815-833, (2007).
18 Schinzel, A. C. et al. Cyclophilin D is a component of mitochondrial permeability transition and mediates neuronal cell death after focal cerebral ischemia. Proc Natl Acad Sci U S A 102, 12005-12010, (2005).
19 Nazareth, W., Yafei, N. & Crompton, M. Inhibition of anoxia-induced injury in heart myocytes by cyclosporin A. J Mol Cell Cardiol 23, 1351-1354, (1991).
20 Krauss, S., Zhang, C. Y. & Lowell, B. B. The mitochondrial uncoupling-protein homologues. Nature reviews 6, 248-261, (2005).
21 Brand, M. D. et al. Mitochondrial superoxide: production, biological effects, and activation of uncoupling proteins. Free Radic Biol Med 37, 755-767, (2004).
22 Andrews, Z. B. et al. Uncoupling protein-2 is critical for nigral dopamine cell survival in a mouse model of Parkinson's disease. J Neurosci 25, 184-191, (2005).
23 Zhang, C. Y. et al. Genipin inhibits UCP2-mediated proton leak and acutely reverses obesity- and high glucose-induced beta cell dysfunction in isolated pancreatic islets. Cell Metab 3, 417-427, (2006).
24 Papa, S. & Skulachev, V. P. Reactive oxygen species, mitochondria, apoptosis and aging. Mol Cell Biochem 174, 305-319, (1997).
25 Echtay, K. S. et al. Superoxide activates mitochondrial uncoupling proteins. Nature 415, 96-99, (2002).
26 Trifunovic, A. Mitochondrial DNA and ageing. Biochim Biophys Acta 1757, 611-617, (2006).
27 Bender, A. et al. High levels of mitochondrial DNA deletions in substantia nigra neurons in aging and Parkinson disease. Nat Genet 38, 515-517, (2006).
28 Bender, A. et al. Dopaminergic midbrain neurons are the prime target for mitochondrial DNA deletions. J Neurol 255, 1231-1235, (2008).
29 Krishnan, K. J., Greaves, L. C., Reeve, A. K. & Turnbull, D. M. Mitochondrial DNA mutations and aging. Ann N Y Acad Sci 1100, 227-240, (2007).
30 Nicholls, D. G. Oxidative stress and energy crises in neuronal dysfunction. Ann N Y Acad Sci 1147, 53-60, (2008).
31 Ekstrand, M. I. et al. Progressive parkinsonism in mice with respiratory-chain-deficient dopamine neurons. Proc Natl Acad Sci U S A 104, 1325-1330, (2007).
32 Stark, A. K. & Pakkenberg, B. Histological changes of the dopaminergic nigrostriatal system in aging. Cell Tissue Res 318, 81-92, (2004).
33 Collier, T. J. et al. Aging-related changes in the nigrostriatal dopamine system and the response to MPTP in nonhuman primates: diminished compensatory mechanisms as a prelude to parkinsonism. Neurobiol Dis 26, 56-65, (2007).
34 Riederer, P. & Wuketich, S. Time course of nigrostriatal degeneration in parkinson's disease. A detailed study of influential factors in human brain amine analysis. J Neural Transm 38, 277-301, (1976).
35 Betarbet, R. et al. Intersecting pathways to neurodegeneration in Parkinson's disease: Effects of the pesticide rotenone on DJ-1, alpha-synuclein, and the ubiquitin-proteasome system. Neurobiol Dis 22, 404-420, (2006).

36 Braak, H., Ghebremedhin, E., Rub, U., Bratzke, H. & Del Tredici, K. Stages in the development of Parkinson's disease-related pathology. Cell Tissue Res 318, 121-134, (2004).
37 Eisenberg, M. J., Brox, A. & Bestawros, A. N. Calcium channel blockers: an update. Am J Med 116, 35-43, (2004).
38 Becker, C., Jick, S. S. & Meier, C. R. Use of antihypertensives and the risk of Parkinson disease. Neurology 70, 1438-1444, (2008).
39 Ritz, B. et al. L-Type Calcium Channel blockers and Parkinson's Disease in Denmark. Annals Neurology, (in press).

Competing Financial Interests: None

Acknowledgments: We acknowledge the technical help of Philip Hockberger, Nicholas Schwarz, Sasha Ulrich and Karen Saporito. We acknowledge the gifts of DJ-1 knockout mice from Ted and Valina Dawson, Johns Hopkins University, UCP2 knockout mice from Dong Kong and Bradford Lowell, Harvard University and cyclophilin D knockout mice from Stanley J. Korsmeyer, Harvard University. This work was supported by the Picower Foundation, the Hartman Foundation, the Falk Trust and NIH grants NS047085 (DJS), NS 054850 (DJS) and HL35440 (PTS) and RR025355 (PTS) and DOD contract W81XWH-07-1-0170 (DJS).

Author contributions: Dr. Surmeier was responsible for the overall direction of the experiments, analysis of data, construction of figures and communication of the results. Drs. Guzman and Sanchez were responsible for the design and execution of experiments, as well as the analysis of results. Dr. Wokosin was responsible for the construction of the imaging workstations and the design of the mitochondrial imaging experiments. Dr. Ilijic assisted with image processing and analysis of data.Drs. Schumacker and Kondapalli were responsible for the generation of the TH-mito-roGFP mice; they also participated in the design, analysis and communication of the results.

Figure legends:

Figure 1. Calcium influx through L-type calcium channels during pacemaking increases mitochondrial oxidant stress in SNc dopaminergic neurons. (a) Whole cell recording from an SNc dopaminergic neuron (shown to the left as a projection image) in pacemaking mode. At the bottom of the trace, a 2PLSM measurement of dendritic Fluo-4 fluorescence (red trace) before and after blocking L-type calcium channels with 5 μM isradipine. Calcium transients in SNc neuron were absent following isradipine (green trace) (n=10 neurons, $P<0.05$). (b) As in panel a but with a VTA neuron which do not display calcium oscillation in dendrites (n=6 neurons). (c) Schematic of the TH-mito-roGFP construct. Below the construct, single-cell RT-PCR analysis of mito-roGFP expressing SNc dopaminergic neurons showing expression of tyrosine hydroxyalse (TH) and Cav1.3 but not calbindin or GAD67; similar results were obtained in all 5 neurons examined. (d) Top, a low magnification image of the mesencephalon of a transgenic TH-mito-roGFP mouse showing expression in SNc and VTA neurons; Bottom, a high magnification image of an SNc neuron showing labeling in cytoplasmic but not nuclear compartments; Right, overlay of mitoTracker red staining showing colocalization with mito-roGFP. (f) mito-roGFP measurements from a VTA neuron; before (control, black trace), and after application of 2 mM dithiothreitol (DTT) (green trace), and 100 μM alditriol (red trace). Relative oxidation $(1-(F-F_{ald})/(F_{DTT}-F_{ald}))$ was plotted as a function of time and treatement condition. (g) mito-roGFP measurements from an SNc dopaminergic neuron (black trace), revealing a higher basal oxidation than in VTA neurons; treatment with 5 μM isradipine diminished mitochondrial oxidation (green trace). (h) Left, box-plots summarizing mean redox measurements in VTA (n=9) and SNc dopaminergic neurons (n=14) in control conditions; SNc neurons were significantly more oxidized ($P<0.05$); Right, box plots of mean redox measurements after antagonizing L-type channels with isradipine (5 μM, n=9) or blocking the mitochondrial uniporter with Ru360 (10 μM, n=8), both were significantly less oxidized than controls ($P<0.05$). (i) Box plots summarizing mean mito-roGFP measurements in SNc dopaminergic neurons in brain slices held at near physiological temperature (30-32°C)(n=14) and at room temperature (20-22°C) (n=5); oxidation was significantly less at room temperature ($P<0.05$). Statistical significance in all plots is shown by an asterisk.

Figure 2. Activity-dependent oxidant stress is elevated in SNc dopaminergic neurons from DJ-1 knockout mice. (a) Whole cell recording from a SNc dopaminergic neuron in a brain slice from a DJ-1

knockout mouse showing normal pacemaking (top) and normal intracellular calcium oscillations (bottom); similar results were seen in all five neurons examind. (b) In SNc dopaminergic neurons from DJ-1 knockouts, mitochondrial mito-roGFP oxidation was higher (red trace) than in control neurons (black trace); isradipine (200 nM) pretreatment normalized oxidation of mito-roGFP (green trace); experiments were done at 20-22 °C. (c) Box plot summarizing mean mito-roGFP measurements in wild-type SNc neurons (n=9), DJ-1 knockout SNc neurons (n=6) and DJ-1 knockout neurons after isradipine pretreatment (n=7); differences between wild-type and DJ-1 knockout were significant ($P<0.05$), as were differences between knockouts with and without isradipine treatment ($P<0.05$). (d) Box plot summarizing mean mito-roGFP measurements from wild-type VTA dopaminergic neurons (n=9), wild-type SNc dopaminergic neurons (n=14) and DJ-1 knockout VTA dopaminergic neurons (red box) (n=4) and at 34-35 °C. In contrast to SNc dopaminergic neurons, mito-roGFP oxidation in VTA dopaminergic neurons were unaffected by DJ-1 deletion ($P>0.05$).

Figure 3. Oxidant stress induces DJ-1-dependent oscillation in mitochondrial membrane potential (a) SNc dopaminergic neuron in a brain slice incubated with tetramethyl rhodamine methyl ester (TMRM), revealing mitochondrial labeling; a region of interest (ROI) from which fluorescence measurments were taken is shown (yellow circle). (b) Representative fluorescence time-series from an SNc dopaminergic neuron (black trace) before and after rotenone (200 nM) (red trace) application; similar results were seen in all cells examined (n>21). For comparison, a time series from a typical VTA dopaminergic neuron is shown (blue trace). (c) Left, TMRM fluorescence measurements before (black trace) and after bath application of isradipine (green trace); Right, box plots summarizing the mean frequency of flickering in control cells and after application of isradipine (5 μM, n=5) or Ru360 (10 μM, n=6), both drugs significantly slowed flickering frequency ($P<0.05$); box plots summarizing the mean amplitude of voltage change inferred from the fluorescence measurement (relative to the maximum potential), the amplitudes were similar in all conditions. in the same conditions. (d) Left, fluorescence time series before and after bath application of the ROS scavenger MPG (2 mM) (green trace), showing a drop in flickering frequency but not amplitude; Right, box plots summarizing mean frequency and amplitude measurements (n=5); MPG significantly reduced the frequency ($P<0.05$) but not the amplitude ($P>0.05$) of flickering. (e) Left, fluorescence time series in control and after application of genipin (100 μM) (green trace), which decreased the frequency and amplitude of the

flickering; Right, box plots summarizing mean amplitude and frequency measurements in control , and after genipin (n=5), genipin significantly decreased both parameters ($P<0.05$); also shown are plots of data from cyclophilin D knockouts, which did not affect either measure (n=10; $P>0.05$). (f) Left, mito-roGFP measurements as in Figure 1 before and after application of genipin (100 μM) (red trace) to an SNc dopaminergic neuron, which increased oxidation; Right, box plots summarizing mean oxidation measurements following isradipine application (green box) (n=9), genipin (red box) (n=6) to SNc dopaminergic neurons, isradipine significantly decreased oxidation, whereas genipin increased oxidation ($P<0.05$); also show are oxidation measurements from VTA dopaminergic neurons following genipin where there was no change from control measurements (n=5, $P>0.05$). (g) Left, TMRM fluorescence measurement from a wild-type SNc dopaminergic neuron (black trace) and a DJ-1 knockout (red trace), showing a reduction in flickering amplitude and frequency; Right, box plots of mean frequency and amplitude data from wild-type (n=21) and DJ-1 knockout neurons (n=7); both amplitude and frequency of flickering were decreased in DJ-1 knockouts ($P<0.05$).

Figure 4. Schematic summary of the results presented linking calcium entry through L-type channels during pacemaking with elevated mitochondrial oxidant stress. The model proposes that oxidant stress arises from ATP utilization and calcium entry into mitochondria through the uniporter. This combined stimulus drives OXPHOS leading to increased production of superoxide, the opening of uncoupling proteins (UCPs) to mildly uncouple the inner mitochondrial membrane diminishing superoxide generation. This negative feedback mechanism should have a threshold, accounting for the turning on and off of UCPs. Schematic also shows the potential contribution of NMDA receptors to the calcium mediated metabolic stress.

## Supplementary Movie:

Time lapsed 2PLSM image showing TMRM fluorescence in a SNc dopaminergic neuron before and after bath application of isradipine (5 μM). Note the decreased flickering after application of isradipine. Similar results were seen in all of the neurons examined (n>20).

## ONLINE METHODS

Tissue Preparation. Acute midbrain coronal slices (220 μm-thick) were obtained from male mice between postnatal ages 21 and 28 days, unless specified otherwise. The handling of mice and all procedures performed on them were approved by the institutional Animal Care and Use Committee and were in accordance with the 'National Institutes of Health Guide to the Care and Use of Laboratory Animals' and Society for Neuroscience guidelines. Mice were anesthetized with a ketamine/xylazine mixture followed by a transcardial perfusion with ice-cold, oxygenated artificial cerebrospinal fluid (ACSF) containing (in mM): 125 NaCl, 2.5 KCl, 25 $NaHCO_3$, 1.25 $NaH_2PO_4$, 2 $CaCl_2$, 1 $MgCl_2$, and 25 dextrose, pH 7.3, osmolality 315-320 mOsm/L. After perfusion, mice were decapitated and brains were removed rapidly, followed by sectioning in ice-cold oxygenated ACSF using a vibratome (VT1000S Leica Microsystems, Nusslock, Germany). Midbrain slices were kept at 34 degrees centigrade for 30 minutes prior to two-photon laser scanning microscopy (2PLSM) imaging experiments. dopaminergic neurons from the ventral tier of the SNc were identified during the imaging experiments based on anatomical location in the slice and cell body size (bregma -2.92 mm), and VTA neurons were identified on its anatomical location medial to the SNc.

Generation of transgenic mice carrying tyrosine hydroxylase promoter driven mitochondrial targeted roGFP gene. The oxidation-reduction status of the mitochondrial matrix was assessed by targeting the expression of a redox-sensitive green fluorescence protein (roGFP) to that compartment. This sensor exhibits ratiometric changes in absorption at 400 and 484 nm in response to changes in the oxidation status of two cysteine thiols located in the outer surface of the protein [4]. roGFP plasmid was generated from the pEGFP-N1 plasmid (CLONTECH, Palo Alto, CA) by substitutingsurface-exposed residues on eGFP with cysteines in appropriate positions as previously described using a QuickChange site directed mutagenesis kit (Stratagene). To express roGFP to mitochondria, the matrix targeting sequence (MTS) from cytochrome oxidase subunit 4 was added at the amino terminus using a primer pair 5'AAT GCC GCT AGC GCC ACC ATG CTG AGC CTG CGC CAG AGC ATC CGC TTC TTC AAG CGC AGC GG CAT CAT GGT GAG CAA GGG CGA GGA GCT G -3' and 5'-CCG CTC GAG TTA CTT GTA CAG CTC GTC CAT GCC-3' while adding restriction sites for Nhe I and Xho I (underlined?). The resulting PCR product was cloned into the pcDNA 3.1(+) vector (invitrogen). MTS-roGFP was again amplified using primer pair 5'-AAT GCC GAT ATC GCC ACC ATG CTG AGC - 3' and 5'-CCG CTC GAG TTA CTT GTA CAG CTC GTC CAT GCC -3' while adding restriction sites for EcoRV and Xho I (underlined?). PCR products were cloned in pCR4-TOPO vector (invitrogen) and excised with EcoRI.

To drive expression in dopaminergic neurons, this construct was ligated into the TH-SK3-PA plasmid containing the tyrosine hydroxylase (TH) promoter, a 9.0 kb genomic fragment, located 5' to the EcoRI restriction site. The TH-SK3-PA vector was kindly provided by Dr. Xiaoxi Zhuang at the University of Chicago, with permission from Dr. Jin H. Son, Laboratory of Molecular Neurobiology, The W. M. Burke Medical Research Institute, White Plains, New York) [5]. Correct orientation of the gene was verified by sequencing. To enable in vivo expression of MTS-roGFP in dopaminergic neurons, a 10.5 kb Sal I and Hind III fragment containing TH promoter/MTS-roGFP/polyadenylation sequences was purified by 0.8% agarose gel electrophoresis, and eluted with an Elutip column as per the manufacturer's instructions (Whatman Schleicher & Schuell). The purified DNA was used to generate transgenic mice by pronuclear microinjection in the University Transgenic and Targeted Mutagenesis core. Several founder transgenic mice were identified by PCR using primers that hybridize with eGFP. The founders for the roGFP mice were generated in a B6SJL genetic background and backcrossed to C57BL6 for our imaging experiments.

2PLSM: Calcium Imaging: For dendritic measurements, SNc dopaminergic neurons in tissue slices (as described above) were loaded with Alexa Fluor 594 (50 μM) and Fluo-4 (200 μM) through the patch pipette. All experiments were performed at 32-34° C. Images were acquired with a 60X/0.9NA water-immersion lens. Dyes were allowed to equilibrate for at least 15 minutes prior to imaging. The two-photon excitation source was a Chameleon-ultra2 tunable laser system (680 nm to 1080 nm) utilizing Ti:sapphire gain medium with all-solid-state active components and a computer-optimized algorithm to ensure reproducible excitation wavelength, average power, and peak power (Coherent Laser Group, Santa Clara, CA). Optical signals were acquired using 810 nm excitation beam (80MHz pulse repetition frequency and ~250fs pulse duration) to simultaneously excite Alexa and Fluor-4 dyes. Laser power attenuation was achieved with two Pockel cell electro-optic modulators (models 350-80, Con Optics, Danbury, CT). The two cells are aligned in series to provide enhanced modulation range for fine control of the excitation dose (0.1% steps over four decades). The laser-scanned images were acquired with a Bio-Rad Radiance MPD system (Hemel Hempstead, England, UK). The fluorescence emission was collected by external or non-de-scanned photomultiplier tubes (PMTs). The green fluorescence (500-550 nm) was detected by a bialkali-cathode PMT and the red fluorescence (580-640 nm) was collected by a multi-alkali-cathode (S-20) PMT. The system digitizes the current from detected photons to 12 bits. The laser light transmitted through the sample was collected by the condenser lens and sent to another PMT to provide a bright-field transmission image in registration with the fluorescent images. Measurements were taken in a sample plane along dendritic segments (100-150 mm from the soma). Line scan signals were

acquired (as described above) at 6 ms per line and 512 pixels per line with 0.18 μm pixels and 10 μs pixel dwell time. The time between the control and isradipine treatment measurements was 5-7 minutes.

2PLSM: Tetramethyl rhodamine methyl ester (TMRM) mitochondrial imaging. Brain slices from wild-type or DJ-1 knock-out mice (mixed background C57BL6x129SvEv) were incubated in 2-4 μTMRM for 30 minutes at 32-34followed by excess dye wash-out in TMRM-free ACSF solution. Imaging experiments were performed with TMRM-free ACSF solution at physiological temperatures (32-34). fluorescence (550-640 nm) was collected by a multi-alkali-cathode (S-20) PMT and a DODT contrast detector system provided bright-field transmission image (Prairie Technologies). The two-photon excitation source was a Chameleon-ultra2 tunable laser system (706 nm to 1000 nm) utilizing Ti:sapphire gain medium with all-solid-state active components and a computer-optimized algorithm to ensure reproducible excitation wavelength, average power, and peak power (Coherent Laser Group, Santa Clara, CA). Flickering activity was taken until a stable baseline activity was obtained. Slices with drifting baseline activity (due to photobleaching of dye and/or wash-out) were discarded from data. signals were acquired using 830 nm excitation beam (80MHz pulse repetition frequency and ~250fs pulse duration), in a fixed plane of focus with a pixel size between 0.18-0.21 μm. Time-series scanning (1000 frames) in a fixed plane was performed with a 4 μs dwell time at a rate of 2.5 frames per second. Time course of drug incubation was performed for all experiments with periods of drug incubation ranging between 30-60 minutes and compared to baseline control activity. Four to five regions of interest (ROIs) in the cell body plus one ROI in the nucleus with fixed location and dimensions were taken and changes in TMRM fluorescence (in arbitrary units) were plotted as a function of time. Flickering frequency was determined by counting the number of transitions in 100 sec epochs; and fluorescence histograms were calculated with MatLab. ROIs were compared before and after drug treatment. The change in mitochondrial membrane potential during flickering was estimated from the fluorescence in an ROI using a Nernst equation: $V= (RT/zF)\ln(\beta/F)$ where R is the gas constant, T is temperature, F is Faraday's constant, z=1, F=the fluorescence in the mitochondrial ROI, Fis the fluorescence of the nucleus in the same optical plane and βis a scaling factor . The scaling factor was calculated by assuming that the mitochondrial membrane potential was -150 mV when Fmaximal. For each flickering event, the percent change in Vwas calculated by taking the difference in the estimates before and then during the drop in fluorescence; the fluorescence during the drops was averaged to allow a single number to be generated. Because the application of oligomycin did not significantly change the maximal TMRM fluorescence in any of the situations described here, Vestimates could reasonably be compared across cells and experiments.

2PLSM: Mitochondrial roGFP imaging. Midbrain slices from wild-type roGFP transgenic mice or DJ-1 knock-out mice (crossed to roGFP transgenic mice) were incubated in ACSF at physiological temperatures (32-34) followed by a recovery period at room temperature. Optical imaging of roGFP signals acquired using 920 nm excitation beam (80MHz pulse repetition frequency and ~250fs pulse duration), in a fixed plane of focus with a pixel size between 0.18-0.21 μm and a 2-3 μs pixel dwell time. two-photon excitation source was a Chameleon-ultra2 tunable laser system (706 nm to 1000 nm) utilizing Ti:sapphire gain medium with all-solid-state active components and a computer-optimized algorithm to ensure reproducible excitation wavelength, average power, and peak power (Coherent Laser Group, Santa Clara, CA). The roGFP fluorescence (490-560 nm) was detected by a bialkali-cathode PMT and a DODT contrast detector system provided bright-field transmission image (Prairie Technologies). Sixty frames of the roGFP signal were collected in one optical plane at a rate of 3-4 frames per second. All experiments were performed at room temperature followed by physiological temperatures (-34). with drifting baseline activity (due to photobleaching or photooxidation of roGFP signal) were discarded from data. the end of all experiments, relative oxidation before and after drug was monitored following application of 2 mM dithiothreitol (DTT) to fully reduce the mitochondria, then 200 μalditriol (ald) to fully oxidize mitochondria. Relative oxidation was then calculated by the equation '1-[(F-F)/FF)]'.

Statistical Analysis: Imaging data collected was analyzed with Igor Pro 6.0 (Wavemetrics, CA) or Matlab (Mathworks, Inc., Natick, MA). The stimulation, display, and analysis software for the two-photon imaging data was analyzed using a custom-written shareware package, WinFluor, PicViewer and PowerCAL kindly provided by John Dempster (Strathclyde University, Glasgow, Scotland; UK). Data was summarized either using box-plots showing median values for small sample sizes (n=6-10 neurons). Statistical analysis was done with SigmaStat 3.5 (Systat Software, Chicago, IL) using non-parametric testing Mann-Whitney Rank Sum Test for comparing between two groups or Kruskal Wallis ANOVA with Dunnet's post hoc for multiple group comparison. Before-after statistical analyses were performed using the Wilcoxon Signed Rank Test. Probability (p) threshold for statistical significance was $p<0.05$.

Pharmacological Reagents and channel ligands: Reagents were purchased from Sigma (St.Louis, MO) except for isradipine, DTT, (Tocris-Cookson), TMRM and Fura-2, (Invitrogen/Molecular Probes), genipin (Sigma and Wako Reagents). Drugs stocks solutions were prepared in deionized water, DMSO, ethanol, or methanol as instructed by manufacturer on the day of experiment. Stocks were diluted to final concentrations in ACSF to achieve a final solvent concentration of less than 0.1% v/v.

References:

1 J. N. Guzman, J. Sanchez-Padilla, C. S. Chan et al., J Neurosci 29 (35), 11011 (2009).

2 C. S. Chan, J. N. Guzman, E. Ilijic et al., Nature 447 (7148), 1081 (2007).

3 Hanson GT, Aggeler R, Oglesbee D et al., J Biol Chem 279 (13), 13044 (2004).

4 Dooley CT, Dore TM, Hanson GT et al., J Biol Chem 279 (21), 22284 (2004).

5 Son JH, Chun HS, Joh TH et al., J Neurosci 19 (1), 10 (1999).

6 W. J. Koopman, F. Distelmaier, J. J. Esseling et al., Methods (San Diego, Calif 46 (4), 304 (2008).

Figure 1: Guzman et al.

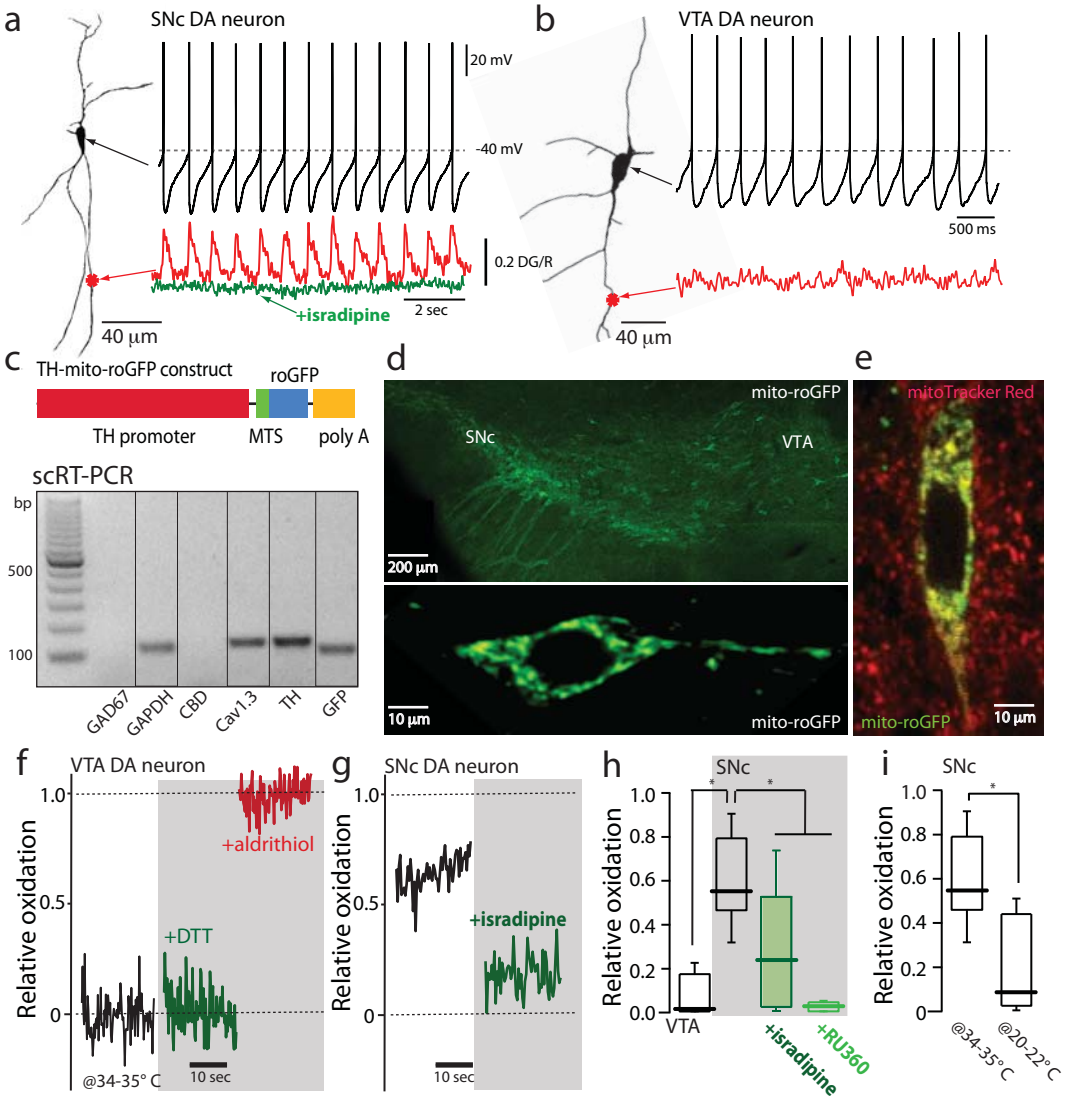

Figure 2: Guzman et al.

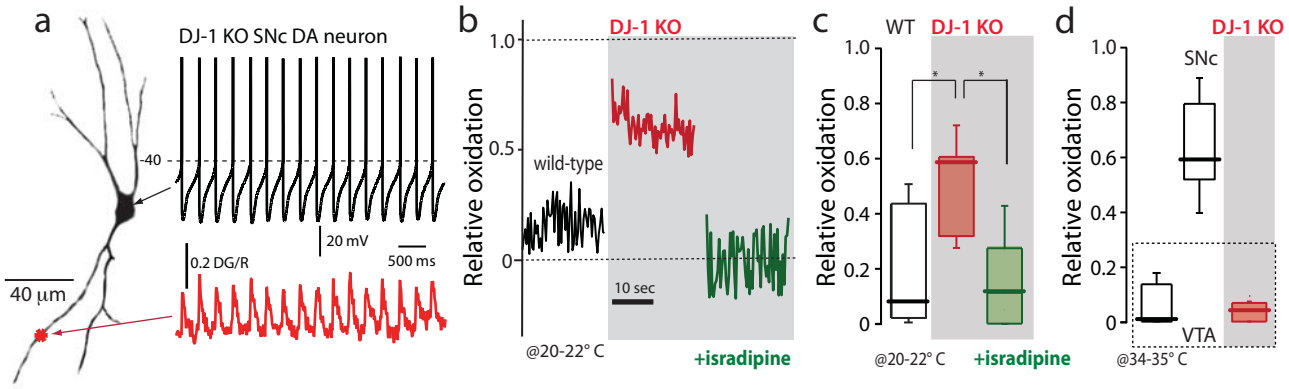

Figure 3: Guzman et al.

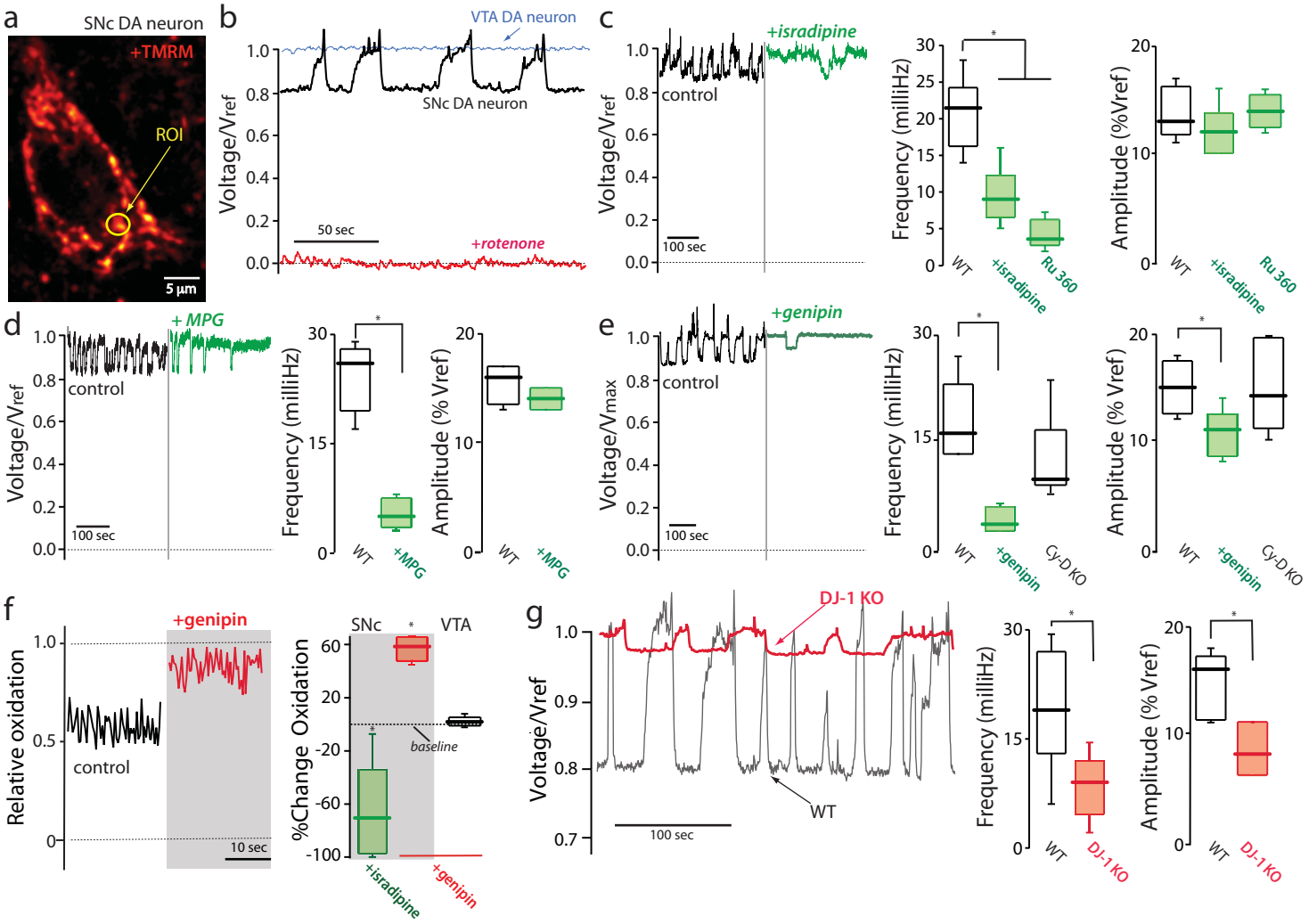

Figure 4: Guzman et al.

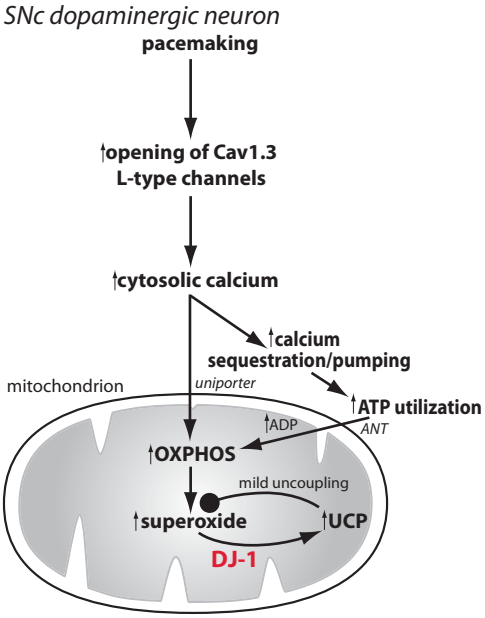

Cell Calcium 47 (2010) 175–182

Contents lists available at ScienceDirect

Cell Calcium

journal homepage: www.elsevier.com/locate/ceca

Review

# Calcium, cellular aging, and selective neuronal vulnerability in Parkinson's disease

D. James Surmeier*, Jaime N. Guzman, Javier Sanchez-Padilla

*Department of Physiology, Feinberg School of Medicine, Northwestern University, 303 E. Chicago Ave., Chicago, IL 60611, United States*

ARTICLE INFO

*Article history:*
Received 24 November 2009
Accepted 2 December 2009
Available online 6 January 2010

*Keywords:*
Substantia nigra
Dopamine
Mitochondria
Channel
Cav1.3

ABSTRACT

Parkinson's disease (PD) is the second most common neurodegenerative disease in developed countries. The core motor symptoms are attributable to the degeneration of dopamine (DA) neurons in the substantia nigra pars compacta (SNc). Why these neurons, and other restricted sets of non-dopamine neuron, succumb in PD is not clear. One potential clue has come from the observation that the engagement of L-type $Ca^{2+}$ channels during autonomous pacemaking elevates the sensitivity of SNc DA neurons to mitochondrial toxins used to create animal models of PD, suggesting that $Ca^{2+}$ entry is a factor in their selective vulnerability. Epidemiological data also supports a linkage between L-type $Ca^{2+}$ channels and the risk of developing PD. This review examines the hypothesis that the primary factor driving neurodegenerative changes in PD is the metabolic stress created by sustained $Ca^{2+}$ entry, particularly in the face of genetic or environmental factors that compromise oxidative defenses or proteostatic competence.



PD is a disabling neurodegenerative disorder that is strongly associated with aging, increasing exponentially in incidence above the age of 65 [1,2]. The incidence of PD is expected to rise dramatically worldwide in the next 25 years with the extension of life expectancy by improved health care [3]. Although there are signs of distributed neuropathology (as judged by Lewy body formation) [4], the motor symptoms of PD, including bradykinesia, rigidity, and resting tremor, are clearly linked to the degeneration and death of SNc DA neurons [5,6]. Although there are pathological changes in other select regions of the brains [4], the efficacy of the clinical gold-standard treatment of L-DOPA – a DA precursor – is testament to the centrality of DA neurons in the motor symptoms of PD.

## 1. What causes SNc DA neurons to die in PD?

The mechanisms responsible for the preferential loss of DA neurons in PD have been debated for decades. A widely held theory implicates DA itself, suggesting that oxidation of cytosolic DA (and its metabolites) leads to the production of cytotoxic free radicals [7,8]. However, there are reasons to doubt this type of cellular stress *alone* is responsible for the loss of DA neurons in PD. For example, there is considerable regional variability in the vulnerability of DA neurons in PD, with some being devoid of pathological markers [9–13]. Moreover, L-DOPA administration (which relieves symptoms by elevating DA levels in PD patients) does not appear to accelerate disease progression [14], suggesting that DA is not a significant source of reactive oxidative stress, at least in the short term. Sulzer and co-workers have recently reported that $Ca^{2+}$ entry through L-type channels stimulates DA metabolism in SNc DA neurons, pushing cytosolic DA concentrations into a toxic range with L-DOPA loading [15]. For this mechanism to be relevant to selective vulnerability, one would have to posit that modest elevations in cytosolic DA over decades leads to an accumulation of cellular defects that ultimately produces cell death. Although plausible, the hypothesis is not readily testable. It does suggest that treating patients in the early stages of the disease with direct acting agonists, rather than L-DOPA, should lead to a slower progression of the disease. That said, the frank death or phenotypic decline of a variety of non-dopaminergic neurons in PD argues that DA itself is not likely to be the principal culprit in the disease.

If not DA, then what? In recent years, attention has turned to the role of mitochondrial dysfunction in PD [16–18]. In addition to the ability of several toxins that target mitochondria to create a parkinsonian phenotype [19,20], compelling evidence for mitochondrial involvement in PD comes from the study of human PD patients. In postmortem tissue samples of the SNc from sporadic PD patients, there is a substantial decrease in the activity of mitochondrial NADH ubiquinone reductase, referred to as complex I of the electron transport chain (ETC) [21]; this deficit is specific to PD patients [22] and appears to reflect oxidative damage to complex I [23]. Oxidative damage to other cellular components such as lipids, proteins and DNA also has been found in the SNc of PD brains [24]. The source of this oxidative stress is likely to be mitochrondrial. Reactive oxygen species (ROS) and other radicals are generated by

* Corresponding author. Tel.: +1 312 503 4904; fax: +1 312 503 4400.
*E-mail address:* j-surmeier@northwestern.edu (D.J. Surmeier).

0143-4160/$ – see front matter © 2009 Elsevier Ltd. All rights reserved.
doi:10.1016/j.ceca.2009.12.003

inefficiencies in the ETC, which is responsible for creating the electrochemical gradient across the inner mitochondrial membrane that drives ATP synthase and the conversion of adenosine diphosphate to ATP [25]. ROS also are thought to be responsible for the high level of somatic DNA and mitochondrial DNA mutations in SNc DA neurons [26–28]. Lastly, although deficits in the complex I activity of platelets, skeletal muscle, fibroblasts, and lymphocytes have been reported in some PD patients [29], this is not a consistent feature of the disease, arguing that mitochondrial dysfunction is regionally selective [30]. Further support for a mitochondrial link in PD comes from the rapidly expanding literature on genetic mutations associated with familial forms of PD [16].

Another organelle that has been widely linked to pathogenesis in PD is the endoplasmic reticulum (ER). The ER is an integral component of the cellular machinery responsible for the production, delivery and degradation of proteins, a process referred to as proteostasis [31]. One of the hallmarks of PD is the formation of Lewy bodies (LBs), an abnormal protein aggregate found in SNc DA neurons and elsewhere in the brain [32]. These depositions reflect a deficiency in proteostasis that is accompanied by signs of ER stress and an attempt to sequester cytotoxic proteins [33]. In part, LBs in PD must reflect the decline in proteostatic competence that accompanies normal aging [31]. What appears to distinguish PD is the presence of an additional proteostatic burden that causes an aged DA neuronal ensemble to fail *en masse* (see below) [18,34,35].

Taken together, the evidence for the *involvement* of mitochondria and ER in the PD pathogenesis is unequivocal. The critical question is whether the disease begins with the dysfunction of these organelles. The striking regional distribution of deficits argues against this proposition. There is no evidence that mitochondria in cortical pyramidal neurons (which show little to no sign of pathology in PD) differ in any important respect from mitochondria in SNc DA neurons. There is no evidence for substantive variation in the ER (or other proteostatic elements) between vulnerable and resistant neurons either. Furthermore, there is no evidence of selective regional expression of genes associated with familial forms of PD that would be predictive of disease progression [36]. The most straightforward conclusion to be drawn from the evidence at hand is that the cellular environment in which these organelles find themselves accelerates their decline with age, making them more vulnerable to genetic or environmental stress. *What then is distinctive about the organelle environment created by SNc DA neurons?*

## 2. SNc DA neurons have a distinctive physiological phenotype

SNc DA neurons have an unusual physiological phenotype. Unlike the vast majority of neurons in the brain, adult SNc DA neurons are autonomously active, generating action potentials regularly (2–4 Hz) in the absence of synaptic input [37]. This pacemaking activity is believed to be important in maintaining ambient DA levels in regions that are innervated by these neurons, particularly the striatum [38]. While most neurons rely exclusively on monovalent cation channels to drive pacemaking, SNc DA neurons also engage ion channels that allow $Ca^{2+}$ to enter the cytoplasm [39–41], leading to elevated intracellular $Ca^{2+}$ concentrations [42,43]. The L-type $Ca^{2+}$ channels used by SNc DA neurons in pacemaking have a distinctive Cav1.3 pore-forming subunit encoded by *Cacna1d* [43,44]. Cav1.3 $Ca^{2+}$ channels are relatively rare, constituting only about 10% of the all the L-type $Ca^{2+}$ channels found in the brain [45]. Channels with this subunit differ from other L-type $Ca^{2+}$ channels in that they open at relatively hyperpolarized potentials, allowing them to contribute to the mechanisms driving the membrane potential to spike threshold underlying autonomous pacemaking [41,43,46].

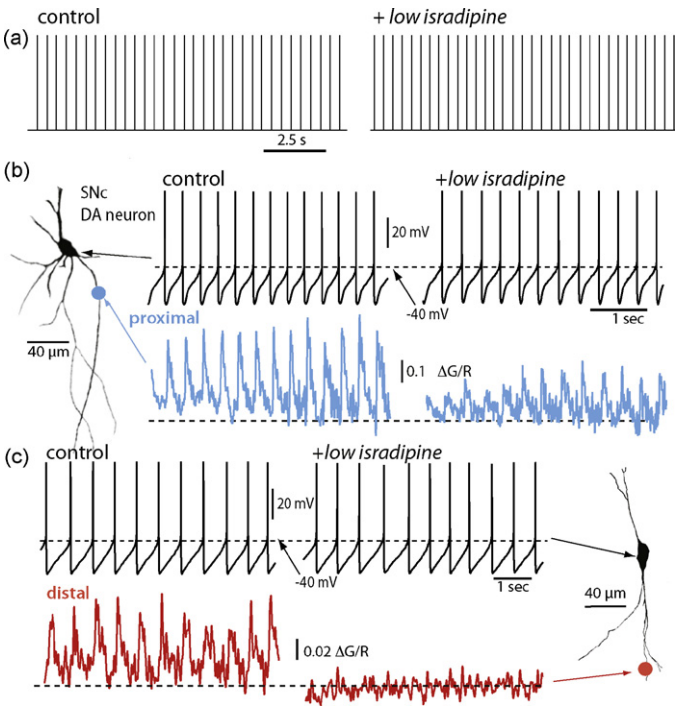


**Fig. 1.** Low concentrations of DHPs suppress dendritic $Ca^{2+}$ oscillations but do not slow pacemaking. (a) Digitized cell-attached patch recordings from an SNc DA neuron before and after application of isradipine (5 μM). The median discharge rate before isradipine application was 2.2 Hz and 2.4 Hz after ($p > 0.05$, $n = 4$). (b) Whole cell recording from the cell shown to the left (projection image) before and after isradipine (5 μM) application; there was no significant change in discharge rate in this cell or in 10 others. At the bottom, 2PLSM measurements of Fluo-4 fluorescence (G) at a proximal dendritic location (~40 μm from the soma) normalized by the fluorescence of the red Alexa dye used to image the cell. (c) Somatic recording during imaging at a more distal dendritic location (~120–200 μm from the soma). Note the complete elimination of the spike associated dendritic $Ca^{2+}$ transient at the distal imaging site. Similar results were obtained in 6 other neurons. From [46].

Until recently, it was thought that L-type $Ca^{2+}$ channels were essential for pacemaking in SNc DA neurons making them less than ideal drug targets if pacemaking was necessary to maintain physiologically important levels of DA in target structures [47,48]. This inference was based upon the ability of L-type channel antagonists (dihydropyridines) to halt pacemaking. However, we know now that at the concentrations of dihydropyridine (DHP) necessary to stop pacemaking, other ion channels are being antagonized, complicating the interpretation of previous studies. This discovery was made possible by the integration of traditional patch clamp electrophysiology and two photon laser scanning microscopy in brain slices. The combination of approaches allowed dendritic $Ca^{2+}$ oscillations to be monitored with high temporal resolution at the same time as somatic voltage, revealing that at lower, channel-specific DHP concentrations, pacemaking continues in SNc DA neurons, unaltered in rate and regularity, even when dendritic L-type $Ca^{2+}$ channels were effectively antagonized (Fig. 1) [46]. The ability of SNc DA neurons to continue pacemaking under these circumstances reflects the robustness of the multi-channel pacemaking mechanism and that Cav1.3 $Ca^{2+}$ channels play a supportive, but not necessary role. In addition to this role, Cav1.3 $Ca^{2+}$ channels participate in the postsynaptic response to activation of glutamatergic synapses and burst spiking in response to reward prediction errors [M. Bevan, unpublished observations]. However, as with pacemaking, this role is supportive, rather than necessary.

The sustained engagement of Cav1.3 $Ca^{2+}$ channels during pacemaking comes at an obvious metabolic cost to SNc DA neurons. Because of its involvement in cellular processes ranging from the

regulation of enzyme activity to programmed cell death, $Ca^{2+}$ is under very tight homeostatic control, with a cytosolic set point near 100 nM – 10,000 times lower than the concentration of $Ca^{2+}$ in the extracellular space [49–51]. $Ca^{2+}$ entering neurons is rapidly sequestered or pumped back across the steep plasma membrane concentration gradient; this process requires energy stored in ATP or in ion gradients that are maintained with ATP-dependent pumps. In most neurons, $Ca^{2+}$ channel opening is a rare event, occurring primarily during very brief action potentials. This makes the task and the metabolic cost to the cell readily manageable. But in SNc DA neurons, where Cav1.3 $Ca^{2+}$ channels are open much of the time, the magnitude and the spatial extent of $Ca^{2+}$ influx are much larger [42].

Another distinctive feature of SNc DA neurons, and many of the other neurons that succumb in PD (e.g., locus ceruleus neurons), is their enormous axonal field. Recent anatomical work has estimated that a typical SNc DA neuron has mean axonal length of 470,000 μm [52]. Furthermore, each axon supports ~370,000 synapses, orders of magnitude higher than the number supported by cortical pyramidal neurons for example [53]. Although the oxidative stress experienced by each of these terminals might very well be normal (this has yet to be determined), it could be that the proteostatic burden created by maintaining this extraordinary axonal tree creates a substantial metabolic load in and of itself. Moreover, the need to supply this axonal field with mitochondria to maintain ionic gradients and exocytosis could create an axonal sink for these organelles, potentially depriving the somatic region of an adequate mitochondrial complement. In fact, mitochondrial density in the somatodendritic region of SNc DA neurons appears to be abnormally low [54]. Asking a depleted mitochondrial complement in the somatodendritic region to meet the challenge posed by sustained $Ca^{2+}$ entry and this large axonal tree should lead to a sustained elevation in oxidative phosphorylation and the production of superoxide and ROS.

## 3. Is PD a manifestation of $Ca^{2+}$-accelerated aging?

One of the oldest and most popular theories of aging is that it is a direct consequence of accumulated mtDNA and organelle damage produced by ROS and related reactive molecules generated by the ETC in the course of oxidative phosphorylation [55,56]. A corollary of this hypothesis is that the rate of aging is directly related to metabolic rate. There is no obvious reason not to extend this organismal postulate to individual cells. The reliance of SNc DA neurons on a metabolically expensive strategy to generate autonomous activity that taxes mitochondria should mean that they age more rapidly than other types of neuron. Is then PD simply a reflection of accelerated aging in neurons that rely too heavily upon $Ca^{2+}$ channels to do their business? Age is undoubtedly the single strongest risk factor for PD [57,58]. Stereological estimates of normal aging related cell death in humans argue that SNc DA neurons at a higher risk than other neurons *in the absence of environmental toxins or pathogens*, as they are lost at a significantly higher rate than many other types of neurons (some of which show no appreciable loss over a 6–7 decade span) [59]. In mammals with significantly shorter life-spans, loss of SNc DA neurons with age has not been seen reliably, but there is a clear decline in phenotypic markers with age that matches that seen in PD, as well as an increased susceptibility to toxins [60–65]. Taken together, these studies make a case that SNc DA neurons age more rapidly than the vast majority of the neurons in the brain.

This 'wear and tear' theory suggests that PD is first and foremost a consequence of aging. Why then do some people become symptomatic in their 50's, others in their 60's or 70's or not at all in an 80 or 90 year life? Genetic factors certainly could account for a large part of this variation [8,36,57]. These factors could increase the rate at which vulnerable neurons age by compromising mitochondrial function or $Ca^{2+}$ homeostasis. Several of the genetic mutations associated with early-onset forms of PD are directly linked to mitochondrial dysfunction [16]. Unfortunately, animal models of these forms of PD have failed to recapitulate the disease. For example, mutations of *DJ-1* (*PARK7*) are associated with an early-onset form of PD. It has been putatively categorized as an atypical mitochondrial "peroxiredoxin-like peroxidase," decreasing the accumulation of hydrogen peroxide and damage due to ETC superoxide generation [66]. But, how this happens is not clear. DJ-1 is redox sensitive, giving it the capacity to signal oxidative challenges and potentially coordinate a variety of mitochondrial oxidative defense mechanisms [67]. Although deleting *DJ-1* increases the sensitivity of cells generally to heroic oxidative challenge, it remains to be determined how it compromises SNc DA neurons under more physiological conditions. Studies of *DJ-1* knockouts have not revealed any loss of SNc DA neurons or a fundamental shift in their physiology, only a modest deficit in DA release during burst stimulation that is difficult to tie to an increased vulnerability [68]. But there have been no studies in these mice of mitochondrial physiology in mature SNc DA neurons where $Ca^{2+}$ influx during pacemaking has fully developed. This could prove to be critical to an understanding of the mechanisms that could accelerate the loss of these cells over decades.

Two other genes linked to familial PD have unequivocal linkages to mitochondria. One is Parkin (*PARK2*). Fruit flies with functional deletions of Parkin have fragmented and apoptotic mitochrondria [69]; knockout mice have a less dramatic but a clear mitochondrial phenotype (including decreased mitochondrial (respiratory) function, decreased metabolic drive, and increased lipid and protein phosphorylation) [70]. Another is PTEN-induced putative kinase 1 or *PINK1* (*PARK6*). Its deletion leads to an identical phenotype in Drosophila as does Parkin deletion – fragmented cristae and apoptotic mitochondria; this phenotype can be rescued by Parkin over-expression, suggesting involvement in some common biochemical pathway [71,72]. Although found both in cytosolic and mitochrondrial preparations, PINK1 has an N-terminus mitochondrial targeting sequence [73]. PINK1 deletion also compromises DA release during burst stimulation, like DJ-1 [74]. It is not difficult to infer that loss of function mutations in either of these genes should have their biggest impact in a cell type that had a high basal level of metabolic activity, creating a mitochondrial oxidative stress. But to date, this has not been convincingly demonstrated.

Can the $Ca^{2+}$-mediated cellular aging hypothesis account for the vulnerability of other cell types in PD? Other regions of the brain that have cell loss paralleling that of the SNc are the locus ceruleus (LC) and hypothalamic tuberomamillary nucleus [32,75]. The neurons of the LC and the tuberomamillary neurons are similar to SNc DA neurons in several respects. Like SNc DA neurons, both LC and tuberomamillary neurons are autonomous pacemakers that depend upon L-type $Ca^{2+}$ channels [76–78]. In contrast, DA neurons in the VTA do not rely upon L-type $Ca^{2+}$ channels for pacemaking and are relatively intact in PD patients and in animal models of PD [11,43,79–81]. DA neurons in the olfactory bulb also are autonomous pacemakers and rely upon $Ca^{2+}$ channels (although not L-type channels) [81]. While olfactory deficits have been associated with PD [82], there is no obvious loss of olfactory bulb DA neurons [83]. Although this would seem to run counter to the $Ca^{2+}$ hypothesis, this could simply be a consequence of the capacity of this region for adult neurogenesis [84].

## 4. Can PD be prevented?

If PD is a consequence of $Ca^{2+}$-accelerated aging in SNc DA neurons (and in those neurons with a similar phenotype), then reducing $Ca^{2+}$ flux should delay the onset of PD symptoms as well as slow

its progression. This might be possible with orally deliverable, DHP L-type channel antagonists shown to be safe in humans [43]. Adult SNc DA neurons readily compensate for the antagonism of L-type Cav1.3 $Ca^{2+}$ channels and continue pacemaking at a normal rate [46]. More importantly, although the impact on mitochondrial and ER stress can only be inferred at this point, reducing $Ca^{2+}$ influx during pacemaking dramatically diminishes the sensitivity of SNc DA neurons to toxins used to generate animal models of PD [43]. SNc DA neurons that express the $Ca^{2+}$ binding protein calbindin also have a diminished sensitivity to PD toxins [79,85]. Furthermore, at neuroprotective doses of an L-type channel antagonist, mice have no obvious motor, learning or cognitive deficits, suggesting that the patterned activity of SNc DA neurons is functionally unchanged [39,46,86].

Is there evidence that this strategy might work in humans to prevent or slow PD? Calcium channel antagonists (CCAs), including the DHPs used in animal studies, are commonly used in clinical practice to treat hypertension, creating a potential database to be mined. A case–control study of hypertensive patients found a significant reduction in the observed risk of PD with CCA use, but not with medications that reduce blood pressure in other ways [87]. More recently, a large Danish data set has been examined [88]. The authors agreed with the main conclusions of the Becker et al. study but extended their findings by showing that only DHPs that cross the blood–brain barrier (BBB) are associated with reduced PD risk (~30%). Given the short period of treatment in many cases (~2 years), variable dosing, and low relative affinity of DHPs for Cav1.3 $Ca^{2+}$ channels (compared to Cav1.2 channels) [89–91], this is a surprisingly strong association and lends further credence to the proposition that a BBB permeable and potent Cav1.3 antagonist could be a very effective neuroprotective agent.

That said, these studies are not a substitute for a controlled clinical trial. In the absence of a selective Cav1.3 $Ca^{2+}$ channel antagonist, the DHP isradipine is the most attractive drug for such a trial. Isradipine has a relatively higher affinity for Cav1.3 $Ca^{2+}$ channels than the other known DHP and has good brain bioavailability [92,93]. At the doses used to treat hypertension, isradipine has relatively minor side effects [94]. The question is whether it will prove neuroprotective at doses tolerated by the general population. Pharmacokinetic studies by our group have found that serum concentrations of isradipine achieved in mice that are protected (~2 ng/ml) against 1-methyl-4-phenyl-1,2,3,6-tetrahydropyridine and 6-hydroxydopamine toxicity are very close to those achieved in humans with a very well-tolerated daily dose (10 mg/day, Dynacirc CR), suggesting that neuroprotection is achievable.

It is also worth considering how DHPs might be used in combination with other drugs that are being tested in clinical neuroprotection trials for PD. Although early trials with creatine, coenzyme Q10, and other antioxidant supplements have been disappointing [95], they share the hypothesis that oxidative stress exacerbates the symptoms and progression of PD. Coenzyme Q10 is an electron acceptor for complexes I and II that appears compromised in PD patients [96] and is neuroprotective in animal models of PD [97]. Creatine is a substrate for ATP production that can both improve mitochondrial efficiency and reduce oxidative stress by buffering fluctuations in cellular energy production [98]. Both approaches are aimed at improving mitochondrial function rather than attacking the source of stress on mitochondria. Rasagline or deprenyl also could prove to have neuroprotective effects by virtue not of its ability to inhibit monoamine oxidase B, but by their ability to its ability to induce the expression of antioxidant defenses [99,100]. Because their sites of action differ within the chain of events leading to oxidative stress and mitochondrial dysfunction, a combination therapy could prove more effective than any one therapy alone.

## 5. Gaps in our understanding of the role of $Ca^{2+}$ in the etiology of PD

There are a number of major gaps in our understanding of the role $Ca^{2+}$ might play in the neuronal pathology seen in PD. Filling these gaps not only could provide novel therapeutic strategies for preventing or slowing the progression of the disease but could also help to create strategies for 'successful aging' generally. Fig. 2 graphically summarizes some of the key points of the review and points of uncertainty.

One major gap is the mechanistic linkage between activity dependent $Ca^{2+}$ entry into neurons and mitochondrial oxidative stress. In spite of its plausibility, there is no direct evidence that plasma membrane $Ca^{2+}$ influx elevates mitochondrial oxidative phosphorylation and the production of superoxide. Limiting plasma membrane $Ca^{2+}$ influx certainly diminishes the sensitivity of SNc DA neurons to mitochondrial toxins, but this effect could be indirect. The development of redox sensitive optical probes [101–103] and two photon laser scanning microscopy to allow imaging of mitochondria *in situ* puts this question within reach. A related, albeit more difficult question, is whether the role of mitochondria in intracellular $Ca^{2+}$ buffering contributes to neuronal apoptosis in slowly progressing neurodegenerative diseases, like PD. Although mitochondria do not normally flux $Ca^{2+}$ from the cytoplasm at physiological concentrations, $Ca^{2+}$ released from the ER through inositol trisphosphate (IP3) or ryanodine receptors can enter mitochondria at points of apposition between the organelles, which form functional $Ca^{2+}$ microdomains in which $Ca^{2+}$ concentrations can rise into the micromolar range [104–106]. Through these junctions, 'dumping' of ER $Ca^{2+}$ stores into mitochondria could trigger apoptosis in marginally competent mitochondria [107]. However, the vast majority of the studies demonstrating the existence of close interactions between mitochondria and the ER have been performed in cell lines, none have been performed in SNc dopaminergic neurons where the functional relationship between these organelles could be quite different. That said, mechanisms like this seem to be in play in Alzheimer's disease [108].

A closely related question is whether non-autonomous oxidative stress could synergize with that created by the $Ca^{2+}$ phenotype. There is ample evidence that inflammation and the production of ROS and reactive nitrogen species (RNS) could accelerate the loss of SNc DA neurons and the progression of PD. Recent work has identified another possible player in translating extrinsic oxidative stress into mitochondria dysfunction. ROS mediated activation of protein kinase C beta (PKCb) phosphorylates 66-kilodalton isoform of the growth factor adapter Shc ($p66^{shc}$), promoting transport into mitochondria where it alters $Ca^{2+}$ responses and promotes apoptosis [109]. Because it controls life-span [110], $p66^{shc}$ could be particularly important in regulating the aging of neurons, like SNc DA neurons, that are stressed by $Ca^{2+}$ flux across the plasma membrane.

A second major gap in our understanding is how genetic mutations associated with PD interact with $Ca^{2+}$ triggered events in SNc DA neurons. Although DA could be a factor [8], $Ca^{2+}$ must be considered the prime suspect in making these mutations lethal. As outlined here, this is most likely mediated by metabolic, oxidative stress. It is easy to imagine that a negative dominant mutation of a gene like *DJ-1* could exacerbate the basal oxidative stress in an SNc DA neuron and accelerate mitochondrial and proteostatic collapse, leaving neurons lacking the same basal stress largely unaffected. But, these types of interaction between mutations and cellular phenotype have not been pursued.

A third gap is our understanding is whether non-dopaminergic neurons that are vulnerable in PD share the $Ca^{2+}$ phenotype. As mentioned above, there is some evidence that at least a subset of the neurons that die or functionally decline are pacemakers that

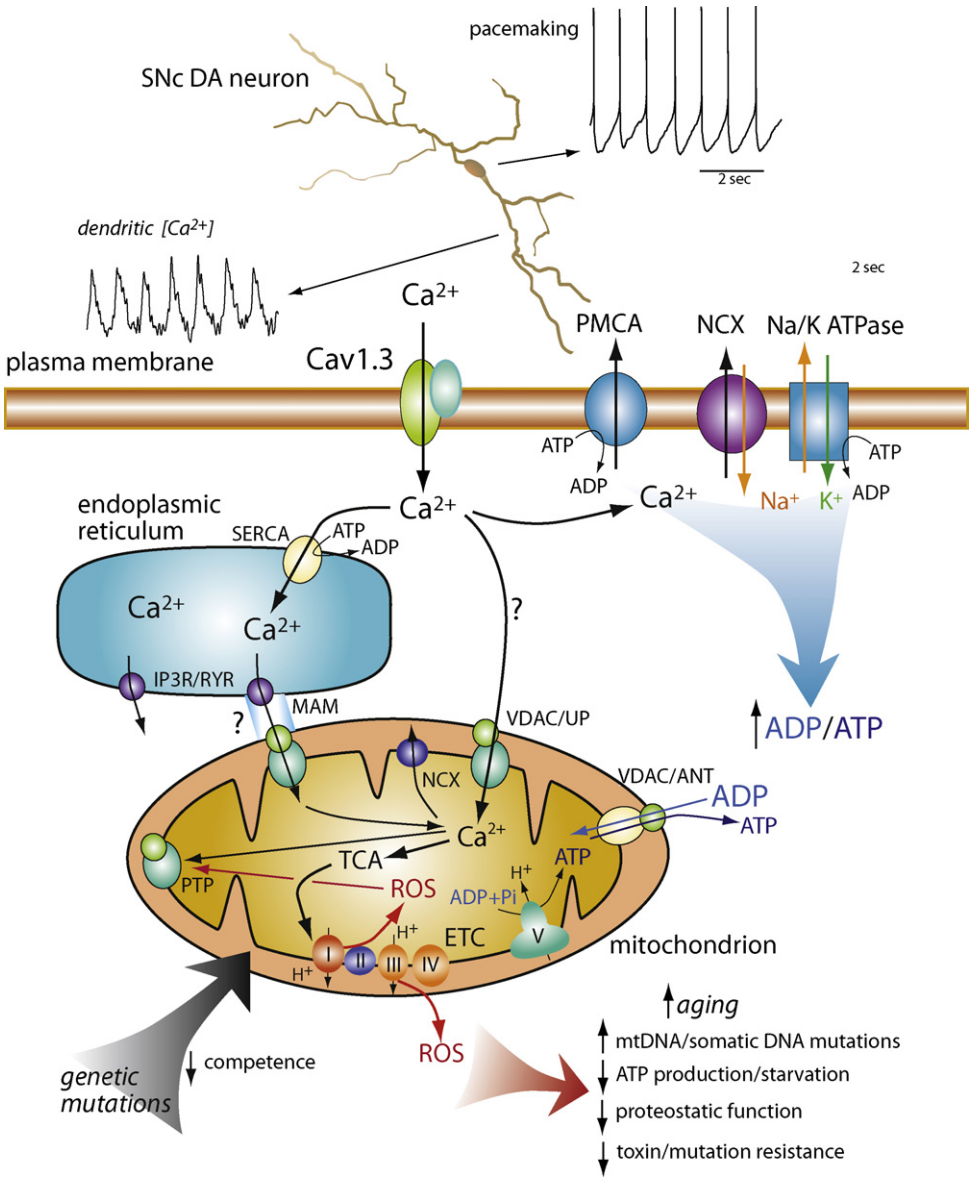


**Fig. 2.** A schematic summarizing a model of how $Ca^{2+}$ entry during pacemaking in SNc DA neurons might lead to mitochondrial oxidative stress, accelerated aging and eventual cell death. At the top is an image of a reconstructed SNc DA neuron showing the pacemaker driven somatic spiking and dendritic $Ca^{2+}$ oscillations associated with pacemaking. This dendritic $Ca^{2+}$ influx is attributable almost entirely to flux through Cav1.3 $Ca^{2+}$ channels. At the bottom is a cartoon depicting the hypothetical mechanisms involved in elevating mitochondrial oxidative stress. $Ca^{2+}$ influx through Cav1.3 channels is either sequestered in the endoplasmic reticulum by uptake through smooth endoplasmic reticulum $Ca^{2+}$ (SERCA) pumps or taken up by mitochondria through channels created by voltage-dependent anion channels (VDAC) and $Ca^{2+}$ uniporter (UP); the extent to which this pathway is important is in question (hence the question mark on the arrow). $Ca^{2+}$ could also enter mitochondria through this VDAC/UP channel at points of apposition between the ER and mitochondra where inositol trisphosphate receptors (IP3) and/or ryanodine receptors (IP3R/RYR) are positioned at specializations – mitochondrial associated membrane (MAM). This entry route has not been established in SNc DA neurons, hence the question mark. $Ca^{2+}$ entering through Cav1.3 channels is moved back across the plasma membrane through either the $Ca^{2+}$-ATPase (PMCA) or through a $Na^+/Ca^{2+}$ exchanger (NCX) that relies upon the $Na^+$ gradient maintained by the Na/K ATPase at energetic cost; leading to conversion of ATP to ADP. ADP and ATP are exchanged by mitochondria with the VDAC and adenine nucleotide transporter (ANT). ADP stimulates oxidative phosphorylation. $Ca^{2+}$ entering the mitochondrial matrix can stimulate enzymes of the tricarboxylic acid (TCA) cycle that produces reducing equivalents for the electron transport chain (ETC); complex I through V are shown at the inner mitochondrial membrane; complex V (ATP synthase) uses the electrochemical gradient to convert adenosine diphosphate (ADP) and inorganic phosphate to adenosine triphosphate (ATP). Electron movement along the ETC generates superoxide, leading to the production of reactive oxygen species (ROS) that can produce a variety of deleterious effects that can be viewed as accelerated aging (red arrow at the bottom). One other action of ROS is to promote opening of the mitochondrial permeability transition pore (mPTP); irreversible opening of the mPTP leads to release of pro-apoptetic factors into the cytosol. A basic question is whether *reversible* opening of the mPTP is possible under conditions of mild oxidative stress; mPTP opening and depolarization of the inner mitochondrial membrane could serve to diminish ROS production. $Ca^{2+}$ is removed from mitochondrial through mitochrondrial $Na^+/Ca^{2+}$ exchangers (NCXs). Lastly, genetic mutations associated with Parkinson's disease, like those to DJ-1 or PINK1, might directly compromise the competence of mitochondria, leading to accelerated aging or increased oxidative stress.

engage L-type $Ca^{2+}$ channels. However, the phenotypic characterization must be explored more systematically in those cell types at greatest risk (dorsal motor nucleus of the vagus, locus ceruleus, basal forebrain cholinergic neurons, dorsal raphe, etc.). Moreover, this should be done *in situ* (either with in vivo recording or in brain slices from adult mice) where the behavior of the neurons is as close as possible to that found in humans.

## 6. Conclusions

$Ca^{2+}$ mediated cellular stress has long been thought to be important in neurodegeneration, but it usually is envisioned as a late stage consequence of organelle damage inflicted by some other challenge. The unusual reliance of SNc DA neurons on voltage-dependent L-type $Ca^{2+}$ channels in autonomous pacemak-

ing suggests that the mitochondrial stress created by sustained $Ca^{2+}$ entry could be responsible for their selective vulnerability, rather than simply a late stage consequence. This hypothesis is consistent with the centrality of mitochondria in prevailing models of pathogenesis in PD. Genetic mutations and environmental challenges could easily synergize with this basal stress, hastening cellular aging and eventual death. Although plausible and consistent with regional deficits seen in normal aging and PD, the proposition that $Ca^{2+}$ entry during pacemaking compromises mitochondrial function remains to be fully untested. The tools necessary to conduct this test are now becoming available. Nevertheless, given the plausibility of the link between $Ca^{2+}$ and the loss of SNc DA neurons, the absence of any proven neuroprotective therapy in PD and the availability of $Ca^{2+}$ channel antagonists that are well-tolerated and approved for human use, it would seem that the human experiment should proceed now in the form of clinical neuroprotection trials.

## Conflict of interest

None of the authors have any financial conflict of interest.

## Acknowledgments

This work was supported by grants from the Hartman Foundation, USAMRMC and NIH (NS047085).

## References

[1] L.M. de Lau, P.C. Giesbergen, M.C. de Rijk, A. Hofman, P.J. Koudstaal, M.M. Breteler, Incidence of parkinsonism and Parkinson's disease in a general population: the Rotterdam Study, Neurology 63 (2004) 1240–1244.
[2] M.C. de Rijk, C. Tzourio, M.M. Breteler, J.F. Dartigues, L. Amaducci, S. Lopez-Pousa, J.M. Manubens-Bertran, A. Alperovitch, W.A. Rocca, Prevalence of parkinsonism and Parkinson's disease in Europe: the EUROPARKINSON Collaborative Study. European Community Concerted Action on the Epidemiology of Parkinson's disease, J. Neurol. Neurosurg. Psychiatry 62 (1997) 10–15.
[3] E.R. Dorsey, R. Constantinescu, J.P. Thompson, K.M. Biglan, R.G. Holloway, K. Kieburtz, F.J. Marshall, B.M. Ravina, G. Schifitto, A. Siderowf, C.M. Tanner, Projected number of people with Parkinson's disease in the most populous nations, 2005 through 2030, Neurology 68 (2007) 384–386.
[4] H. Braak, E. Ghebremedhin, U. Rub, H. Bratzke, K. Del Tredici, Stages in the development of Parkinson's disease-related pathology, Cell Tissue Res. 318 (2004) 121–134.
[5] O. Hornykiewicz, Dopamine (3-hydroxytyramine) and brain function, Pharmacol. Rev. 18 (1966) 925–964.
[6] P. Riederer, S. Wuketich, Time course of nigrostriatal degeneration in Parkinson's disease. A detailed study of influential factors in human brain amine analysis, J. Neural. Transm. 38 (1976) 277–301.
[7] J.T. Greenamyre, T.G. Hastings, Biomedicine. Parkinson's—divergent causes, convergent mechanisms, Science 304 (2004) 1120–1122.
[8] D. Sulzer, Multiple hit hypotheses for dopamine neuron loss in Parkinson's disease, Trends Neurosci. 30 (2007) 244–250.
[9] P. Damier, E.C. Hirsch, Y. Agid, A.M. Graybiel, The substantia nigra of the human brain. II. Patterns of loss of dopamine-containing neurons in Parkinson's disease, Brain 122 (Pt 8) (1999) 1437–1448.
[10] H. Ito, S. Goto, S. Sakamoto, A. Hirano, Calbindin-D28k in the basal ganglia of patients with parkinsonism, Ann. Neurol. 32 (1992) 543–550.
[11] S.J. Kish, K. Shannak, O. Hornykiewicz, Uneven pattern of dopamine loss in the striatum of patients with idiopathic Parkinson's disease. Pathophysiologic and clinical implications, N. Engl. J. Med. 318 (1988) 876–880.
[12] M.M. Matzuk, C.B. Saper, Preservation of hypothalamic dopaminergic neurons in Parkinson's disease, Ann. Neurol. 18 (1985) 552–555.
[13] C.B. Saper, D.M. Sorrentino, D.C. German, S. de Lacalle, Medullary catecholaminergic neurons in the normal human brain and in Parkinson's disease, Ann. Neurol. 29 (1991) 577–584.
[14] S. Fahn, Does levodopa slow or hasten the rate of progression of Parkinson's disease? J. Neurol. 252 (Suppl. 4) (2005) IV37–IV42.
[15] E.V. Mosharov, K.E. Larsen, E. Kanter, K.A. Phillips, K. Wilson, Y. Schmitz, D.E. Krantz, K. Kobayashi, R.H. Edwards, D. Sulzer, Interplay between cytosolic dopamine, calcium, and alpha-synuclein causes selective death of substantia nigra neurons, Neuron 62 (2009) 218–229.
[16] A.H. Schapira, Mitochondria in the aetiology and pathogenesis of Parkinson's disease, Lancet Neurol. 7 (2008) 97–109.
[17] M. Vila, D. Ramonet, C. Perier, Mitochondrial alterations in Parkinson's disease: new clues, J. Neurochem. 107 (2008) 317–328.
[18] C. Henchcliffe, M.F. Beal, Mitochondrial biology and oxidative stress in Parkinson's disease pathogenesis, Nat. Clin. Pract. Neurol. 4 (2008) 600–609.
[19] S. Przedborski, K. Tieu, C. Perier, M. Vila, MPTP as a mitochondrial neurotoxic model of Parkinson's disease, J. Bioenerg. Biomembr. 36 (2004) 375–379.
[20] R. Betarbet, T.B. Sherer, G. MacKenzie, M. Garcia-Osuna, A.V. Panov, J.T. Greenamyre, Chronic systemic pesticide exposure reproduces features of Parkinson's disease, Nat. Neurosci. 3 (2000) 1301–1306.
[21] V.M. Mann, J.M. Cooper, S.E. Daniel, K. Srai, P. Jenner, C.D. Marsden, A.H. Schapira, Complex I, iron, and ferritin in Parkinson's disease substantia nigra, Ann. Neurol. 36 (1994) 876–881.
[22] M. Gu, M.T. Gash, J.M. Cooper, G.K. Wenning, S.E. Daniel, N.P. Quinn, C.D. Marsden, A.H. Schapira, Mitochondrial respiratory chain function in multiple system atrophy, Movement Disord. 12 (1997) 418–422.
[23] P.M. Keeney, J. Xie, R.A. Capaldi, J.P. Bennett Jr., Parkinson's disease brain mitochondrial complex I has oxidatively damaged subunits and is functionally impaired and misassembled, J. Neurosci. 26 (2006) 5256–5264.
[24] J. Zhang, G. Perry, M.A. Smith, D. Robertson, S.J. Olson, D.G. Graham, T.J. Montine, Parkinson's disease is associated with oxidative damage to cytoplasmic DNA and RNA in substantia nigra neurons, Am. J. Pathol. 154 (1999) 1423–1429.
[25] D.G. Nicholls, S.J. Ferguson, Bioenergetics 3 (2002).
[26] N.W. Soong, D.R. Hinton, G. Cortopassi, N. Arnheim, Mosaicism for a specific somatic mitochondrial DNA mutation in adult human brain, Nat. Genet. 2 (1992) 318–323.
[27] Y. Kraytsberg, E. Kudryavtseva, A.C. McKee, C. Geula, N.W. Kowall, K. Khrapko, Mitochondrial DNA deletions are abundant and cause functional impairment in aged human substantia nigra neurons, Nat. Genet. 38 (2006) 518–520.
[28] A. Bender, K.J. Krishnan, C.M. Morris, G.A. Taylor, A.K. Reeve, R.H. Perry, E. Jaros, J.S. Hersheson, J. Betts, T. Klopstock, R.W. Taylor, D.M. Turnbull, High levels of mitochondrial DNA deletions in substantia nigra neurons in aging and Parkinson's disease, Nat. Genet. 38 (2006) 515–517.
[29] L. Tretter, I. Sipos, V. Adam-Vizi, Initiation of neuronal damage by complex I deficiency and oxidative stress in Parkinson's disease, Neurochem. Res. 29 (2004) 569–577.
[30] P. Jenner, Parkinson's disease, pesticides and mitochondrial dysfunction, Trends Neurosci. 24 (2001) 245–247.
[31] W.E. Balch, R.I. Morimoto, A. Dillin, J.W. Kelly, Adapting proteostasis for disease intervention, Science 319 (2008) 916–919.
[32] K. Del Tredici, H. Braak, Idiopathic Parkinson's disease: staging an alpha-synucleinopathy with a predictable pathoanatomy, in: P.J. Kahle, C. Haas (Eds.), Molecular Mechanisms of Parkinson's Disease, Landes Bioscience, Georgetown, TX, 2004, pp. 1–32.
[33] E.J. Ryu, H.P. Harding, J.M. Angelastro, O.V. Vitolo, D. Ron, L.A. Greene, Endoplasmic reticulum stress and the unfolded protein response in cellular models of Parkinson's disease, J. Neurosci. 22 (2002) 10690–10698.
[34] S. Kaushik, A.M. Cuervo, Chaperone-mediated autophagy, Methods Mol. Biol. 445 (2008) 227–244.
[35] H.Q. Wang, R. Takahashi, Expanding insights on the involvement of endoplasmic reticulum stress in Parkinson's disease, Antioxid. Redox Signal. 9 (2007) 553–561.
[36] D.J. Moore, A.B. West, V.L. Dawson, T.M. Dawson, Molecular pathophysiology of Parkinson's disease, Annu. Rev. Neurosci. 28 (2005) 57–87.
[37] A.A. Grace, B.S. Bunney, Intracellular and extracellular electrophysiology of nigral dopaminergic neurons. 2. Action potential generating mechanisms and morphological correlates, Neuroscience 10 (1983) 317–331.
[38] R. Romo, W. Schultz, Dopamine neurons of the monkey midbrain: contingencies of responses to active touch during self-initiated arm movements, J. Neurophysiol. 63 (1990) 592–606.
[39] A. Bonci, P. Grillner, N.B. Mercuri, G. Bernardi, L-type calcium channels mediate a slow excitatory synaptic transmission in rat midbrain dopaminergic neurons, J. Neurosci. 18 (1998) 6693–6703.
[40] H.X. Ping, P.D. Shepard, Apamin-sensitive Ca(2+)-activated K+ channels regulate pacemaker activity in nigral dopamine neurons, Neuroreport 7 (1996) 809–814.
[41] M. Puopolo, E. Raviola, B.P. Bean, Roles of subthreshold calcium current and sodium current in spontaneous firing of mouse midbrain dopamine neurons, J. Neurosci. 27 (2007) 645–656.
[42] C.J. Wilson, J.C. Callaway, Coupled oscillator model of the dopaminergic neuron of the substantia nigra, J. Neurophysiol. 83 (2000) 3084–3100.
[43] C.S. Chan, J.N. Guzman, E. Ilijic, J.N. Mercer, C. Rick, T. Tkatch, G.E. Meredith, D.J. Surmeier, 'Rejuvenation' protects neurons in mouse models of Parkinson's disease, Nature 447 (2007) 1081–1086.
[44] J. Striessnig, A. Koschak, M.J. Sinnegger-Brauns, A. Hetzenauer, N.K. Nguyen, P. Busquet, G. Pelster, N. Singewald, Role of voltage-gated L-type Ca2+ channel isoforms for brain function, Biochem. Soc. Trans. 34 (2006) 903–909.
[45] M.J. Sinnegger-Brauns, I.G. Huber, A. Koschak, C. Wild, G.J. Obermair, U. Einzinger, J.C. Hoda, S.B. Sartori, J. Striessnig, Expression and 1,4-dihydropyridine-binding properties of brain L-type calcium channel isoforms, Mol. Pharmacol. 75 (2009) 407–414.
[46] J.N. Guzman, J. Sanchez-Padilla, C.S. Chan, D.J. Surmeier, Robust pacemaking in substantia nigra dopaminergic neurons, J. Neurosci. 29 (2009) 11011–11019.
[47] S. Nedergaard, J.A. Flatman, I. Engberg, Nifedipine- and omega-conotoxin-sensitive Ca2+ conductances in guinea-pig substantia nigra pars compacta neurones, J. Physiol. 466 (1993) 727–747.
[48] N.B. Mercuri, A. Bonci, P. Calabresi, F. Stratta, A. Stefani, G. Bernardi, Effects of dihydropyridine calcium antagonists on rat midbrain dopaminergic neurones, Br. J. Pharmacol. 113 (1994) 831–838.

[49] R. Rizzuto, Intracellular Ca(2+) pools in neuronal signalling, Curr. Opin. Neurobiol. 11 (2001) 306–311.
[50] S. Orrenius, B. Zhivotovsky, P. Nicotera, Regulation of cell death: the calcium-apoptosis link, Nat. Rev. Mol. Cell Biol. 4 (2003) 552–565.
[51] M.J. Berridge, P. Lipp, M.D. Bootman, The versatility and universality of calcium signalling, Nat. Rev. Mol. Cell Biol. 1 (2000) 11–21.
[52] W. Matsuda, T. Furuta, K.C. Nakamura, H. Hioki, F. Fujiyama, R. Arai, T. Kaneko, Single nigrostriatal dopaminergic neurons form widely spread and highly dense axonal arborizations in the neostriatum, J. Neurosci. 29 (2009) 444–453.
[53] G.W. Arbuthnott, J. Wickens, Space, time and dopamine, Trends Neurosci. 30 (2007) 62–69.
[54] C.L. Liang, T.T. Wang, K. Luby-Phelps, D.C. German, Mitochondria mass is low in mouse substantia nigra dopamine neurons: implications for Parkinson's disease, Exp. Neurol. 203 (2007) 370–380.
[55] D. Harman, The biologic clock: the mitochondria? J. Am. Geriatr. Soc. 20 (1972) 145–147.
[56] D.C. Wallace, A mitochondrial paradigm of metabolic and degenerative diseases, aging, and cancer: a dawn for evolutionary medicine, Annu. Rev. Genet. 39 (2005) 359–407.
[57] D.B. Calne, J.W. Langston, Aetiology of Parkinson's disease, Lancet 2 (1983) 1457–1459.
[58] W.R. Gibb, A.J. Lees, Anatomy, pigmentation, ventral and dorsal subpopulations of the substantia nigra, and differential cell death in Parkinson's disease, J. Neurol. Neurosurg. Psychiatry 54 (1991) 388–396.
[59] A.K. Stark, B. Pakkenberg, Histological changes of the dopaminergic nigrostriatal system in aging, Cell Tissue Res. 318 (2004) 81–92.
[60] A.L. McCormack, D.A. Di Monte, K. Delfani, I. Irwin, L.E. DeLanney, W.J. Langston, A.M. Janson, Aging of the nigrostriatal system in the squirrel monkey, J. Comp. Neurol. 471 (2004) 387–395.
[61] T. Ishikawa, V. Dhawan, K. Kazumata, T. Chaly, F. Mandel, J. Neumeyer, C. Margouleff, B. Babchyck, I. Zanzi, D. Eidelberg, Comparative nigrostriatal dopaminergic imaging with iodine-123-beta CIT-FP/SPECT and fluorine-18-FDOPA/PET, J. Nucl. Med. 37 (1996) 1760–1765.
[62] L. Backman, N. Ginovart, R.A. Dixon, T.B. Wahlin, A. Wahlin, C. Halldin, L. Farde, Age-related cognitive deficits mediated by changes in the striatal dopamine system, Am. J. Psychiatry 157 (2000) 635–637.
[63] T.J. Collier, J. Lipton, B.F. Daley, S. Palfi, Y. Chu, C. Sortwell, R.A. Bakay, J.R. Sladek Jr., J.H. Kordower, Aging-related changes in the nigrostriatal dopamine system and the response to MPTP in nonhuman primates: diminished compensatory mechanisms as a prelude to parkinsonism, Neurobiol. Dis. 26 (2007) 56–65.
[64] N.M. Kanaan, J.H. Kordower, T.J. Collier, Age-related accumulation of Marinesco bodies and lipofuscin in rhesus monkey midbrain dopamine neurons: relevance to selective neuronal vulnerability, J. Comp. Neurol. 502 (2007) 683–700.
[65] N.M. Kanaan, J.H. Kordower, T.J. Collier, Age-related changes in dopamine transporters and accumulation of 3-nitrotyrosine in rhesus monkey midbrain dopamine neurons: relevance in selective neuronal vulnerability to degeneration, Eur. J. Neurosci. 27 (2008) 3205–3215.
[66] E. Andres-Mateos, C. Perier, L. Zhang, B. Blanchard-Fillion, T.M. Greco, B. Thomas, H.S. Ko, M. Sasaki, H. Ischiropoulos, S. Przedborski, T.M. Dawson, V.L. Dawson, DJ-1 gene deletion reveals that DJ-1 is an atypical peroxiredoxin-like peroxidase, Proc. Natl. Acad. Sci. U.S.A. 104 (2007) 14807–14812.
[67] P.J. Kahle, J. Waak, T. Gasser, DJ-1 and prevention of oxidative stress in Parkinson's disease and other age-related disorders, Free Radical Biol. Med. 47 (2009) 1354–1361.
[68] M.S. Goldberg, A. Pisani, M. Haburcak, T.A. Vortherms, T. Kitada, C. Costa, Y. Tong, G. Martella, A. Tscherter, A. Martins, G. Bernardi, B.L. Roth, E.N. Pothos, P. Calabresi, J. Shen, Nigrostriatal dopaminergic deficits and hypokinesia caused by inactivation of the familial Parkinsonism-linked gene DJ-1, Neuron 45 (2005) 489–496.
[69] J.C. Greene, A.J. Whitworth, I. Kuo, L.A. Andrews, M.B. Feany, L.J. Pallanck, Mitochondrial pathology and apoptotic muscle degeneration in Drosophila parkin mutants, Proc. Natl. Acad. Sci. U.S.A. 100 (2003) 4078–4083.
[70] J.J. Palacino, D. Sagi, M.S. Goldberg, S. Krauss, C. Motz, M. Wacker, J. Klose, J. Shen, Mitochondrial dysfunction and oxidative damage in parkin-deficient mice, J. Biol. Chem. 279 (2004) 18614–18622.
[71] I.E. Clark, M.W. Dodson, C. Jiang, J.H. Cao, J.R. Huh, J.H. Seol, S.J. Yoo, B.A. Hay, M. Guo, Drosophila pink1 is required for mitochondrial function and interacts genetically with parkin, Nature 441 (2006) 1162–1166.
[72] J. Park, S.B. Lee, S. Lee, Y. Kim, S. Song, S. Kim, E. Bae, J. Kim, M. Shong, J.M. Kim, J. Chung, Mitochondrial dysfunction in Drosophila PINK1 mutants is complemented by parkin, Nature 441 (2006) 1157–1161.
[73] N. Exner, B. Treske, D. Paquet, K. Holmstrom, C. Schiesling, S. Gispert, I. Carballo-Carbajal, D. Berg, H.H. Hoepken, T. Gasser, R. Kruger, K.F. Winklhofer, F. Vogel, A.S. Reichert, G. Auburger, P.J. Kahle, B. Schmid, C. Haass, Loss-of-function of human PINK1 results in mitochondrial pathology and can be rescued by parkin, J. Neurosci. 27 (2007) 12413–12418.
[74] T. Kitada, A. Pisani, D.R. Porter, H. Yamaguchi, A. Tscherter, G. Martella, P. Bonsi, C. Zhang, E.N. Pothos, J. Shen, Impaired dopamine release and synaptic plasticity in the striatum of PINK1-deficient mice, Proc. Natl. Acad. Sci. U.S.A. 104 (2007) 11441–11446.
[75] D.C. German, K.F. Manaye, C.L. White, 3rd, D.J. Woodward, D.D. McIntire, W.K. Smith, R.N. Kalaria, D.M. Mann, Disease-specific patterns of locus coeruleus cell loss, Ann. Neurol. 32 (1992) 667–676.
[76] J.T. Williams, R.A. North, S.A. Shefner, S. Nishi, T.M. Egan, Membrane properties of rat locus coeruleus neurones, Neuroscience 13 (1984) 137–156.
[77] D.R. Stevens, H.L. Haas, Calcium-dependent prepotentials contribute to spontaneous activity in rat tuberomammillary neurons, J. Physiol. 493 (Pt 3) (1996) 747–754.
[78] A. Taddese, B.P. Bean, Subthreshold sodium current from rapidly inactivating sodium channels drives spontaneous firing of tuberomammillary neurons, Neuron 33 (2002) 587–600.
[79] D.C. German, K.F. Manaye, P.K. Sonsalla, B.A. Brooks, Midbrain dopaminergic cell loss in Parkinson's disease and MPTP-induced parkinsonism: sparing of calbindin-D28k-containing cells, Ann. NY Acad. Sci. 648 (1992) 42–62.
[80] S. Belzunegui, W. San Sebastian, P. Garrido-Gil, A. Izal-Azcarate, M. Vazquez-Claverie, B. Lopez, I. Marcilla, J.L. Lanciego, M.R. Luquin, The number of dopaminergic cells is increased in the olfactory bulb of monkeys chronically exposed to MPTP, Synapse 61 (2007) 1006–1012.
[81] A. Pignatelli, K. Kobayashi, H. Okano, O. Belluzzi, Functional properties of dopaminergic neurones in the mouse olfactory bulb, J. Physiol. 564 (2005) 501–514.
[82] R.B. Postuma, A.E. Lang, J. Massicotte-Marquez, J. Montplaisir, Potential early markers of Parkinson's disease in idiopathic REM sleep behavior disorder, Neurology 66 (2006) 845–851.
[83] E. Huisman, H.B. Uylings, P.V. Hoogland, Gender-related changes in increase of dopaminergic neurons in the olfactory bulb of Parkinson's disease patients, Movement Disord. 23 (2008) 1407–1413.
[84] A. Pignatelli, J.B. Ackman, D. Vigetti, A.P. Beltrami, S. Zucchini, O. Belluzzi, A potential reservoir of immature dopaminergic replacement neurons in the adult mammalian olfactory bulb, Pflugers Arch. 457 (2009) 899–915.
[85] T. Yamada, P.L. McGeer, K.G. Baimbridge, E.G. McGeer, Relative sparing in Parkinson's disease of substantia nigra dopamine neurons containing calbindin-D28K, Brain Res. 526 (1990) 303–307.
[86] A.A. Grace, B.S. Bunney, The control of firing pattern in nigral dopamine neurons: single spike firing, J. Neurosci. 4 (1984) 2866–2876.
[87] C. Becker, S.S. Jick, C.R. Meier, Use of statins and the risk of Parkinson's disease: A retrospective case–control study in the UK, Drug Saf. 31 (2008) 399–407.
[88] B. Ritz, L. Qian, S.L. Rhodes, E. Schernhammer, J. Olsen, S. Friis, L-type calcium channel blockers and Parkinson's disease in Denmark, Ann. Neurol., in press.
[89] A. Kupsch, J. Sautter, J. Schwarz, P. Riederer, M. Gerlach, W.H. Oertel, 1-Methyl-4-phenyl-1,2,3,6-tetrahydropyridine-induced neurotoxicity in non-human primates is antagonized by pretreatment with nimodipine at the nigral, but not at the striatal level, Brain Res. 741 (1996) 185–196.
[90] R. Mannhold, R.F. Rekker, C. Sonntag, A.M. ter Laak, K. Dross, E.E. Polymeropoulos, Comparative evaluation of the predictive power of calculation procedures for molecular lipophilicity, J. Pharm. Sci. 84 (1995) 1410–1419.
[91] M.J. Eisenberg, A. Brox, A.N. Bestawros, Calcium channel blockers: an update, Am. J. Med. 116 (2004) 35–43.
[92] A. Koschak, D. Reimer, I. Huber, M. Grabner, H. Glossmann, J. Engel, J. Striessnig, alpha 1D (Cav1.3) subunits can form l-type Ca2+ channels activating at negative voltages, J. Biol. Chem. 276 (2001) 22100–22106.
[93] A. Scholze, T.D. Plant, A.C. Dolphin, B. Nurnberg, Functional expression and characterization of a voltage-gated CaV1.3 (alpha1D) calcium channel subunit from an insulin-secreting cell line, Mol. Endocrinol. 15 (2001) 1211–1221.
[94] A. Fitton, P. Benfield, Isradipine. A review of its pharmacodynamic and pharmacokinetic properties, and therapeutic use in cardiovascular disease, Drugs 40 (1990) 31–74.
[95] A.Y. Hung, M.A. Schwarzschild, Clinical trials for neuroprotection in Parkinson's disease: overcoming angst and futility? Curr. Opin. Neurol. 20 (2007) 477–483.
[96] C.W. Shults, R.H. Haas, D. Passov, M.F. Beal, Coenzyme Q10 levels correlate with the activities of complexes I and II/III in mitochondria from parkinsonian and nonparkinsonian subjects, Ann. Neurol. 42 (1997) 261–264.
[97] M.F. Beal, R.T. Matthews, A. Tieleman, C.W. Shults, Coenzyme Q10 attenuates the 1-methyl-4-phenyl-1,2,3,tetrahydropyridine (MPTP) induced loss of striatal dopamine and dopaminergic axons in aged mice, Brain Res. 783 (1998) 109–114.
[98] R.T. Matthews, R.J. Ferrante, P. Klivenyi, L. Yang, A.M. Klein, G. Mueller, R. Kaddurah-Daouk, M.F. Beal, Creatine and cyclocreatine attenuate MPTP neurotoxicity, Exp. Neurol. 157 (1999) 142–149.
[99] K. Magyar, B. Szende, (−)-Deprenyl, a selective MAO-B inhibitor, with apoptotic and anti-apoptotic properties, Neurotoxicology 25 (2004) 233–242.
[100] A.H. Schapira, Progress in neuroprotection in Parkinson's disease, Eur. J. Neurol. 15 (Suppl. 1) (2008) 5–13.
[101] W. Wang, H. Fang, L. Groom, A. Cheng, W. Zhang, J. Liu, X. Wang, K. Li, P. Han, M. Zheng, J. Yin, M.P. Mattson, J.P. Kao, E.G. Lakatta, S.S. Sheu, K. Ouyang, J. Chen, R.T. Dirksen, H. Cheng, Superoxide flashes in single mitochondria, Cell 134 (2008) 279–290.
[102] J.R. Desireddi, K.N. Farrow, J.D. Marks, G.B. Waypa, P.T. Schumacker, Hypoxia increases ROS signaling and cytosolic Ca2+ in pulmonary artery smooth muscle cells of mouse lungs slices, Antioxid. Redox Signal. (2009), doi:10.1089/ars.2009.2862.
[103] G.T. Hanson, R. Aggeler, D. Oglesbee, M. Cannon, R.A. Capaldi, R.Y. Tsien, S.J. Remington, Investigating mitochondrial redox potential with redox-sensitive green fluorescent protein indicators, J. Biol. Chem. 279 (2004) 13044–13053.
[104] R. Rizzuto, T. Pozzan, Microdomains of intracellular Ca2+: molecular determinants and functional consequences, Physiol. Rev. 86 (2006) 369–408.
[105] G. Csordas, C. Renken, P. Varnai, L. Walter, D. Weaver, K.F. Buttle, T. Balla, C.A. Mannella, G. Hajnoczky, Structural and functional features and significance

of the physical linkage between ER and mitochondria, J. Cell Biol. 174 (2006) 915–921.
[106] O.M. de Brito, L. Scorrano, Mitofusin 2 tethers endoplasmic reticulum to mitochondria, Nature 456 (2008) 605–610.
[107] G. Hajnoczky, E. Davies, M. Madesh, Calcium signaling and apoptosis, Biochem. Biophys. Res. Commun. 304 (2003) 445–454.
[108] I. Bezprozvanny, Calcium signaling and neurodegenerative diseases, Trends Mol. Med. 15 (2009) 89–100.
[109] P. Pinton, A. Rimessi, S. Marchi, F. Orsini, E. Migliaccio, M. Giorgio, C. Contursi, S. Minucci, F. Mantovani, M.R. Wieckowski, G. Del Sal, P.G. Pelicci, R. Rizzuto, Protein kinase C beta and prolyl isomerase 1 regulate mitochondrial effects of the life-span determinant p66Shc, Science 315 (2007) 659–663.
[110] E. Migliaccio, M. Giorgio, S. Mele, G. Pelicci, P. Reboldi, P.P. Pandolfi, L. Lanfrancone, P.G. Pelicci, The p66shc adaptor protein controls oxidative stress response and life span in mammals, Nature 402 (1999) 309–313.